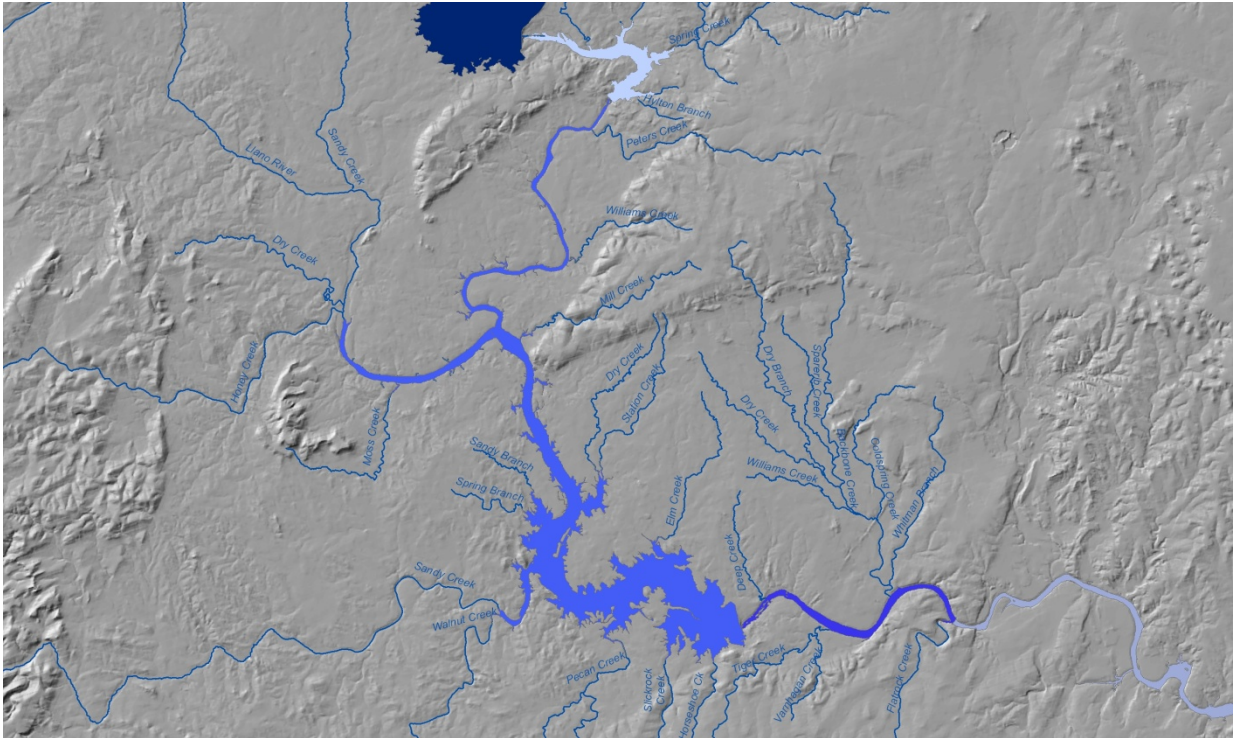


FINAL REPORT

COLORADO RIVER ENVIRONMENTAL MODELS PHASE 3: INKS LAKE, LAKE LBJ, LAKE MARBLE FALLS



Prepared for:

LOWER COLORADO RIVER AUTHORITY



Prepared by:

PARSONS

In conjunction with



MARCH 2011

FINAL REPORT

COLORADO RIVER ENVIRONMENTAL MODELING SYSTEM
PHASE 3: INKS LAKE, LAKE LBJ, LAKE MARBLE FALLS

Prepared for:

LOWER COLORADO RIVER AUTHORITY



Prepared by:

PARSONS

8000 Centre Park Drive, Suite 200
Austin, TX 78754

in conjunction with



901 S Mopac, Bldg IV, Suite 280
Austin, TX 78746

MARCH 2011

TABLE OF CONTENTS

SECTION 1 INTRODUCTION	1-1
1.1 Background.....	1-1
1.1.1 Inks Lake System	1-1
1.1.2 Lake LBJ System.....	1-2
1.1.3 Lake Marble Falls System	1-2
1.1.4 Relevant Ordinances.....	1-3
1.1.4.1 TCEQ Highland Lakes Discharge Ban.....	1-3
1.1.4.2 Highland Lake Watershed Ordinance.....	1-3
1.2 Summary of the Phase 1 Effort.....	1-3
1.3 Objectives of the CREMs Phase 2 and 3 Effort.....	1-4
1.4 Overview of the Phase 3 Report	1-5
SECTION 2 MONITORING PROGRAM	2-1
2.1 Overview.....	2-1
2.2 Program 1: Expanded Routine Monitoring.....	2-1
2.2.1 Expanded List of Parameters	2-3
2.2.1.1 Laboratory Parameters.....	2-3
2.2.1.2 Additional Field Parameters	2-4
2.2.2 Higher Resolution Sampling at Boundaries.....	2-5
2.2.3 Higher Resolution Sampling in the Lake.....	2-5
2.2.4 Additional Lake Stations	2-5
2.2.5 Additional Tributary Stations.....	2-5
2.2.6 Expanded Vertical Sampling	2-5
2.2.7 Lower Detection Limits	2-5
2.3 Program 2: Storm Water Monitoring	2-6
2.3.1 Storm Types and Sampling Frequency.....	2-7
2.3.2 Tributary and Lake Stations.....	2-8
2.4 Program 3: Remote Monitoring	2-8
2.4.1 Thermistors and Thermistor Chains	2-8
2.4.2 Automated Profilers.....	2-9
2.5 Program 4: Special Manual Monitoring	2-9
2.5.1 Phytoplankton Investigation Study.....	2-9
SECTION 3 WATERSHED MODEL	3-1
3.1 Introduction.....	3-1
3.1.1 State Variables of Concern and Model Timestep.....	3-1

3.1.2	Model Input and Development.....	3-2
3.1.2.1	Geospatial Input Data and Hydrologic Response Unit Generation.....	3-2
3.1.2.2	Climatic Temporal Input Data	3-2
3.1.2.3	Point Source Dischargers.....	3-3
3.1.3	General Description of Calibration	3-3
3.1.4	Calibration Data	3-3
3.2	Lake LBJ Watershed	3-4
3.2.1	Lake LBJ Watershed Spatial Domain	3-4
3.2.1.1	Geology.....	3-5
3.2.1.2	Climate.....	3-5
3.2.1.3	Topography	3-6
3.2.1.4	Soils	3-6
3.2.1.5	Land Cover.....	3-7
3.2.1.6	Watershed Ordinance	3-7
3.2.1.7	Point Sources.....	3-7
3.2.1.8	Sub-Watershed Delineation	3-10
3.2.2	Lake LBJ SWAT Model Calibration.....	3-10
3.2.2.1	Hydrology Calibration Data.....	3-10
3.2.2.2	Hydrology Calibration Approach.....	3-12
3.2.2.3	Water Quality Calibration Data	3-14
3.2.2.4	Water Quality Calibration Approach.....	3-16
3.2.2.5	Watershed Operations.....	3-18
3.2.3	Lake LBJ SWAT Model Results.....	3-18
3.2.3.1	Hydrology Calibration Results.....	3-18
3.2.3.2	Sediment Calibration Results.....	3-20
3.2.3.3	Nutrient Calibration Results	3-21
3.3	Lake Marble Falls Watershed	3-24
3.3.1	Lake Marble Falls Watershed Spatial Domain	3-24
3.3.1.1	Geology.....	3-25
3.3.1.2	Climate.....	3-25
3.3.1.3	Topography	3-25
3.3.1.4	Soils	3-25
3.3.1.5	Land Cover.....	3-26
3.3.1.6	Watershed Ordinance	3-26
3.3.1.7	Point Sources.....	3-26

3.3.1.8	Sub-watershed Delineation	3-26
3.3.1.9	Lake Marble Falls SWAT Model Calibration.....	3-27
3.3.1.10	Hydrology Calibration Data.....	3-27
3.3.1.11	Hydrology Calibration Approach.....	3-27
3.3.1.12	Water Quality Calibration Data	3-28
3.3.1.13	Water Quality Calibration Approach.....	3-28
3.3.1.14	Watershed Operations.....	3-29
3.3.2	Lake Marble Falls SWAT Model Results.....	3-29
3.3.2.1	Hydrology Calibration Results.....	3-29
3.3.2.2	Water Quality Calibration Results	3-30
3.4	Inks Lake Watershed	3-30
3.4.1	Inks Lake Watershed Spatial Domain	3-30
3.4.1.1	Geology.....	3-31
3.4.1.2	Climate.....	3-31
3.4.1.3	Topography	3-31
3.4.1.4	Soil.....	3-32
3.4.1.5	Land Cover.....	3-32
3.4.1.6	Watershed Ordinance	3-33
3.4.1.7	Point Sources.....	3-33
3.4.1.8	Sub-watershed Delineation	3-33
3.4.2	Inks Lake SWAT Model Results.....	3-33
3.5	Sensitivity Analysis.....	3-36
SECTION 4 LAKE MODEL.....		4-1
4.1	Introduction.....	4-1
4.1.1	Spatial Domain, Model Segmentation, and Bathymetry	4-1
4.1.1.1	Inks Lake.....	4-2
4.1.1.2	Lake LBJ.....	4-3
4.1.1.3	Lake Marble Falls.....	4-4
4.1.2	Model Time Period.....	4-5
4.1.3	General Processes Modeled	4-5
4.1.4	Calibration Metrics and Goals	4-5
4.2	Model Overview.....	4-7
4.2.1	State Variables of Concern	4-7
4.3	Water Balance	4-8
4.4	Hydrodynamics and Temperature Model Development and Calibration.....	4-9

4.4.1	Model Inputs	4-9
4.4.1.1	Initial Conditions	4-9
4.4.1.2	Flows	4-9
4.4.1.2.1	Inks Lake	4-9
4.4.1.2.2	Lake LBJ.....	4-10
4.4.1.2.3	Lake Marble Falls	4-12
4.4.1.3	Boundary Temperatures.....	4-13
4.4.1.3.1	Upstream Water Temperatures	4-13
4.4.1.3.2	Tributary Water Temperatures.....	4-13
4.4.1.4	Direct Drainage Water Temperature	4-14
4.4.1.5	Meteorological Data	4-14
4.4.2	Model Parameterization.....	4-14
4.4.3	Hydrodynamic and Temperature Calibration Approach	4-16
4.4.4	Calibration Data	4-16
4.4.5	Calibration Results	4-17
4.4.5.1	Inks Lake.....	4-17
4.4.5.2	Lake LBJ.....	4-17
4.4.5.3	Lake Marble Falls.....	4-19
4.5	Water Quality Model Development and Calibration	4-20
4.5.1	Model Inputs	4-20
4.5.1.1	Upstream Boundary Water Column Concentrations.....	4-20
4.5.1.1.1	Total Dissolved Solids.....	4-22
4.5.1.1.2	Algae	4-22
4.5.1.1.3	Organic Matter.....	4-23
4.5.1.1.4	Organic Nitrogen.....	4-24
4.5.1.1.5	Organic Phosphorus	4-25
4.5.1.1.6	Inorganic Suspended Solids.....	4-25
4.5.1.2	Initial Conditions.....	4-25
4.5.1.3	Tributary and Runoff Water Quality Concentrations.....	4-25
4.5.1.3.1	Flow.....	4-26
4.5.1.3.2	Organic Matter, Organic Nitrogen, and Organic Phosphorus	4-26
4.5.1.3.3	Bioavailable Orthophosphorus.....	4-27
4.5.1.3.4	Nitrate/Nitrite Nitrogen	4-27
4.5.1.3.5	Ammonia Nitrogen.....	4-28
4.5.1.3.6	Dissolved Oxygen	4-28

4.5.1.3.7	Suspended Sediments	4-28
4.5.1.3.8	Generic Constituents	4-28
4.5.1.3.9	Algae	4-28
4.5.1.4	Direct Wastewater Discharges	4-28
4.5.1.5	Utility Water Discharge	4-29
4.5.1.6	Sediment Fluxes	4-29
4.5.2	Loading Summaries	4-29
4.5.3	Water Quality Parameterization	4-30
4.5.3.1	Light Extinction.....	4-30
4.5.3.2	Algae.....	4-31
4.5.4	Water Quality Calibration Approach.....	4-31
4.5.5	Calibration Data	4-33
4.5.6	Calibration Results for the Inks Lake Model.....	4-34
4.5.6.1	Conservatives (Specific Conductance and Chloride).....	4-34
4.5.6.2	Dissolved Oxygen	4-34
4.5.6.3	Organic Matter (Total Organic Carbon).....	4-35
4.5.6.4	Nitrogen	4-35
4.5.6.5	Phosphorus.....	4-36
4.5.6.6	Algae and Chlorophyll-a.....	4-37
4.5.6.7	Model Parameters.....	4-38
4.5.7	Calibration Results for the Lake LBJ Model	4-42
4.5.7.1	Conservatives (Specific Conductance and Chloride).....	4-42
4.5.7.2	Dissolved Oxygen	4-43
4.5.7.3	Organic Matter (Total Organic Carbon).....	4-43
4.5.7.4	Nitrogen	4-44
4.5.7.5	Phosphorus.....	4-45
4.5.7.6	Chlorophyll-a	4-46
4.5.7.7	Model Parameters.....	4-47
4.5.8	Calibration Results for the Lake Marble Falls Model.....	4-51
4.5.8.1	Conservatives (Specific Conductance and Chloride).....	4-51
4.5.8.2	Dissolved Oxygen	4-51
4.5.8.3	Organic Matter (Total Organic Carbon).....	4-52
4.5.8.4	Nitrogen	4-52
4.5.8.5	Phosphorus.....	4-54
4.5.8.6	Chlorophyll-a	4-54

4.5.8.7	Model Parameters.....	4-55
4.6	Sensitivity Analysis.....	4-59
4.7	Bounding Calibration.....	4-62
SECTION 5 SUMMARY		5-1
SECTION 6 REFERENCES.....		6-1

Appendix A.1	Water Balance Methodology Memo
Appendix A.2	Summary of Water Balance Discussions with ROC
Appendix B	Vertical Profiles of Temperature, Specific Conductance, Chloride, and Dissolved Oxygen
Appendix C	CE-QUAL-W2 Model Calibration Metrics and Objectives

LIST OF TABLES

Table 2-1	Program 1 – RSS and Expanded RSS Monitoring Locations.....	2-2
Table 2-2	Program 1 – List of Parameters for Expanded RSS Sampling	2-3
Table 2-3	Program 2 – Storm Monitoring Locations and Number of Monitoring Events...	2-6
Table 2-4	Program 2 - Summary of Storm Sampling	2-7
Table 2-5	Program 3 - Summary of Remote Sampling.....	2-8
Table 3-1	Meteorological Stations Used for the Lake LBJ SWAT Model	3-5
Table 3-2	Lake LBJ Watershed Land Cover	3-8
Table 3-3	Permitted Discharger Flow and Concentrations in the Lake LBJ Watershed	3-9
Table 3-4	Lake LBJ Watershed Hydrologic Calibration Stations	3-11
Table 3-5	Lake LBJ SWAT Hydrologic Calibration Parameters	3-13
Table 3-6	Lake LBJ Watershed Water Quality Calibration Stations.....	3-15
Table 3-7	Uncertainty Associated with Lake LBJ Watershed Rating Curve Predictions..	3-15
Table 3-8	Lake LBJ SWAT Water Quality Calibration Parameters.....	3-17
Table 3-9	Lake LBJ SWAT Monthly Hydrologic Calibration Metrics for Primary Calibration Locations	3-19
Table 3-10	Lake LBJ SWAT Monthly Hydrologic Calibration Metrics for Secondary Calibration Locations	3-19
Table 3-11	Lake LBJ SWAT Monthly Sediment (TSS) Calibration Metrics	3-21
Table 3-12	Lake LBJ SWAT Monthly Nutrient Calibration Metrics	3-22
Table 3-13	Comparison of Lake LBJ (Llano near Llano) and Lake Travis SWAT Monthly Nutrient Calibration Metrics	3-24
Table 3-14	Meteorological Stations Used for the Lake Marble Falls SWAT Model	3-25
Table 3-15	Lake Marble Falls Watershed Land Cover	3-26
Table 3-16	Lake Marble Falls Watershed Hydrologic Calibration Stations	3-27
Table 3-17	Lake Marble Falls SWAT Hydrologic Calibration Parameters	3-28
Table 3-18	Lake Marble Falls SWAT Water Quality Calibration Parameters.....	3-29
Table 3-19	Lake Marble Falls SWAT Hydrologic Calibration Metrics for Backbone Creek.....	3-30
Table 3-20	Lake Marble Falls SWAT Water Quality Calibration Metrics for Backbone Creek.....	3-30
Table 3-21	Meteorological Stations used for the Inks Lake SWAT Model.....	3-31
Table 3-22	Soil Distribution within the Inks Lake Watershed	3-32
Table 3-23	Inks Lake Watershed Land Cover	3-32

Table 3-24	Parameters Changed for Base Run of the Inks Lake SWAT Model (same as calibration parameters for basin 63 of the LBJ SWAT model)	3-33
Table 3-25	Summary of SWAT Results for the Two Major Tributaries of Inks Lake	3-36
Table 3-26	SWAT Parameters Selected for Sensitivity Analysis.....	3-37
Table 3-27	Sensitivity Results for the Lake LBJ SWAT Model	3-38
Table 3-28	Sensitivity Results for the Lake Marble Falls SWAT Model	3-40
Table 3-29	Sensitivity Results for the Inks Lake SWAT Model	3-42
Table 4-1	Summary of Longitudinal Segmentation for Inks Lake CE-QUAL-W2 Model..	4-2
Table 4-2	Summary of Longitudinal Segmentation for Lake LBJ CE-QUAL-W2 Model..	4-3
Table 4-3	Summary of Longitudinal Segmentation for Lake Marble Falls CE-QUAL-W2 Model.....	4-4
Table 4-4.	Calibration Goals† for Absolute Mean Error	4-6
Table 4-5	List of Water Quality State Variables in CE-QUAL-W2 Version 3.6	4-7
Table 4-6	Inks Lake Model Flows: Tributaries, Outflows and Directly Connected Watersheds	4-10
Table 4-7	Lake LBJ Model Inflows: Tributaries, Discharges, Outflows, Withdrawals, and Directly Connected Watersheds	4-11
Table 4-8	Lake Marble Falls Model Flows: Outflows and Directly Connected Watersheds	4-12
Table 4-9	Model Parameters Affecting Hydrodynamic and Thermal Calibration	4-14
Table 4-10	Inks Lake Model Performance Metrics for Water Temperature	4-17
Table 4-11	Lake LBJ Model Performance Metrics for Water Temperature	4-18
Table 4-12	Lake Marble Falls Model Performance Metrics for Water Temperature	4-19
Table 4-13	Measured Water Quality Parameters at Inks Lake Upstream Boundary Site....	4-21
Table 4-14	Relative Abundance (%) of Algal Cells by Class	4-23
Table 4-15	Estimated Algal Biovolume by Major Group†	4-23
Table 4-16	Model Performance Metrics for Specific Conductance and Chloride at Station 12336 of Inks Lake	4-34
Table 4-17	Model Performance Metrics for DO at Station 12336 of Inks Lake	4-35
Table 4-18	Model Performance Metrics for TOC at Station 12336 of Inks Lake	4-35
Table 4-19	Model Performance Metrics for Nitrogen at Station 12336 of Inks Lake	4-35
Table 4-20	Model Performance Metrics for Phosphorus at Station 12336 of Inks Lake.....	4-37
Table 4-21	Model Performance Metrics for Chlorophyll-a at Station 12336 of Inks Lake .	4-37
Table 4-22	Default and Calibrated Parameter Values for the Inks Lake Model	4-38
Table 4-23	Overall Model Performance Metrics for Specific Conductance and Chloride at Lake LBJ Monitoring Stations	4-42

Table 4-24	Overall Model Performance Metrics for DO at Lake LBJ Monitoring Stations	4-43
Table 4-25	Overall Model Performance Metrics for TOC at Lake LBJ Stations	4-44
Table 4-26	Overall Model Performance Metrics for Nitrogen at Lake LBJ Stations	4-44
Table 4-27	Overall Model Performance Metrics for Phosphorus Species in Lake LBJ	4-46
Table 4-28	Overall Model Performance Metrics for Chlorophyll-a in Lake LBJ	4-46
Table 4-29	Default and Calibrated Parameter Values for the Lake LBJ Model	4-47
Table 4-30	Model Performance Metrics for Specific Conductance and Chloride at Station 12319 of Lake Marble Falls	4-51
Table 4-31	Model Performance Metrics for DO at Station 12319 of Lake Marble Falls	4-52
Table 4-32	Model Performance Metrics for TOC at Station 12319 of Lake Marble Falls	4-52
Table 4-33	Model Performance Metrics for Nitrogen at Station 12319 of Lake Marble Falls	4-53
Table 4-34	Model Performance Metrics for Phosphorus Species at Station 12319 of Lake Marble Falls	4-54
Table 4-35	Model Performance Metrics for Chlorophyll-a at Station 12319 of Lake Marble Falls	4-55
Table 4-36	Calibrated Parameter Values for the Lake Marble Falls Model	4-55
Table 4-37	Sensitivity Indices for Model Parameters and Inputs	4-60
Table 4-38	Inks Lake Model Performance Metrics for Original and Bounding Calibration	4-63
Table 4-39	Lake LBJ Model Performance Metrics for Original and Bounding Calibration	4-64
Table 4-40	Lake Marble Falls Model Performance Metrics for Original and Bounding Calibration	4-65

LIST OF FIGURES

- Figure 3-1 Phase 3 Watershed
- Figure 3-2 Lake LBJ Watershed and Stream Network
- Figure 3-3 Lake LBJ Watershed Geologic Regions (Modified TWDB 2009)
- Figure 3-4 Lake LBJ Watershed Average Annual Precipitation and Meteorological Stations
- Figure 3-5 Lake LBJ Watershed with Digital Elevation Model
- Figure 3-6 Lake LBJ Watershed STATSGO Soils
- Figure 3-7 Lake LBJ Watershed Land Cover
- Figure 3-8 Development near Lake LBJ
- Figure 3-9 Lake LBJ Watershed within the HLWO
- Figure 3-10 Lake LBJ Watershed Permitted Dischargers
- Figure 3-11 Lake LBJ Lake Model Segmentation and Watershed Model Pour Points
- Figure 3-12 Lake LBJ Sub-watershed Delineation
- Figure 3-13 Lake LBJ SWAT Model Monthly Average Flow Calibration by Reach Using Default Model Parameters
- Figure 3-14 Llano River Average Daily Flows at Junction, Mason, and Llano in 2006
- Figure 3-15a Rating Curves Predicted by LOADEST for Llano River near Llano
- Figure 3-15b Rating Curves Predicted by LOADEST for Llano River near Junction
- Figure 3-15c Rating Curves Predicted by LOADEST for Sandy Creek near Kingsland
- Figure 3-15d Rating Curves Predicted by LOADEST for Llano River near Mason
- Figure 3-16a Lake LBJ SWAT Model Average Daily Flows Calibration for Llano River at Llano (Reach 13)
- Figure 3-16b Lake LBJ SWAT Model Average Daily Flows Calibration for Llano River near Mason (Reach 32)
- Figure 3-16c Lake LBJ SWAT Model Average Daily Flows Calibration for Llano River near Junction (Reach 69)
- Figure 3-16d Lake LBJ SWAT Model Average Daily Flows Calibration for Sandy creek near Kingsland (Reach 63)
- Figure 3-17a Lake LBJ SWAT Model Average Monthly Flows Calibration for Llano River at Llano (Reach 13)
- Figure 3-17b Lake LBJ SWAT Model Average Monthly Flows Calibration for Llano River near Mason (Reach 32)
- Figure 3-17c Lake LBJ SWAT Model Average Monthly Flows Calibration for Llano River near Junction (Reach 69)

Figure 3-17d Lake LBJ SWAT Model Average Monthly Flows Calibration for Sandy Creek near Kingsland (Reach 63)

Figure 3-18a Lake LBJ SWAT Model Average Annual Flows Calibration for Llano River at Llano (Reach 13)

Figure 3-18b Lake LBJ SWAT Model Average Annual Flows Calibration for Llano River near Mason (Reach 32)

Figure 3-18c Lake LBJ SWAT Model Average Annual Flows Calibration for Llano River near Junction (Reach 69)

Figure 3-18d Lake LBJ SWAT Model Average Annual Flows Calibration for Sandy Creek near Kingsland (Reach 63)

Figure 3-19 Lake LBJ SWAT Model Monthly Average Flow Calibration by Reach

Figure 3-20 Lake LBJ SWAT Model Monthly Average TSS Load Calibration by Reach

Figure 3-21a Lake LBJ SWAT Model Monthly Average OrgP Load Calibration by Reach

Figure 3-21b Lake LBJ SWAT Model Monthly Average PO₄ Load Calibration by Reach

Figure 3-21c Lake LBJ SWAT Model Monthly Average TP Load Calibration by Reach

Figure 3-21d Lake LBJ SWAT Model Monthly Average OrgN Load Calibration by Reach

Figure 3-21e Lake LBJ SWAT Model Monthly Average NH₄ Load Calibration by Reach

Figure 3-21f Lake LBJ SWAT Model Monthly Average NO_x Load Calibration by Reach

Figure 3-21g Lake LBJ SWAT Model Monthly Average TN Load Calibration by Reach

Figure 3-22 Lake Marble Falls Watershed and Stream Network

Figure 3-23 Lake Marble Falls Watershed Average Annual Precipitation and Meteorological Stations

Figure 3-24 Lake Marble Falls Watershed with Digital Elevation Model

Figure 3-25 Lake Marble Falls Watershed STATSGO Soils

Figure 3-26 Lake Marble Falls Watershed Land Cover

Figure 3-27 Extent of the HLWO within Lake Marble Falls Watershed

Figure 3-28 SWAT Model Subbasins for the Lake Marble Falls Watershed

Figure 3-29 Lake Marble Falls Calibration Station

Figure 3-30 SWAT Modeled and Reported Daily Flows for Backbone Creek (Reach 7) Draining to Lake Marble Falls

Figure 3-31a SWAT Modeled and Reported Monthly Average Flows for Backbone Creek (Reach 7) Draining to Lake Marble Falls

Figure 3-31b SWAT Modeled and Reported Monthly Average Flows for Backbone Creek (Reach 7) Draining to Lake Marble Falls

Figure 3-32	SWAT Modeled and Reported Yearly Average Flows for Backbone Creek (Reach 7) Draining to Lake Marble Falls
Figure 3-33	Inks Lake Watershed and Stream Network
Figure 3-34	Inks Lake Watershed Geologic Units
Figure 3-35	Inks Lake Watershed Average Annual Precipitation and Meteorological Stations
Figure 3-36	Inks Lake Watershed with Digital Elevation Model
Figure 3-37	Inks Lake Watershed STATSGO Soil Classification
Figure 3-38	Inks Lake Watershed NLCD Land Cover
Figure 3-39	Inks Lake Watershed within the HLWO
Figure 3-40	Inks Lake Watershed Permitted Dischargers
Figure 3-41	Inks Lake Watershed Model Segmentation
Figure 3-42	Inks Lake SWAT Model Annual Average Flows and Loads for Spring Creek (Reach 29)
Figure 3-43	Inks Lake SWAT Model Annual Average Flows and Loads for Clear Creek (Reach 10)
Figure 4-1	Segmentation of the Inks Lake Model
Figure 4-2	Longitudinal profile of the Inks Lake Model
Figure 4-3	Elevation-Volume Relationship for the Inks Lake Model
Figure 4-4	Segmentation of the Lake LBJ Model
Figure 4-5	Longitudinal Profile of the Lake LBJ Model
Figure 4-6	Elevation-Volume Relationship for the Lake LBJ Model
Figure 4-7	Segmentation of the Lake Marble Falls Model
Figure 4-8	Longitudinal Profile of the Lake Marble Falls Model
Figure 4-9	Elevation-Volume Relationship for the Lake Marble Falls Model
Figure 4-10	Water Level Calibration Results for the Inks Lake Model
Figure 4-11	Water Temperature Calibration Results for the Inks Lake Model
Figure 4-12	Water Level Calibration of the Lake LBJ Model
Figure 4-13	Water Temperature Calibration Results for Lake LBJ near Wirtz Dam
Figure 4-14	Water Temperature Calibration Results for Lake LBJ at the Narrows
Figure 4-15	Water Temperature Calibration Results for Lake LBJ at Confluence with Sandy Creek Arm
Figure 4-16	Water Temperature Calibration Results for Lake LBJ at Confluence with Llano River Arm

Figure 4-17	Water Temperature Calibration Results for Lake LBJ at FM 1431
Figure 4-18	Water Temperature Calibration Results for Lake LBJ at Kingsland Cove
Figure 4-19	Water Temperature Calibration Results for Lake LBJ at Headwaters
Figure 4-20	Water Temperature Calibration Results for Lake LBJ at FM 2900
Figure 4-21	Water Temperature Calibration Results for Lake LBJ at Lake Shore Drive
Figure 4-22	Water Temperature Calibration Results for Lake LBJ at Horseshoe Bay Cove
Figure 4-23	Water Level Calibration of the Lake Marble Falls Model
Figure 4-24	Water Temperature Calibration Results for Lake Marble Falls near Max Starcke Dam
Figure 4-25	Water Temperature Calibration Results for Lake Marble Falls near US 281 Bridge
Figure 4-26	Water Temperature Calibration Results for Lake Marble Falls at Hefner Ranch
Figure 4-27	Water Temperature Calibration Results for Lake Marble Falls at Headwaters
Figure 4-28	Percentage Contribution to Inks Lake by Source Type for Input Constituent Mass
Figure 4-29	Percentage Contribution to Lake LBJ by Source Type for Input Constituent Mass
Figure 4-30	Percentage Contribution to Lake Marble Falls by Source Type for Source Type for Input Constituent Mass
Figure 4-31	Specific Conductance Calibration Results for the Inks Lake Model
Figure 4-32	Chloride Calibration Results for the Inks Lake Model
Figure 4-33	Dissolved Oxygen Calibration Results for the Inks Lake Model
Figure 4-34	Total Organic Carbon Calibration Results for the Inks Lake Model
Figure 4-35	Total Kjeldahl Nitrogen Calibration Results for the Inks Lake Model
Figure 4-36	Ammonia Nitrogen Calibration Results for the Inks Lake Model
Figure 4-37	Nitrate Nitrogen Calibration Results for the Inks Lake Model
Figure 4-38	Total Phosphorus Calibration Results for the Inks Lake Model
Figure 4-39	Orthophosphorus Calibration Results for the Inks Lake Model
Figure 4-40	Chlorophyll-a Calibration Results for the Inks Lake Model
Figure 4-41	Predicted Seasonal Abundances of Major Algal Groups in Inks Lake
Figure 4-42	Algal Growth Limiting Factors by Year in Inks Lake
Figure 4-43	Algal Growth Limiting Factors by Month in Inks Lake
Figure 4-44	Specific Conductance Calibration Results for Lake LBJ near Wirtz Dam
Figure 4-45	Specific Conductance Calibration Results for Lake LBJ at the Narrows

- Figure 4-46 Specific Conductance Calibration Results for Lake LBJ at Confluence with Sandy Creek Arm
- Figure 4-47 Specific Conductance Calibration Results for Lake LBJ near Confluence with Llano River Arm
- Figure 4-48 Specific Conductance Calibration Results for Lake LBJ at FM 1431
- Figure 4-49 Specific Conductance Calibration Results for Lake LBJ at Kingsland Cove
- Figure 4-50 Specific Conductance Calibration Results for Lake LBJ at Headwaters
- Figure 4-51 Specific Conductance Calibration Results for Lake LBJ at FM 2900 Bridge
- Figure 4-52 Specific Conductance Calibration Results for Lake LBJ near Lake Shore Drive
- Figure 4-53 Specific Conductance Calibration Results for Lake LBJ at Horseshoe Bay Cove
- Figure 4-54 Chloride Calibration Results for Lake LBJ near Wirtz Dam
- Figure 4-55 Chloride Calibration Results for Lake LBJ near Sandy Creek Confluence
- Figure 4-56 Chloride Calibration Results for Lake LBJ near Confluence with Llano River Arm
- Figure 4-57 Chloride Calibration Results for Lake LBJ at Kingsland Cove
- Figure 4-58 Chloride Calibration Results for Lake LBJ at Headwaters
- Figure 4-59 Chloride Calibration Results for Lake LBJ at FM 2900
- Figure 4-60 Chloride Calibration Results for Lake LBJ near Lake Shore Drive
- Figure 4-61 Chloride Calibration Results for Lake LBJ at Horseshoe Bay Cove
- Figure 4-62 Dissolved Oxygen Calibration Results for Lake LBJ near Wirtz Dam.
- Figure 4-63 Dissolved Oxygen Calibration Results for Lake LBJ at The Narrows.
- Figure 4-64 Dissolved Oxygen Calibration Results for Lake LBJ near Sandy Creek Confluence.
- Figure 4-65 Dissolved Oxygen Calibration Results for Lake LBJ near confluence with Llano River Arm
- Figure 4-66 Dissolved Oxygen Calibration Results for Lake LBJ at FM 1431
- Figure 4-67 Dissolved Oxygen Calibration Results for Lake LBJ at Kingsland Cove
- Figure 4-68 Dissolved Oxygen Calibration Results for Lake LBJ at Headwaters
- Figure 4-69 Dissolved Oxygen Calibration Results for Lake LBJ at FM 2900
- Figure 4-70 Dissolved Oxygen Calibration Results for Lake LBJ near Lake Shore Drive
- Figure 4-71 Dissolved Oxygen Calibration Results for Lake LBJ at Horseshoe Bay Cove
- Figure 4-72 Total Organic Carbon Calibration Results for Lake LBJ near Wirtz Dam
- Figure 4-73 Total Organic Carbon Calibration Results for Lake LBJ near Sandy Creek Confluence

- Figure 4-74 Total Organic Carbon Calibration Results for Lake LBJ near Confluence with Llano River Arm
- Figure 4-75 Total Organic Carbon Calibration Results for Lake LBJ at Kingsland Cove
- Figure 4-76 Total Organic Carbon Calibration Results for Lake LBJ at Headwaters
- Figure 4-77 Total Organic Carbon Calibration Results for Lake LBJ at FM 2900
- Figure 4-78 Total Organic Carbon Calibration Results for Lake LBJ near Lake Shore Drive
- Figure 4-79 Total Organic Carbon Calibration Results for Lake LBJ at Horseshoe Bay Cove
- Figure 4-80 Total Kjeldahl Nitrogen Calibration Results for Lake LBJ near Wirtz Dam
- Figure 4-81 Total Kjeldahl Nitrogen Calibration Results for Lake LBJ near Sandy Creek Confluence
- Figure 4-82 Total Kjeldahl Nitrogen Calibration Results for Lake LBJ near Confluence with Llano River Arm
- Figure 4-83 Total Kjeldahl Nitrogen Calibration Results for Lake LBJ at Kingsland Cove
- Figure 4-84 Total Kjeldahl Nitrogen Calibration Results for Lake LBJ at Headwaters
- Figure 4-85 Total Kjeldahl Nitrogen Calibration Results for Lake LBJ at FM 2900
- Figure 4-86 Total Kjeldahl Nitrogen Calibration Results for Lake LBJ near Lake Shore Drive
- Figure 4-87 Total Kjeldahl Nitrogen Calibration Results for Lake LBJ at Horseshoe Bay Cove
- Figure 4-88 Ammonia Nitrogen Calibration Results for Lake LBJ near Wirtz Dam
- Figure 4-89 Ammonia Nitrogen Calibration Results for Lake LBJ near Sandy Creek Confluence
- Figure 4-90 Ammonia Nitrogen Calibration Results for Lake LBJ near Confluence with Llano River Arm
- Figure 4-91 Ammonia Nitrogen Calibration Results for Lake LBJ at Kingsland Cove
- Figure 4-92 Ammonia Nitrogen Calibration Results for Lake LBJ at Headwaters
- Figure 4-93 Ammonia Nitrogen Calibration Results for Lake LBJ at FM 2900
- Figure 4-94 Ammonia Nitrogen Calibration Results for Lake LBJ near Lake Shore Drive
- Figure 4-95 Ammonia Nitrogen Calibration Results for Lake LBJ at Horseshoe Bay Cove
- Figure 4-96 Nitrate Nitrogen Calibration Results for Lake LBJ near Wirtz Dam
- Figure 4-97 Nitrate Nitrogen Calibration Results for Lake LBJ near Sandy Creek Confluence
- Figure 4-98 Nitrate Nitrogen Calibration Results for Lake LBJ near Confluence with Llano River Arm
- Figure 4-99 Nitrate Nitrogen Calibration Results for Lake LBJ at Kingsland Cove
- Figure 4-100 Nitrate Nitrogen Calibration Results for Lake LBJ at Headwaters

- Figure 4-101 Nitrate Nitrogen Calibration Results for Lake LBJ at FM 2900
- Figure 4-102 Nitrate Nitrogen Calibration Results for Lake LBJ near Lake Shore Drive
- Figure 4-103 Nitrate Nitrogen Calibration Results for Lake LBJ at Horseshoe Bay Cove
- Figure 4-104 Total Phosphorus Calibration Results for Lake LBJ near Wirtz Dam
- Figure 4-105 Total Phosphorus Calibration Results for Lake LBJ near Sandy Creek Confluence
- Figure 4-106 Total Phosphorus Calibration Results for Lake LBJ near Confluence with Llano River Arm
- Figure 4-107 Total Phosphorus Calibration Results for Lake LBJ at Kingsland Cove
- Figure 4-108 Total Phosphorus Calibration Results for Lake LBJ at Headwaters
- Figure 4-109 Total Phosphorus Calibration Results for Lake LBJ at FM 2900
- Figure 4-110 Total Phosphorus Calibration Results for Lake LBJ near Lake Shore Drive
- Figure 4-111 Total Phosphorus Calibration Results for Lake LBJ at Horseshoe Bay Cove
- Figure 4-112 Orthophosphorus Calibration Results for Lake LBJ near Wirtz Dam
- Figure 4-113 Orthophosphorus Calibration Results for Lake LBJ near Sandy Creek Confluence
- Figure 4-114 Orthophosphorus Calibration Results for Lake LBJ near Confluence with Llano River Arm
- Figure 4-115 Orthophosphorus Calibration Results for Lake LBJ at Kingsland Cove
- Figure 4-116 Orthophosphorus Calibration Results for Lake LBJ at Headwaters
- Figure 4-117 Orthophosphorus Calibration Results for Lake LBJ at FM 2900
- Figure 4-118 Orthophosphorus Calibration Results for Lake LBJ near Lake Shore Drive
- Figure 4-119 Orthophosphorus Calibration Results for Lake LBJ at Horseshoe Bay Cove
- Figure 4-120 Chlorophyll-a Calibration Results for Lake LBJ near Wirtz Dam
- Figure 4-121 Chlorophyll-a Calibration Results for Lake LBJ near Sandy Creek Confluence
- Figure 4-122 Chlorophyll-a Calibration Results for Lake LBJ near Confluence with Llano River Arm
- Figure 4-123 Chlorophyll-a Calibration Results for Lake LBJ at Kingsland Cove
- Figure 4-124 Chlorophyll-a Calibration Results for Lake LBJ at Headwaters
- Figure 4-125 Chlorophyll-a Calibration Results for Lake LBJ at FM 2900
- Figure 4-126 Chlorophyll-a Calibration Results for Lake LBJ near Lake Shore Drive
- Figure 4-127 Chlorophyll-a Calibration Results for Lake LBJ at Horseshoe Bay Cove
- Figure 4-128 Predicted Seasonal Abundances of Major Algal Groups in Lake LBJ
- Figure 4-129 Algal Growth Limiting Factors by Year at Lake LBJ near Wirtz Dam
- Figure 4-130 Algal Growth Limiting Factors by Month at Lake LBJ near Wirtz Dam

- Figure 4-131 Specific Conductance Calibration Results for Lake Marble Falls near Max Starcke Dam
- Figure 4-132 Specific Conductance Calibration Results for Lake Marble Falls near US 281 Bridge
- Figure 4-133 Specific Conductance Calibration Results for Lake Marble Falls at Hefner Ranch
- Figure 4-134 Specific Conductance Calibration Results for Lake Marble Falls at Headwaters
- Figure 4-135 Chloride Calibration Results for Lake Marble Falls near Max Starcke Dam
- Figure 4-136 Chloride Calibration Results for Lake Marble Falls at Headwaters
- Figure 4-137 Dissolved Oxygen Calibration Results for Lake Marble Falls near Max Starcke Dam
- Figure 4-138 Dissolved Oxygen Calibration Results for Lake Marble Falls near US 281 Bridge
- Figure 4-139 Dissolved Oxygen Calibration Results for Lake Marble Falls at Hefner Ranch
- Figure 4-140 Dissolved Oxygen Calibration Results for Lake Marble Falls at Headwaters
- Figure 4-141 Total Organic Carbon Calibration Results for Lake Marble Falls near Max Starcke Dam
- Figure 4-142 Total Organic Carbon Calibration Results for Lake Marble Falls at Headwaters
- Figure 4-143 Total Kjeldahl Nitrogen Calibration Results for Lake Marble Falls near Max Starcke Dam
- Figure 4-144 Total Kjeldahl Nitrogen Calibration Results for Lake Marble Falls at Headwaters
- Figure 4-145 Ammonia Nitrogen Calibration Results for Lake Marble Falls near Max Starcke Dam
- Figure 4-146 Ammonia Nitrogen Calibration Results for Lake Marble Falls at Headwaters
- Figure 4-147 Nitrate Nitrogen Calibration Results for Lake Marble Falls near Max Starcke Dam
- Figure 4-148 Nitrate Nitrogen Calibration Results for Lake Marble Falls at Headwaters
- Figure 4-149 Total Phosphorus Calibration Results for Lake Marble Falls near Max Starcke Dam
- Figure 4-150 Total Phosphorus Calibration Results for Lake Marble Falls at Headwaters
- Figure 4-151 Orthophosphorus Calibration Results for Lake Marble Falls near Max Starcke Dam
- Figure 4-152 Orthophosphorus Calibration Results for Lake Marble Falls at Headwaters
- Figure 4-153 Chlorophyll-a Calibration Results for Lake Marble Falls near Max Starcke Dam
- Figure 4-154 Chlorophyll-a Calibration Results for Lake Marble Falls at Headwaters
- Figure 4-155 Predicted Seasonal Abundances of Major Algal Groups in Lake Marble Falls

- Figure 4-156 Algal Growth Limiting Factors by Year in Lake Marble Falls near Max Starcke Dam
- Figure 4-157 Algal Growth Limiting Factors by Month in Lake Marble Falls near Max Starcke Dam
- Figure 4-158 Sensitivity Analysis Results
- Figure 4-159 Ranking and Scree Plot
- Figure 4-160 Dissolved Oxygen Calibration Results for the Inks Lake Model – Bounding Calibration
- Figure 4-161 Total Organic Carbon Calibration Results for the Inks Lake Model – Bounding Calibration
- Figure 4-162 Total Kjeldahl nitrogen Calibration Results for the Inks Lake Model – Bounding Calibration
- Figure 4-163 Ammonia nitrogen Calibration Results for the Inks Lake Model – Bounding Calibration
- Figure 4-164 Nitrate nitrogen Calibration Results for the Inks Lake Model – Bounding Calibration
- Figure 4-165 Total phosphorus Calibration Results for the Inks Lake Model – Bounding Calibration
- Figure 4-166 Orthophosphorus Calibration Results for the Inks Lake Model – Bounding Calibration
- Figure 4-167 Chlorophyll-a Calibration Results for the Inks Lake Model – Bounding Calibration
- Figure 4-168 Dissolved Oxygen Calibration Results for Lake LBJ near Wirtz Dam – Bounding Calibration
- Figure 4-169 Total Organic Carbon Calibration Results for Lake LBJ near Wirtz Dam – Bounding Calibration
- Figure 4-170 Total Kjeldahl Nitrogen Calibration Results for Lake LBJ near Wirtz Dam – Bounding Calibration
- Figure 4-171 Ammonia Nitrogen Calibration Results for Lake LBJ near Wirtz Dam – Bounding Calibration
- Figure 4-172 Nitrate Nitrogen Calibration Results for Lake LBJ near Wirtz Dam – Bounding Calibration
- Figure 4-173 Total Phosphorus Calibration Results for Lake LBJ near Wirtz Dam – Bounding Calibration
- Figure 4-174 Orthophosphorus Calibration Results for Lake LBJ near Wirtz Dam – Bounding Calibration

- Figure 4-175 Chlorophyll-a Calibration Results for Lake LBJ near Wirtz Dam – Bounding Calibration
- Figure 4-176 Dissolved Oxygen Calibration Results for Lake Marble Falls at Starcke Dam – Bounding Calibration
- Figure 4-177 Total Organic Carbon Calibration Results for Lake Marble Falls at Starcke Dam – Bounding Calibration
- Figure 4-178 Total Kjeldahl Nitrogen Calibration Results for Lake Marble Falls at Starcke Dam – Bounding Calibration
- Figure 4-179 Ammonia Nitrogen Calibration Results for Lake Marble Falls at Starcke Dam – Bounding Calibration
- Figure 4-180 Nitrate Nitrogen Calibration Results for Lake Marble Falls at Starcke Dam – Bounding Calibration
- Figure 4-181 Total Phosphorus Calibration Results for Lake Marble Falls at Starcke Dam – Bounding Calibration
- Figure 4-182 Orthophosphorus Calibration Results for Lake Marble Falls at Starcke Dam – Bounding Calibration
- Figure 4-183 Chlorophyll-a Calibration Results for Lake Marble Falls at Starcke Dam – Bounding Calibration

ACRONYMS AND ABBREVIATIONS

°C	Degrees Celsius
ACHLA	Stoichiometric Ratio of Algal Biomass to Chlorophyll-a, in mg per µg
AG	Algal Growth Rate
ALGP	Algal Phosphorus Content
ALPHA_BF	Baseflow Recession Coefficient (SWAT)
AM	Mortality Rate of Algae
AME	Absolute Mean Error
APHA	American Public Health Association
BASINS	Better Assessment Science Integrating Point and Nonpoint Sources
BMP	Best Management Practice
BOD5	5-Day Biochemical Oxygen Demand
CBOD	Carbonaceous Biochemical Oxygen Demand
CFS	Cubic Feet per Second
CMS	Cubic Meters per Second
CH_K2	Effective River Channel Hydraulic Conductivity (SWAT)
Chl-a	Chlorophyll-a
CN	Curve Number (SWAT)
COD	Chemical Oxygen Demand
CREMs	Colorado River Environmental Models
DKN	Dissolved Kjeldahl Nitrogen
DMR	Discharge Monitoring Report
DO	Dissolved Oxygen
DOM	Dissolved Organic Matter
DON	Dissolved Organic Nitrogen
DOP	Dissolved Organic Phosphorus
DP	Dissolved Phosphorus
EPCO	Plant Uptake Compensation Factor
EPSC	Evapotranspiration Potential for Plants
ESCO	Soil Evaporation Compensation Factor
ET	Evapotranspiration
EXA	Light Extinction Attributable to Algae (CE-QUAL-W2)
EXH2O	Light Extinction Attributable to Water (CE-QUAL-W2)
EXM	Light Extinction Attributable to Macrophytes (CE-QUAL-W2)
EXOM	Light Extinction Attributable to Organic Suspended Solids (CE-QUAL-W2)
EXSS	Light Extinction Attributable to Inorganic Suspended Solids (CE-QUAL-W2)
EXZ	Light Extinction Attributable to Zooplankton (CE-QUAL-W2)
ft	Feet
FM	Farm-to-Market Road
GOF	Goodness of Fit
GPS	Global Positioning System
GW_DELAY	Groundwater Delay Parameter

ha	Hectare
HLWO	Highland Lakes Watershed Ordinance
HRU	Hydrologic Response Unit
HUC	Hydrologic Unit Code
HUMUS	Hydrologic Unit Model of the United States
in	Inch
ISS	Inorganic Suspended Solids
kg	Kilogram
km	Kilometer
L	Liter
LBJ	Lyndon Baines Johnson
LCRA	Lower Colorado River Authority
LDOM	Labile Dissolved Organic Matter
LOADEST	Load Estimator (USGS)
LPOM	Labile Particulate Organic Matter
LPOMDK	Labile Particulate Organic Matter
LTI	LimnoTech, Inc.
m	Meters
MDL	Method Detection Limit
ME	Mean Error
MGD	Million Gallons per Day
mg/L	Milligrams per Liter
mi	Mile
MINP	Mineral Phosphorus (SWAT), aka Orthophosphorus
mL	Milliliters
mm	Millimeters
mph	Miles per Hour
MUD	Municipal Utility District
MUMAX	Maximum Specific Algal Growth Rate
MUSLE	Modified Universal Soil Loss Equation
NADV88	North American Vertical Datum of 1988
NCDC	National Climatic Data Center
NED	National Elevation Dataset
NGVD 29	National Geodetic Vertical Datum of 1929
NH3N	Ammonia Nitrogen
NH ₄	Ammonium, also NH ₄ -N
NLCD	National Land Cover Dataset
NO ₂	Nitrite, also NO ₂ -N
NO ₃	Nitrate, also NO ₃ -N
NO _x	Nitrate + Nitrite, also NO _x -N
NPS	Non-Point Source
NRCS	Natural Resource Conservation Service
NS	Nash-Sutcliffe Model Efficiency Coefficient
NTU	Nephelometric Turbidity Unit
OrgN	Organic Nitrogen

OrgP	Organic Phosphorus
P_UPDIS	Phosphorus Uptake Distribution Parameter
PO4	Orthophosphate, also PO ₄ -P
POM	Particulate Organic Matter
PON	Particulate Organic Nitrogen
POR	Period of Record
PSP	Phosphorus Availability Index
QMLE	Quasi-Maximum Likelihood Estimator
R ²	Squared Correlation Coefficient
RCHRG_DP	Percent of Infiltrated Water Lost to a Regional Aquifer (SWAT)
RDOM	Refractory Dissolved Organic Matter
RI	Reliability Index
RMSE	Root Mean Square Error
RPOM	Refractory Particulate Organic Matter
RSS	Reservoir and Stream Sampling
SEDP	Phosphorus Sorbed to Eroded Sediment
SH	State Highway
SI	Sensitivity Index
SLSUBBSN	Average Slope Length
SOD	Sediment Oxygen Demand
SOL_AWC	Soil Available Water Content (SWAT)
SOL_K	Saturated Hydraulic Conductivity (SWAT)
SOLP	Soluble Phosphorus (SWAT)
SPCOND	Specific Conductance
SSURGO	Soil Survey Geographic Database (NRCS)
STATSGO	State Soil Geographic Database (NRCS)
SU	Standard Units (of pH)
SWAT	Soil and Water Assessment Tool
SYLD	Sediment Yield (SWAT)
TAMU	Texas A&M University
TCEQ	Texas Commission on Environmental Quality
TDS	Total Dissolved Solids
TKN	Total Kjeldahl Nitrogen
TN	Total Nitrogen
TOC	Total Organic Carbon
TON	Total Organic Nitrogen
TOP	Total Organic Phosphorus
TP	Total Phosphorus
TSED	Temperature of Sediment Bed (CE-QUAL-W2)
TSS	Total Suspended Solids
TWDB	Texas Water Development Board
USACE	United States Army Corps of Engineers
USEPA	United States Environmental Protection Agency
USGS	United States Geological Survey
USLE	Universal Soil Loss Equation

USLE_P	Universal Soil Loss Equation Support Practice Factor
WSC	Wind Sheltering Coefficient (CE-QUAL-W2)
WWTP	Wastewater Treatment Plant
WYLD	Water Yield (SWAT)
μg/L	Micrograms per Liter
μS/cm ²	Micro-Siemens per Square Centimeter

Acknowledgements

The CREMs Phase 3 model development project was a team effort. Monitoring conducted to support the modeling effort was led by LCRA. Ecological Communications Corporation provided support with data collection and quality control of the databases. Mimi Wallace and Richard Kiesling of the United States Geological Survey (USGS) conducted monitoring of algae in the system. Anchor QEA developed and calibrated the SWAT models of the watersheds of Lake LBJ and Lake Marble Falls, and the CE-QUAL-W2 model of Lake Marble Falls. Working closely with them, Parsons developed and calibrated the SWAT model of the Inks Lake watershed, and the CE-QUAL-W2 models of Inks Lake and Lake LBJ. LimnoTech, Inc. reviewed the modeling approaches and drafts of the final report. LCRA staff, including Lisa Hatzenbuehler, John Wedig, Bryan Cook, Dave Bass, Karen Bondy, Erik Harris, Jerry Guajardo, Susan Meckel, and Suzanne Zarling, provided guidance and feedback throughout the project.

SECTION 1 INTRODUCTION

1.1 Background

The Lower Colorado River Authority (LCRA) initiated development of mathematical models to support water quality management of the lower Colorado River system. This project, referred to as the Colorado River Environmental Models (CREMs) project, was designed to help diagnose existing water quality problems and issues, discern water quality trends, and predict the consequences of various management decisions and associated actions on the water quality of the Highland Lakes, lower Colorado River, and its tributaries. The modeling tools are being designed to provide the information needed by LCRA staff and management to support policy decisions that proactively and effectively protect the integrity of the water resources in the lower Colorado River basin.

The CREMs project has four phases. Phases 1 and 2 focused on Lake Travis, which was selected during the prioritization process described in the CREMs Master Plan (CH2M Hill 2002). Phase 3, which commenced in 2008, focuses on lakes Lyndon Baines Johnson (LBJ), Inks, and Marble Falls. The selection of Lake Travis for Phases 1 and 2 was based on the need to support the evaluation of the Lake Travis non-point source (NPS) pollution control ordinance and to address community questions regarding the effectiveness of the Texas Commission on Environmental Quality's (TCEQ) wastewater discharge ban (also known as the point source discharge ban or the Highland Lakes discharge ban). Phase 1 assessed Lake Travis water quality using existing data to develop a simplified model of the reservoir and watershed. Details on the Phase 1 work can be found in the Phase 1 Lake Travis Model Report (LCRA 2004). Phase 2 involved acquiring additional water quality data and developing refined watershed and water quality models of Lake Travis. Details on the Phase 2 work can be found in the CREMs Phase 2 Lake Travis Final Report (Anchor QEA and Parsons 2009). The fourth and final phase of the project will focus on Lake Buchanan.

1.1.1 Inks Lake System

Inks Lake is the second in a series of six reservoirs on the lower Colorado River known as the Highland Lakes. It is also the second smallest of the Highland Lakes. It was created by the construction of the Roy Inks Dam, completed in 1938. Inks Lake is a run-of-river reservoir impounded between Buchanan Dam and Roy Inks Dam. There are no floodgates on Inks Dam so the bulk of the floodwater passes over an uncontrolled spillway, although a small amount of water is released through turbines for hydroelectric power generation (TWDB 2007a). Inks Lake was built primarily for hydroelectric power generation, but also serves to provide drinking water and recreation for central Texas.

Inks Lake is considered full at an elevation of 888.53 feet (ft; 270.82 m) above mean sea level (NAVD 88), and its normal operating range is 887.21 to 888.01 ft (TWDB 2007a). Inks Lake holds 14,074 acre-feet (1.74×10^7 cubic meters [m^3]) of water when full and covers an area of 788 acres (3.19 square kilometers [km^2]). The main body of Inks Lake is only 4.3 river miles (6.8 km) long, from below Buchanan Dam to Roy Inks Dam. The reservoir is less than 0.1 miles (161 m) wide in the upper reaches of the lake, and widens to approximately 0.4 miles (640 m) at some points above Inks Dam. When the lake is full, the deepest point in Inks Lake

is more than 60 feet (18 m) below the water surface. The local contributing drainage area between Buchanan Dam and Inks Dam covers 24,600 acres (approximately 100 km²). Average annual precipitation in this local contributing drainage area is approximately 32 inches (TWDB 1998). In the Colorado River basin upstream of Inks Lake, average annual rainfall decreases to as little as 20 in (0.5 m) in the upper reaches of the basin in west Texas.

1.1.2 Lake LBJ System

Lake LBJ is the third in the series of six Highland Lakes on the lower Colorado River. It was created by the construction of the Alvin Wirtz Dam, completed in 1951. Lake LBJ was built primarily for hydroelectric power generation, but also serves to provide cooling water for the gas-fired steam electric Thomas C. Ferguson power plant, drinking water and recreation for central Texas. Originally, named Granite Shoals Lake, in 1965 it was renamed in honor of the 36th president of the United States.

Lake LBJ is considered full at an elevation of 828.68 ft (251.67 m) above mean sea level (NAVD 88), and its normal operating range is 825.08 to 825.68 ft (TWDB 2009). Lake LBJ holds 133,090 acre-feet (1.64 x 10⁸ m³) of water and covers an area of 6,273 acres (25.4 km²). The main body of Lake LBJ winds roughly 21 river miles (37 km) through the central Texas Hill Country, from below Inks Dam to Wirtz Dam. The reservoir is less than 0.1 miles (161 m) wide in the upper reaches of the lake, and widens to more than 0.8 miles (1,290 m) near Wirtz Dam. When the lake is full, the deepest point in Lake LBJ is more than 72 ft (22 m) below the water surface in the thalweg near Wirtz Dam. The local contributing drainage area between Wirtz Dam and Inks Dam covers approximately 3.2 million acres (13,000 km²). Average annual precipitation in this local contributing drainage area ranges from approximately 22 inches in the western reaches of the watershed to approximately 32 inches in the east (TWDB 1998).

1.1.3 Lake Marble Falls System

Lake Marble Falls is the fourth in a series of six reservoirs on the lower Colorado River known as the Highland Lakes. It is the smallest of the Highland Lakes and was created by the construction of the Max Starcke Dam (originally named Marble Falls Dam), completed in 1951. Lake Marble Falls is a run-of-river reservoir impounded between Wirtz Dam and Max Starcke Dam. Lake Marble Falls was constructed primarily for the production of hydroelectricity; however, it is also used as a source of water supply and recreation.

Lake Marble Falls is considered full at an elevation of 738.19 ft (225.04 m) above mean sea level (NAVD88), and its normal operating range is 736.39 to 737.19 ft (TWDB 2007b). Lake Marble Falls holds 7,486 acre-feet (9.23 x 10⁶ m³) of water when full and covers an area of 608 acres (2.46 km²) (TWDB 2007b). The main body of Lake Marble Falls is 5.75 miles (9.3 km) long, from below Wirtz Dam to Max Starcke Dam. Lake Marble Falls is 0.2 miles (329 m) at its widest point. When the lake is full, the deepest point is more than 60 ft (18 m) below the water surface in the thalweg near Max Starcke Dam. The local contributing drainage area between Wirtz Dam and Max Starcke Dam covers 50,400 acres (approximately 204 km²). Average annual precipitation in this local contributing drainage area is approximately 30 to 32 inches (TWDB 1998).

1.1.4 Relevant Ordinances

One of the primary missions of the LCRA is to ensure that water quality of the lower Colorado River tributaries and reservoirs will support fishing, swimming, and public water supply uses through monitoring, assessment, advocacy and regulatory oversight to protect against degradation of the lower Colorado River, its reservoirs, and tributaries. Reservoir and watershed management approaches to protecting Highland Lake water quality include TCEQ's ban on point source discharges and the LCRA's implementation of the Highland Lakes Watershed Ordinance (HLWO). Water quality modeling is critical to understanding important processes in the Highland Lakes relevant to protecting water quality and to evaluating the benefits provided by the TCEQ Highland Lakes discharge ban and HLWO.

1.1.4.1 TCEQ Highland Lakes Discharge Ban

In order to protect and maintain the existing water quality of the Highland Lakes, the Texas Water Commission (the predecessor to TCEQ) adopted regulations in October 1986 prohibiting new or expanded discharges of wastewater treatment plant (WWTP) effluent into the Highland Lakes or their tributaries within 10 stream miles of the lakes. Details of the discharge ban can be found in Chapter 311 of the Texas Administrative Code (Inks Lake in Subchapter B and Lakes LBJ and Marble Falls in Subchapter F).

1.1.4.2 Highland Lake Watershed Ordinance

The LCRA responded to the threat of pollution resulting from a construction boom around the Highland Lakes in the early 1990's with two NPS pollution control ordinances. In 2006 the two ordinances were revised into one, entitled the Highland Lakes Watershed Ordinance. The ordinance addresses pollution or storm water runoff and targets three key pollutants: total suspended solids, total phosphorus, and oil and grease. This ordinance applies to development in portions of Travis, Burnet and Llano Counties that drain to the Highland Lakes. The HLWO is a performance-based ordinance, which means that developers and landowners must show that the standards will be met before proceeding with a project. The ordinances apply to all new construction; property that was platted before the ordinance went into effect is exempt.

1.2 Summary of the Phase 1 Effort

The principal objective of the Phase 1 Lake Travis modeling effort was to develop a tool to project long-term and large-scale water quality impacts associated with changes in watershed land use. The watershed model was a derivative of PLOAD (see BASINS documentation for an explanation of PLOAD; U.S. Environmental Protection Agency [USEPA 2001]) and used simplified approaches to estimate watershed hydrologic and pollutant loadings. The reservoir model consisted of a custom, nine-segment model that simulated nitrogen, phosphorus, and chlorophyll-a dynamics in a simplified kinetic framework (LCRA 2004).

The Phase 1 data analysis and modeling effort provided the following insights into the Lake Travis system:

- Data:
 - the Phase 1 dataset has limitations with regard to model development (e.g., lack of storm event data, on-lake wind information, light attenuation measurements,

- phytoplankton speciation, phytoplankton photosynthesis and respiration data, and cove, metalimnion, and phytoplankton bloom data);
 - low concentrations of nutrients and phytoplankton (many below the method detection limits) complicate the discernment of spatial and temporal trends;
 - certain land use types and areas disproportionately contribute to NPS loadings;
 - additional monitoring data were necessary to support the Phase 2 modeling effort.
- Model:
 - upstream source loads are important water quality drivers;
 - the Phase 1 model was not sufficiently refined to detect temporally and spatially localized water quality impacts of existing nutrient loads;
 - nutrient limitations to phytoplankton growth are important; and
 - Lake Travis experiences both nitrogen and phosphorus limitations, as well as co-limitation.

The Phase 1 model can be used to predict long-term, system-wide changes in phytoplankton concentration as a result of changes in land use. However, it cannot be used to predict changes in the duration, extent, and severity of phytoplankton blooms, nor can the Phase 1 model discern what is occurring in the coves of Lake Travis. Algal blooms within the coves are potentially more important to stakeholders than overall average phytoplankton concentrations, as the public strongly associates blooms with degradation of water quality and impairment of recreational opportunities. Hence, while the Phase 1 modeling effort provided valuable insights into the relationships between watershed land use changes and Lake Travis water quality as well as preliminary quantification of hydrologic and nutrient budgets, it lacked the spatial resolution to define localized water quality impacts of potential watershed land use changes. The Phase 2 and Phase 3 modeling efforts were designed to address these shortcomings.

1.3 Objectives of the CREMs Phase 2 and 3 Effort

The principal goal of the Phase 2 modeling effort was to develop a comprehensive, linked watershed and water quality modeling tool of the Lake Travis system. The principal goal of the Phase 3 modeling effort was to develop comprehensive, linked watershed and water quality modeling tools for Inks Lake, Lake LBJ, and Lake Marble Falls. The models will ultimately be applied to investigate system responses (both lake and watershed) to projected growth and/or proposed water quality management practices. Specifically, the Phase 2 and 3 models were developed to:

- evaluate the effectiveness of the HLWO in protecting water quality in the Highland Lakes;
- assess the effectiveness of the TCEQ point source discharge ban in protecting water quality in the Highland Lakes;

- identify and quantify trends in specific water quality indicators (long-term, seasonal, and short-term);
- quantify differences in water quality between the main body of lakes and their coves;
- evaluate the impacts of land use changes on the quality and quantity of runoff and resulting impacts on the lakes and watersheds;
- assess the impacts of existing point source discharges on the water quality of the Highland Lakes;
- evaluate the relative contribution of anthropogenic and natural background sources of nutrients to observed water quality trends;
- predict the impacts of various basin-wide best management practice (BMP) implementation strategies;
- identify tributaries with the highest nutrient loadings;
- evaluate water quality trends with respect to drinking water source issues;
- assist in the regulatory establishment of nutrient standards;
- expand competency of internal LCRA staff with respect to watershed and water quality management and modeling issues; and
- identify and guide potential future water quality protection and restoration projects on the Highland Lakes.

Various LCRA business units have established many of these issues as high priority items, as documented in the CREMs Master Plan (CH2M Hill 2002). As such, the Phase 2 and Phase 3 models are valuable tools for providing information to guide management decisions that are central to the LCRA's mission statement and operational goals. In the short term, the priority application of the models was to understand the effects of the HLWO and TCEQ's Highland Lakes Discharge Ban on water quality (see Anchor QEA and Parsons [2009] for a discussion of the predicted water quality impacts should these two policies change), although these other long-term objectives were considered throughout model development and application.

1.4 Overview of the Phase 3 Report

The purpose of this report is to provide a detailed description of the Phase 3 program, including monitoring and model development and calibration. The ultimate goal of the Phase 3 CREMs effort is to develop tools that the LCRA can use to aid in the management of their reservoirs and address many of the specific objectives outlined in Section 1.3. To reach that goal, steps undertaken in this Phase 3 effort included:

1. conducting increased sampling to aid in the development and calibration of the modeling tools and in the understanding of the Inks Lake, Lake LBJ, and Lake Marble Falls systems;
2. developing comprehensive, linked watershed and water quality modeling tools of the Inks Lake, Lake LBJ, and Lake Marble Falls systems; and
3. evaluating the sensitivity of Inks Lake, Lake LBJ, and Lake Marble Falls to different changes on the watershed, including the impact of land use changes and possible

introductions of point source dischargers on the lake (discussed in a separate document).

This report is divided into four additional sections. Section 2 overviews the Phase 3 sampling efforts, including sampling conducted by the LCRA and the USGS. Sections 3 and 4 discuss the model development and calibration for the watershed and water quality models, respectively. Finally, Section 5 provides a summary of the work.

SECTION 2 MONITORING PROGRAM

2.1 Overview

The purpose of the Phase 3 monitoring effort was to develop a more complete dataset for supporting the development and calibration of the Inks Lake, Lake LBJ, and Lake Marble Falls watersheds and water quality models. The Phase 3 monitoring supplemented the existing data record (and existing monitoring program) by providing information to develop and calibrate a more complex model of these lakes and their surrounding watersheds. For Phase 3, four monitoring programs were designed and implemented: 1) expanded routine monitoring; 2) storm event monitoring; 3) special remote monitoring studies; and 4) special manual sampling studies. Each program started in 2007 and ended before the development and calibration of the Phase 3 models, with varying durations of each monitoring program. Details of each monitoring program are presented in this section.

2.2 Program 1: Expanded Routine Monitoring

The Phase 3 ambient sampling and analysis program was an expansion of the current Reservoir and Stream Sampling (RSS) program, which provides a long-term record and satisfies LCRA and state requirements independent of the CREMs program. From 1982 to the early 1990's, data were collected monthly in the LCRA basin through the RSS program. The existing RSS program includes collection of water samples and field data at four stations in Lake LBJ, and two stations each on Inks Lake and Lake Marble Falls every other month (Figure 2-1). Additionally, field parameters are measured at two other stations in Lake LBJ. Water samples and field data are also collected at two stations at the model boundaries (the Llano River and the headwaters of Lake Travis). Similar to the existing RSS program, the expanded routine monitoring program was limited to regularly scheduled sampling (i.e., it did not target high flow events). Specific components of the expanded monitoring included measuring additional parameters, increasing the sampling temporal resolution at the boundaries (weekly) and in the lakes (monthly), and sampling additional stations in the lake and tributaries. The expanded routine monitoring program started in January 2007 and ended in June 2009 after which the existing RSS program resumed.

As part of CREMs Phase 3, data were collected at two additional sites within Lake LBJ and three sites within its tributaries (Figure 2-1). Table 2-1 lists sampling stations that were monitored during Phase 3. These additional sites are discussed in Section 2.2.4 and 2.2.5.

Throughout this monitoring program, the reservoir stations were sampled at the top (0.3 m below the water surface) and bottom (1 m above the sediments) of the water column, as the existing protocols state. In addition, when a defined thermocline was present, an additional water quality sample was collected at that location (Section 2.2.7). Tributary stations were sampled once at mid-depth.

Table 2-1 Program 1 – RSS and Expanded RSS Monitoring Locations

Site	Site ID ⁴	RSS	Expanded RSS	Number of Sampling Events (during the Phase 3 monitoring period; 2007-2009)
LAKE				
Lake Marble Falls at Max Starcke Dam	12319	x		29
Lake Marble Falls at Headwaters	12323	x		130
Lake LBJ at Wirtz Dam	12324	x		29
Lake LBJ at Horseshoe Bay Cove	LC915		x	29
Lake LBJ near Granite Shoals	12327	x		29
Lake LBJ in Sandy Creek Arm	12328		x	29
Lake LBJ near Kingsland	12330	x		29
Lake LBJ at FM 2900	12331	x ¹		29
Lake LBJ at 30° 50"	12333	x ¹		29
Lake LBJ at Headwaters	12335	x		129
Inks Lake at Inks Dam	12336	x		29
Inks Lake at Headwaters ²	12343	x		131
BOUNDARY				
Lake Travis at Headwaters	12318	x		127
Llano River at FM 3404	12383	x		127
TRIBUTARY				
Walnut Creek	LC917		x	24
Sandy Creek	12214	x		110
Honey Creek	LC918		x	28
Slick Rock Creek	LC916		x	30

Notes:

¹. Field parameters measured only.

². Site is considered a boundary site for this report, but is also considered to be within the main lake.

³. Lake and tributary sites sampled monthly; boundary sites sampled weekly. Sampling frequency at Inks Lake at Headwaters, Lake LBJ, Lake Marble Falls and Lake Travis increased to weekly during Phase 3.

⁴. See Figure 2-1 for map of monitoring locations.

2.2.1 Expanded List of Parameters

2.2.1.1 Laboratory Parameters

Two laboratory parameters, dissolved organic carbon and dissolved phosphorus, were added to the suite of parameters being analyzed under the routine monitoring program (Table 2-2). These were added so that the dynamics between the particulate and dissolved forms of organic matter could be defined better within the lake model. Ideally, particulate organic carbon and particulate nitrogen would also be measured directly (particulate phosphorus is difficult to measure directly), but due to limited resources, their concentrations were calculated as the difference between the measured total and measured dissolved concentrations. For the measurement of dissolved constituents, filtration followed the procedures outlined in Standard Methods (American Public Health Association [APHA] 1998). The data were reported as low as the method detection limit (MDL), which varies for each laboratory calibration of the analytical instrument (Table 2-2).

Table 2-2 Program 1 – List of Parameters for Expanded RSS Sampling

Parameter ^{1,2}	STORET Code	Units	Detection or Precision
MEASURED IN FIELD			
Light extinction	L1001	$\mu\text{mol s}^{-1} \text{m}^{-2}$	0.4%
Oxygen, dissolved	00300	mg/L	0.20
Oxygen, % saturation	00301	%	-
pH	00400	SU	0.20
Secchi depth	00078	m	-
Solar radiation (total)	-	Wm^{-2}	-
Specific conductance	00094	$\mu\text{S/cm}$	1%
Temperature, air	00020	°C	0.20
Temperature, water	00010	°C	0.05
Turbidity	82078	NTU	1%
Wind direction	L1003	°	-
Wind speed	L1002	mph	-
MEASURED IN LABORATORY			
Alkalinity, total	00410	mg/L	0.32
Chloride	00940	mg/L	0.08
Chlorophyll-a	70953	$\mu\text{g/L}$	0.02
Ammonia, nitrogen	00610	mg/L	0.005
Nitrite plus nitrate, nitrogen	00630	mg/L	0.004
Organic carbon, dissolved	00681	mg/L	0.03
Organic carbon, total	00680	mg/L	0.03

Parameter ^{1,2}	STORET Code	Units	Detection or Precision
Pheophytin	32113	µg/L	0.5
Kjeldahl nitrogen, dissolved	00623	mg/L	0.006
Kjeldahl nitrogen, total	00625	mg/L	0.006
Phosphorus, dissolved	00666	mg/L	0.005
Phosphorus, ortho	00671	mg/L	0.005
Phosphorus, total	00665	mg/L	0.005
Sulfate	00945	mg/L	0.02
Suspended solids, total	00530	mg/L	0.5
CALCULATED			
Dissolved solids, total	70952	mg/L	-
Nitrogen, particulate	-	mg/L	-
Organic carbon, particulate	-	mg/L	-
Phosphorus, particulate	-	mg/L	-

Notes:

¹ Parameters added in Expanded RSS shown in bold italics.

² Bacteria were collected only in even months to support routine monitoring.

³ The MDL for each laboratory analyte may vary each time the analytical instrument is calibrated.

2.2.1.2 Additional Field Parameters

Three field parameters – solar radiation, wind direction, wind speed – were added to the suite of parameters measured under the routine monitoring program (Table 2-2). Concentrations for one additional parameter, total dissolved solids, were calculated from the lake specific relationship with specific conductance developed by LCRA.

Solar radiation controls photosynthesis and the temperature cycle of the lake and is a forcing function for the hydrodynamic and water quality calculations in the lake model. Light penetration must also be known and is described by two factors: 1) the fraction of light absorbed/reflected in the surface layer; and 2) the light extinction through the water column. Both of these were measured using a light probe (e.g., the LCRA’s Li-Cor LI-189 probe). Light was measured above the water surface, immediately below the water surface (at 0.33 m depth), and at one meter intervals through the water column down to 10 m concurrently with samples collected in the reservoir (solar radiation data were not needed in the tributaries).

Due to the importance of wind speed and direction on mixing in the lakes, wind data were obtained concurrently with all field samples. This allowed for a point estimate of wind conditions at the time of sampling. These measurements provided information on spatial wind patterns and sheltering over the reservoirs and helped to decrease the uncertainty in specifying wind energy at the lake surface. Wind data were collected with a portable field sensor at 2 m above the water surface concurrently with all water samples collected in the reservoir (collection of wind data in the tributaries was not needed).

2.2.2 Higher Resolution Sampling at Boundaries

Weekly sampling was implemented at each boundary location (Table 2-1).

2.2.3 Higher Resolution Sampling in the Lake

To improve the characterization of water quality in the reservoirs, the sampling frequency was increased from bimonthly to monthly at all non-boundary stations. This allowed for a more complete understanding of seasonal trends in water quality throughout the lakes.

2.2.4 Additional Lake Stations

In Lake LBJ, two new lake sampling stations were added to the program (Table 2-1). Both of these sites were located in different coves of the lake (Horseshoe Bay Cove and the Sandy Creek Arm). Data from these stations facilitated the quantification of water quality in previously unsampled areas of the lake and improved the resolution for calibration of the lake model. For each of these stations, water samples were collected and analyzed for the expanded suite of water quality parameters (Table 2-2) on a monthly basis, in tandem with the other sampling on Lake LBJ.

2.2.5 Additional Tributary Stations

To improve the quantification of base flow loadings to Lake LBJ, the following four tributary stations were added to the sampling program: Slick Rock Creek, Sandy Creek, Walnut Creek, and Honey Creek. The locations of these stations were upstream of the Lake LBJ pool, but as far downstream as practicable, given accessibility and flooding constraints. Because these stations were also used as storm event sampling stations (discussed in Section 2.3), they needed to be positioned in areas where they could be safely accessed and protected from loss (vandalism, flooding, etc.).

Sandy Creek and Honey Creek had an existing stream gauge at the sampling location. Walnut Creek was sampled below its stream gauge during ambient collection, and at the stream gauge during storm water collections. Slick Rock Creek was not gaged, so estimates of flow were recorded at each sampling event. Monthly sampling included the expanded suite of water quality parameters (Table 2-2).

2.2.6 Expanded Vertical Sampling

The routine monitoring program was expanded to include metalimnion sampling. The metalimnion field data were collected by first identifying the depth at which a 0.5 °C or greater temperature change was measured over a one meter depth interval. A sample of the water in the metalimnion was collected one meter below this point.

2.2.7 Lower Detection Limits

For a number of water quality parameters, lower MDLs were applied to the Phase 3 monitoring programs compared to those used historically. This was done to facilitate temporal and spatial trend analysis and to support lake model calibration. Table 2-2 contains the parameter specific MDL.

2.3 Program 2: Storm Water Monitoring

Storm loadings in flood prone areas such as central Texas can account for a large percentage of the total annual loading to a water body. Such loadings are difficult to quantify due to their transient nature and the level of effort required for collecting samples. Due to the lack of historical storm event data on the reservoirs, such sampling comprised a significant portion of the Phase 3 monitoring effort. Table 2-3 lists the storm monitoring locations and the number of monitoring events.

Table 2-3 Program 2 – Storm Monitoring Locations and Number of Monitoring Events

Site	Site ID ¹	Number of Storm Monitoring Events ²
LAKE		
Lake Marble Falls at Max Starcke Dam	12319	3
Lake Marble Falls at Headwaters	12323	6
Lake LBJ at Wirtz Dam	12324	5
Lake LBJ at Horseshoe Bay Cove	LC915	5
Lake LBJ near Granite Shoals	12327	5
Lake LBJ in Sandy Creek Arm	12328	5
Lake LBJ near Kingsland	12330	5
Lake LBJ at FM 2900	12331	5
Lake LBJ at 30° 50"	12333	5
Lake LBJ at Headwaters	12335	7
Inks Lake at Inks Dam	12336	1
Inks Lake at Headwaters	12343	4
BOUNDARY		
Lake Travis at Headwaters	12318	4
Llano River at FM 3404	12383	8
TRIBUTARY		
Walnut Creek	LC917	5
Sandy Creek	12214	7
Honey Creek	LC918	7
Slick Rock Creek	LC916	6

Notes:

¹ See Figure 2-1 for map of monitoring locations.

² Multiple monitoring events happened during a single storm.

2.3.1 Storm Types and Sampling Frequency

From January 2007 to June 2009, storm event monitoring captured two types of storms – Type 1 and Type 2. Type 1 storms were defined as small events producing localized runoff over a small time scale. Only the affected tributaries and coves were sampled, as no lake-wide impacts were expected. Type 2 storms were those that were expected to affect most of the lakes’ watersheds and had the potential to produce substantial in-lake changes in water quality because of the large runoff volume. As summarized in Table 2-4, seven Type 1 and one Type 2 storm events were captured.

Table 2-4 Program 2 - Summary of Storm Sampling

Storm Type	Storm Start Date	Storm Duration (hours)	Approx. Total Rainfall (inches)	Number of Stations Monitored		Number of Samples Collected Over All Stations
				Tributary	Lake	
2	3/12/2007	7	4.3	6	12	47
1	5/24/2007	14	2.9	5	0	53
1	6/3/2007	4	2.1	5	0	17
1	6/16/2007	5	1.6	5	1	56
1	7/2/2007	14	3.0 ¹	5	8	28
1	8/17/2007	12	1.6	2	0	12
1	9/5/2007	10	1.3	3	0	10
1	3/12/2009	14	4.1	2	4	6

¹An 18 inch very localized rain event impacted the area.

Sampling of each storm type followed a different protocol. During a Type 1 storm, only tributaries and coves impacted by the storm were sampled. Sampling occurred at 12-hour intervals for the first day. The impacted tributaries were sampled daily for the next four days. During a Type 2 storm, sampling in coves occurred daily for the first four days and at seven and 14 days following the triggering event. Sampling in tributaries took place daily for the first five days and also seven and 14 days after the storm began.

Starting in January 2007, tributary sampling was initiated based on a prescribed change from base flow that is characteristic of storm events. Immediately after the trigger level was reached, automated samplers were programmed to collect first flush samples followed by hourly discrete samples. Only two of the four tributary locations were equipped to collect storm water samples automatically. On the stations equipped with automatic samplers, first flush samples followed by hourly discrete samples were collected. At sites without automated equipment, grab samples were collected once daily – as near to first flush as possible and each subsequent 24 hours after. In addition, meteorological conditions (a major flood event occurred in June 2007, followed by a drought in 2008 and 2009) resulted in the sampling of essentially all rainfall events greater than one inch.

2.3.2 Tributary and Lake Stations

Tributary sampling stations for the storm event monitoring program were co-located with the four tributary monitoring locations in the expanded routine monitoring program described in Section 2.2.5. On two of these (Sandy Creek and Walnut Creek), sampling was performed using an ISCO® automated sampler as well as via grab sampling at boundary locations. This allowed for a comparison between storm and base flow data. The two other tributary locations (Honey Creek and Slick Rock Creek) were monitored through grab sampling. Tributary samples were analyzed for the expanded suite of water quality parameters (Table 2-2).

Lake samples (both cove and main body) were collected manually during storm events and were analyzed for the expanded suite of water quality parameters (Table 2-2).

2.4 Program 3: Remote Monitoring

Remote monitoring using automatic sampling devices collected data in a continuous manner over time, which is otherwise difficult to accomplish by field teams. The objective of this sampling program was to provide detailed data for the lake model calibration.

Remote data collection equipment was deployed at selected locations to serve a number of purposes. These purposes included helping in the calibration of the Phase 3 models; quantifying the short-circuiting of flood flows and plunging of inflows; measuring stratification and mixing; providing an early warning system to identify algal blooms; and quantifying the occurrence, duration, and intensity of algal blooms. The two types of remote monitoring units used were thermistor chains and an automated profiler.

2.4.1 Thermistors and Thermistor Chains

Thermistors measure water temperature and were deployed at multiple depths in the water column. One thermistor or thermistor chain was installed at each of the stations listed in Table 2-5. Most of the devices were installed at the beginning of Phase 3 sampling and were left in place for the duration of the monitoring program. The units measured temperature every two meters at Horseshoe Bay Cove in Lake LBJ. At the other stations, only surface temperature was measured. The chains measured temperature each hour. Unfortunately, thermistors at several locations were lost due to entanglement with lake debris and storm events, particularly the July 2007 rain event. Unfortunately, because of the lack of confidence in the data collected by the automated profilers due to instrumentation issues, some data collected by the automated profilers were not used in the lake model calibration.

Table 2-5 Program 3 - Summary of Remote Sampling

Site	Site ID ¹	Vertical Spacing (m)	Average Water Depth at Site (m)	Number of Thermistors per Chain
Lake LBJ at Horseshoe Bay Cove	LC915	2	12	6
Inks Lake Headwaters	12343	-	2	1
Lake LBJ Headwaters	12335	-	3	1
Slick Rock Creek	LC916	-	1	1

Site	Site ID ¹	Vertical Spacing (m)	Average Water Depth at Site (m)	Number of Thermistors per Chain
Walnut Creek	LC917	-	1	1
Lake Marble Falls Headwaters	12323	-	1	1

Notes:

¹ See Figure 2-1 for map of monitoring locations.

2.4.2 Automated Profilers

Automated profilers are remotely programmable field stations with probes suitable for measuring standard field parameters as well as chlorophyll-a and turbidity. These systems are also capable of sampling a vertical profile through the water column, not just at a fixed depth. One automated profiler was installed for this monitoring program, near Wirtz Dam on Lake LBJ. It was established to provide information on flow patterns at the dam; stratification, thermocline development, and turnover; oxygen consumption in the hypolimnion; and diurnal fluctuations of dissolved oxygen and pH. The automated profiler measured a full vertical profile (every meter) of field parameters, including chlorophyll-a, generally every day from January 2007 to May 2008. Unfortunately, because of the lack of confidence in the chlorophyll-a and turbidity data collected by the automated profilers due to instrumentation issues, these data were not used in the lake model calibration.

2.5 Program 4: Special Manual Monitoring

To further constrain the lake water quality models, special manual field and laboratory studies were conducted. Special manual sampling for Phase 3 consisted of a phytoplankton investigation study.

2.5.1 Phytoplankton Investigation Study

The USGS conducted a phytoplankton investigation in each lake between April 2007 and June 2009. Surface water plankton was collected on a monthly basis from the dam monitoring stations on each reservoir. Phytoplankton composition and abundance and phytoplankton nutrient-dependent growth rates were investigated. Algal grazing rates by zooplankton were also measured using bioassays. Methods are described in Appendix B of the CREMs Phase II report (Anchor QEA and Parsons 2009).

THIS PAGE INTENTIONALLY LEFT BLANK

SECTION 3 WATERSHED MODEL

Section 3 describes the watershed models developed during Phase 3 of the CREMs project for the Inks Lake, Lake LBJ, and Lake Marble Falls watersheds (Figure 3-1). The introduction presents a general outline of the Soil and Water Assessment Tool (SWAT) watershed modeling software (Arnold et al. 1998), the model state variables of concern, the model input and development, and the model calibration procedures applicable to all three watersheds. Three sub-sections specific to the Lake LBJ, Lake Marble Falls, and Inks Lake watersheds follow the introduction. These sub-sections describe the spatial domain, data considerations, model development, and model calibration procedures and results particular to a given watershed.

3.1 Introduction

The reservoir management tool developed during Phase 3 of the CREMs project consists of hydrodynamic and water quality models of Inks Lake, Lake LBJ, and Lake Marble Falls based on the United States Army Corps of Engineers (USACE) CE-QUAL-W2 model (lake models). To effectively apply the lake models for the current and future management of the basin, tributary loadings and direct runoff under potential watershed scenarios need to be predicted. This was accomplished through the development and calibration of mathematical models of the Inks Lake, Lake LBJ, and Lake Marble Falls watersheds. The watershed modeling software selected for the CREMs project is SWAT2005 (Neitsch et al. 2005), which is the version of SWAT used to model the Lake Travis watershed in Phase 2 of the CREMs project (Anchor QEA and Parsons 2009). SWAT simulates watershed hydrology and constituent loads and accounts for various land-cover types, land uses, and management practices. The watershed model can predict changes in constituent loads to its respective lake arising from changes in land use and practices within the watershed, and thereby provides a mechanism to tie activities in the watershed to resultant water quality in the lake.

A full description of SWAT and its simulated processes can be found in Neitsch, et al. (2005). Selection of SWAT as the modeling platform for the Lake Travis watershed as well as a description of SWAT model theory, structure, and operation as they pertain to the CREMs project are described in the Phase 2 Lake Travis Final Report (Anchor QEA and Parsons 2009). Due to the success in application of this software for modeling the Lake Travis watershed, the same software was applied in Phase 3. The SWAT executable developed for ArcSWAT 2.0.0 (build 1420) was used. ArcSWAT is an ArcGIS extension and a graphical user input interface for SWAT (Di Luzio et al. 2002).

3.1.1 State Variables of Concern and Model Timestep

The primary purpose of the SWAT models developed for CREMs is the calculation of watershed loads to be applied to the receiving water models, in this case the CE-QUAL-W2-based lake models. As a result, the state variables chosen for simulation in SWAT reflect the needs of the lake models. State variables simulated in SWAT to be passed to the lake models include:

- flow
- total suspended solids (TSS)

- organic phosphorus (OrgP)
- orthophosphorus (PO₄-P [aka minP in SWAT])
- total phosphorus (TP)
- organic nitrogen (OrgN)
- ammonia (NH₄-N)
- nitrate+nitrite (NO_x-N)
- total nitrogen (TN)
- dissolved oxygen (DO)
- carbonaceous biological oxygen demand (CBOD)
- chlorophyll-a (chl-a)

A daily timestep was employed with SWAT over the modeling period extending from 1984 through 2008, which is the period that was chosen to simulate water quality for the lake models. SWAT was run for an additional four-year period from January 1, 1980 through December 31, 1984 to provide a four-year “spin-up” time for the model to equilibrate initial model conditions.

3.1.2 Model Input and Development

3.1.2.1 Geospatial Input Data and Hydrologic Response Unit Generation

In SWAT, a watershed is divided into multiple sub-watersheds, which are then further subdivided into hydrologic response units (HRUs) that consist of homogeneous slope, land cover, and soil characteristics. Watershed delineation techniques using the 2002/2004 10-meter USGS National Elevation Dataset (NED) were employed to delineate each lake’s drainage basin. The NED was also used to calculate the slopes and determine the stream network incorporated into SWAT. Slopes were divided into five categories: 0-5, 5-10, 10-30, 30-60, and >60 %. Finally, multiple sub-watersheds were delineated using the NED and user-specified sub-watershed outlet points on the stream network (pour points). HRU generation for each sub-watershed was completed based upon the spatial intersection of the slope categories with the 2001 Multi-Resolution Land Characteristics Consortium National Land Cover Dataset (NLCD) and the National Resource Conservation Service (NRCS) State Soil Geographic (STATSGO) soil database.

3.1.2.2 Climatic Temporal Input Data

Climatic inputs used in SWAT include measured and/or generated records of precipitation, maximum and minimum temperature, solar radiation, relative humidity, and wind speed. Precipitation and temperature data were available for all three watershed models from proximal weather stations from the Texas A&M (TAMU) AgriLIFE Research Center and the National Climatic Data Center (NCDC). Solar radiation, relative humidity, wind speed, and missing precipitation or temperature records were created using the SWAT U.S. database weather generator as needed (Neitsch et al. 2005). The CREMs Phase 2 Lake Travis report (Anchor QEA and Parsons 2009) contains a more detailed description of generated climatic data as they pertain to CREMs SWAT models.

3.1.2.3 Point Source Dischargers

Model inputs for point sources existing within each watershed were developed from the TCEQ's Discharge Monitoring Report (DMR) records for permitted dischargers. Loads were either assumed based on values used in CREMs Phase 2 (Anchor QEA and Parsons 2009), at permitted values, DMR values if available, or estimated based on wastewater treatment plant outfall water quality data collected as part of the 2004 and 2005 LCRA-San Antonio Water System Water Project low-flow surveys (QEA 2004 and 2005).¹

3.1.3 General Description of Calibration

Calibration of a model consists of adjusting input parameters so that the model accurately reproduces trends in observed data. While the model calibration time period was from the start of 1984 through the end of 2008, model-to-data comparison at any particular location depended on data availability during this time period. A three-step calibration process was employed: the watershed hydrology calibration was performed, then the sediment load calibration, and finally, the nutrient load calibration. Calibration progressed in this stepwise manner because watershed hydrology drives constituent loading and sediment transport can impact nutrient loading.

For each of the three steps, final calibration parameter values were derived through iterative runs of the model while implementing small model parameter changes based on graphical and statistical evaluations of the model's agreement with measured data. Graphical evaluations were used in initial stages to approximate model fit for each calibration parameter. The predictive power of the model was evaluated based on calculated coefficient of determination values (R^2) and Nash-Sutcliffe model efficiency coefficient (NS) values (Nash and Sutcliffe 1970). NS measures how much better a model predicts observed values than the average of the observed values. A value of 1 indicates a perfect match, whereas a value of 0 or negative indicates that the model performs no better at predicting observed values than the average of the observed values. The NS is given more weight in model evaluation than the R^2 because NS describes the variability of the model output versus the data (accuracy) whereas R^2 describes the variability of the model output versus a regression line (precision). Finally, the percent difference between the sum of model output and the sum of the observed data over the period of data availability was also compared to evaluate model goodness of fit.

3.1.4 Calibration Data

Daily average USGS and LCRA Hydromet streamflow data were used for watershed model hydrology calibration. If a Hydromet gage was co-located with a USGS gage, the USGS gage data were used due to longer periods of record at those gages and for data consistency.

Water quality data collected as part of the LCRA CREMs and the extended LCRA Reservoir and Stream Sampling programs were used for watershed constituent load calibrations (see Section 2 of this report for a full description of these sampling programs). Constituent data used for watershed sediment and nutrient calibrations were:

¹ Average constituent concentration values from outfalls in the lower Colorado River Basin with measured discharge rates (range of 0.006 to 0.81 million gallons per day [MGD]) similar to the permitted discharge rates of outfalls in the three Phase 3 watersheds were used.

- TSS
- OrgP (calculated from data as TP minus PO₄)
- PO₄
- TP
- OrgN (Total Kjeldahl Nitrogen minus NH₄)
- NH₄
- NO_x (nitrate plus nitrite)
- TN (Total Kjeldahl Nitrogen plus NO_x)

Due to the low frequency of water quality data collection and the need for a continuous record for model calibration, an empirical model was developed to produce a continuous time-series to which the simulated time-series was compared for calibration. The USGS LOAD ESTimator (LOADEST; Runkel et al. 2004), a program for estimating constituent loads in streams and rivers, was used to develop watershed-specific constituent regression models (i.e., rating curves) for those tributaries where sufficient stream flow and constituent concentrations were available. Given paired stream flow and constituent concentration data, LOADEST develops a regression model for the estimation of the constituent loads. The use of LOADEST model output to calibrate a SWAT model is not optimal due to the propagation of model uncertainty. A discussion of the limitations of using a model to calibrate a model can be found in the CREMs Phase 2 Lake Travis (Anchor QEA and Parsons 2009) report. Despite these limitations, the use of a rating curve like that produced by LOADEST for water quality calibration is a viable and often used option when continuous time-series water quality data are not available (Gassman et al. 2007).

3.2 Lake LBJ Watershed

3.2.1 Lake LBJ Watershed Spatial Domain

The spatial extent of the Lake LBJ SWAT model is the drainage basin of the Colorado River from Roy Inks Dam to Alvin Wirtz Dam (Figure 3-2). Lake LBJ is a run-of-river reservoir impounded between these two dams. The Lake LBJ maximum capacity volume is approximately 134,000 acre-feet with a maximum capacity area of approximately 6,500 acres (LCRA 2009). The SWAT model was only required to simulate the watershed of Lake LBJ that either drains directly to the lake or drains to one of the tributaries of the lake because observed data taken at Inks Dam served as the upstream input to the Lake LBJ CE-QUAL-W2 model.

The Lake LBJ watershed area is approximately 3.2 million acres (13,000 km²) spanning the Edwards Plateau in the Texas Hill Country, including portions of the Llano Uplift. As shown on Figure 3-2, the majority of the modeled watershed comprises the Llano River and Sandy Creek watersheds, both of which enter Lake LBJ from the west. The Llano River watershed composes 90% of the total Lake LBJ watershed area, the Sandy Creek watershed composes 8%, and the remaining 2% of the watershed area drains directly to Lake LBJ.

3.2.1.1 Geology

Geological features in the Lake LBJ watershed directly and indirectly impact watershed hydrology and constituent loading. The Lake LBJ watershed comprises two main geologic regions (Figure 3-3). The Llano Uplift, which is a complex of Precambrian and Paleozoic igneous and metamorphic (crystalline) rocks, underlies approximately the lower half of the Lake LBJ watershed. Fracture systems in these crystalline rocks influence groundwater recharge and discharge patterns by providing preferential groundwater flow paths and, therefore, directly affect runoff and baseflow (Mace et al. 2004).

The western half of the watershed is underlain by karstified Cretaceous limestone. The limestone units are sub-horizontal, dipping slightly to the southeast, and contain features such as sinkholes and springs. Karst features provide groundwater preferential flow paths and thus, like the crystalline rock fracture systems, directly affect runoff and baseflow (Mace et al. 2004).

The geology of the Lake LBJ watershed also indirectly impacts watershed hydrology and constituent loading in that soil formation, type, and distribution, which directly impact watershed hydrology and constituent loads, are uniquely derived from the regional parent rocks. Also, soil type and climate determine the vegetative cover of a region. Vegetative cover, in turn, directly impacts watershed hydrology and constituent loads.

3.2.1.2 Climate

The Lake LBJ watershed is in a semi-arid environment that increases in precipitation from west to east. Average annual precipitation ranges from approximately 22 inches in the western reaches of the watershed to approximately 32 inches in the east (TWDB 1998) (Figure 3-4). Precipitation distribution directly affects vegetative cover formation as water-conserving brush and grasses dominate the western portion of the watershed and forest density gradually increases to the east.

Also, rainfall in the region generally occurs as intense convective or frontal thunderstorms followed by extended dry periods (Asquith et al. 2006). These thunderstorms result in ‘flashy’ hydrographs including many ephemeral streams that only flow in response to storm events (Asquith et al. 2006).

Precipitation data were available for input to the Lake LBJ SWAT model from 22 proximal meteorological towers (nine NCDC stations and 13 TAMU stations). Temperature data were available from 10 stations (three NCDC stations and seven TAMU stations) (Table 3-1, Figure 3-4). These time-series precipitation data were imported into the SWAT model along with the station coordinates and SWAT subsequently spatially distributed the precipitation throughout the basin (Neitsch et al. 2005).

Table 3-1 Meteorological Stations Used for the Lake LBJ SWAT Model

Station ID	Station Name	Source	Data Types
413954 06	Harper 1W	NCDC	P
417787	Round MTN 4WNW	NCDC	P

Station ID	Station Name	Source	Data Types
418531	Spicewood	NCDC	P
418863 06	Taylor Ranch	NCDC	P
418877 06	Teague Ranch	NCDC	P
419099	Tow	NCDC	P
414670 06	Junction 4SSW	NCDC	P, T
417232 05	Prade Ranch	NCDC	P, T
417706 06	Rocksprings	NCDC	P, T
410738	Bertram 3 ENE	TAMU	P
412040 06	Cottonwood	TAMU	P
413605 05	Gold	TAMU	P
414363 06	Humble Pump	TAMU	P
414402	Hye	TAMU	P
418897 05	Telegraph	TAMU	P
411250	Burnet	TAMU	P, T
413329 07	Fredericksburg	TAMU	P, T
414605	Johnson City	TAMU	P, T
415272	Llano	TAMU	P, T
415650 06	Mason	TAMU	P, T
415822 06	Menard	TAMU	P, T
418449 05	Sonora	TAMU	P, T

Notes: P = precipitation, T = temperature

3.2.1.3 Topography

The Lake LBJ watershed features rolling hills, which are the result of karst topographic formation and the variable erodibility of Llano Uplift formations. Watershed elevation ranges from 146 to 784 m above mean sea level (Figure 3-5). Slopes in the watershed ranged from 0 to 117% with 58% of the slopes in the 0-5% range, 28% in the 5-10% range, 13% in the 10-30% range, 1% in the 30-60% range, and <1% in the greater than 60% range.

3.2.1.4 Soils

As stated in Section 3.2.1.1, soil formation, type, and distribution are directly related to parent rock type (Figure 3-6). Soil types cross-cut topography in the Llano Uplift area due to the inherent heterogeneity of crystalline rock formations. Alternately, soil formation follows topography in the karst area where the rock formations are sub-horizontal and laterally extensive.

Also, as a part of Phase 2 of the CREMs project, LimnoTech, Inc. (LTI) examined the extent and characterization of Tarrant-series soil in the Pedernales River watershed. LTI reviewed available STATSGO and the Soil Survey Geographic Database (SSURGO) datasets to identify the extent of Tarrant-series soil, and also reviewed descriptions of the various soil series in these areas. Their evaluation concluded that the hydrologic soil group used in SWAT for the Tarrant series be changed from D to C, which increases the permeability of the soil. Because the Pedernales River watershed is adjacent to the Lake LBJ watershed, these changes were applied to the Tarrant-series soil in the Lake LBJ watershed. The LTI soil evaluation is fully described in Appendix C of the Phase 2 Lake Travis Final Report (Anchor QEA and Parsons 2009).

3.2.1.5 Land Cover

The Lake LBJ watershed is predominantly rural. Almost 80% of the watershed land cover is brush and grassland and 18.5% forest (Figure 3-7, Table 3-2). Less than 1% of the watershed is developed, although development is more intense near Lake LBJ (Figure 3-8). Development around the lake is noteworthy because runoff from direct drainage sub-watersheds can deliver urban pollution directly to the lake with minimal attenuation through the basin. Finally, both brush and deciduous forest occur at higher densities in the western karst area whereas grassland and evergreen forest are more common in the eastern crystalline rock area. Vegetation formation within the watershed is likely attributed to variations in both soil type and precipitation.

3.2.1.6 Watershed Ordinance

A portion of the Lake LBJ watershed is covered by the HLWO (Figure 3-9). The HLWO controls storm water runoff and enforces erosion controls to reduce pollution to the Highland Lakes (LCRA 2006). The Lake LBJ sub-watershed delineation, which is described in Section 3.2.1.8, accommodated the extent of the HLWO so that, if changes to HLWO regulations are considered in the future, the model scenario runs that address alternative watershed conditions can accommodate these changes.

3.2.1.7 Point Sources

There are eight permitted point sources in the Lake LBJ watershed (Figure 3-10). Four of the point sources are in sub-watersheds that drain directly to the lake and two are near the city of Junction. The remaining two are at the cities of Mason and Rocksprings. Permitted discharge flow rates were used for point source flows and ranged from 0.02 to 2.16 MGD (Table 3-3). The initial calibration was based on permitted flows for all 8 permittees in the Lake LBJ watershed. Since then, DMRs and additional information on land application permits has become available (as shown in Table 3-3). The calibration was re-run using self-reported average flows and zero constituent loads for land application discharges.

Table 3-2 Lake LBJ Watershed Land Cover

Name	Code	Area (acre)	Percent of Total Watershed Area
Open Water	WATR	9,647	0.30
Developed, Open Space	URLD	20,467	0.65
Developed, Low Intensity	URMD	4,730	0.15
Developed, Medium Intensity	URHD	1,714	0.05
Developed, High Intensity	UIDU	395	0.01
Barren Land	SWRN	341	0.01
Deciduous Forest	FRSD	175,083	5.53
Evergreen Forest	FRSE	406,177	12.83
Mixed Forest	FRST	346	0.01
Scrub/Shrub	RNGB	2,245,961	70.96
Grassland/Herbaceous	RNGE	283,006	8.94
Pasture/Hay	HAY	8,714	0.28
Cultivated Crops	AGRR	8,447	0.27
Woody Wetlands	WETF	251	0.01

Table 3-3 Permitted Discharger Flow and Concentrations in the Lake LBJ Watershed

Permit Number	Permittee	Permitted Flow ^a (MGD)	Average Flow ^d (MGD)	BOD5 (mg/L)	TSS (mg/L)	NH ₃ (mg/L)	TP (mg/L)	DO (mg/L)	PO ₄ (mg/L)	NO _x (mg/L)	TKN (mg/L)	OrgN (mg/L)	OrgP (mg/L)
0011217001	Lake LBJ MUD No. 1	1.50	0.0 ^e	5	10	2	3.2	4	3	20	2.5	0.5	0.2
0011332001	AquaSource Utilities ^f	0.03	0.02	2.0 ^b	1.9 ^b	2	1.0 ^b	5.9 ^b	1.0	20	2.5	0.13	0.01
0011549001	Kingsland MUD ^f	0.75	0.31	3.2 ^c	3.5 ^c	2	1.1 ^c	5.7 ^c	1.1	20	2.5	0.21	0.01
0013459001	Camp Longhorn Inc	0.02	0.0 ^e	5	10	2	3.2	4	3	20	2.5	0.5	0.2
0010199101	City of Junction	0.28	0.25	5	10	2	3.2	4	3	20	2.5	0.5	0.2
0010670001	City of Mason	0.42	0.17	5	10	2	3.2	4	3	20	2.5	0.5	0.2
0013490001	City of Rocksprings	0.13	0.11	5	10	2	3.2	4	3	20	2.5	0.5	0.2
001391000	Murpaks Inc.	2.16	0.75	5	10	2	3.2	4	3	20	2.5	0.5	0.2

Notes:

^a Permit limits provided by Susan Meckel of the LCRA (Meckel 2008; Meckel 2010)

^b Average of self-reported monthly average concentrations for Aquasource Utilities (Permit 0011332001) for the period April 2000 to December 2008

^c Average of self-reported monthly average concentrations for Kingsland MUD (Permit 0011549001) for the period February 1998 to December 2008

All other values estimated based on Low-Flow Survey data (QEA 2004 and 2005) discussed in Section 3.1.2.3.

^d Average of self-reported monthly average flows (1984-2008)

^e Land application permits- no direct discharge

^f AquaSource Utilities and Kingsland MUD discharge directly to Lake LBJ and are included in lake model, not the watershed model; they are shown here for informational purposes

3.2.1.8 Sub-Watershed Delineation

The Lake LBJ sub-watershed delineation accounted for the location of watershed calibration stations, the HLWO, and the Lake LBJ model segmentation. Pour points were co-located with hydrologic and water quality calibration stations so that model output at these points could be compared directly to calibration records. An attempt was made to locate pour points so that the majority of a defined sub-watershed area was either contained within or outside of the HLWO. As a result, specific sub-watersheds can be targeted in future scenario simulations that may involve changes to the HLWO. Also, pour points were added in order to facilitate the spatial linkage between output from the watershed model and input to the lake model (Figure 3-11). Finally, additional pour points were added, as needed, in order to break larger sub-watersheds into more manageable parcels. The sub-watershed delineation resulted in 78 sub-watersheds (Figure 3-12), and the intersection of the slope, land cover, and soil type resulted in 5,309 HRUs. The average HRU area was approximately 600 acres.

3.2.2 Lake LBJ SWAT Model Calibration

As mentioned previously in Section 3.1.3, a stepwise approach was used for the calibration of the Lake LBJ SWAT model starting with hydrology, then sediment loading, and finally, nutrient loading. All three calibration steps, unless noted otherwise, followed a “basin-wide” approach. In other words, identical flow and water quality calibration parameters were applied to identical HRUs (i.e., areas of the same soil type, land cover, and slope), regardless of the sub-watershed in which they were located.

3.2.2.1 Hydrology Calibration Data

Average daily flow data from six USGS gages and eleven LCRA Hydromet gages were available for the Lake LBJ watershed model hydrology calibration (Figure 3-12, Table 3-4). The flow data periods of record (POR) varied by station but, generally, the USGS flow gage PORs spanned the spin-up and calibration period of 1980 through 2008. Most of the Hydromet gages located in the Lake LBJ watershed came online from 1999 to 2001 with the earliest online in 1996.

The four primary hydrology calibration stations were the USGS Llano River near Junction (08150000), USGS Llano River near Mason (08150700), USGS Llano River near Llano (08151500), and USGS Sandy Creek near Kingsland (08152000) gages. Any data gap periods at the calibration stations were not used to calculate model calibration metrics. For example, the Sandy Creek near Kingsland gage was offline from April 1993 to October 1997 and thus no data were available for evaluating model fit at that gage during that time period.

Table 3-4 Lake LBJ Watershed Hydrologic Calibration Stations

Station Name	Station Number	Source	SWAT Sub-watershed Number	Contributing Area to Total Lake LBJ Watershed Area (%)	POR during Model Simulation Period	Average Monthly Flow Rate (cfs)
<i>Llano River near Llano</i>	<i>08151500</i>	<i>USGS</i>	<i>13</i>	<i>84</i>	<i>1980-2009</i>	<i>424</i>
<i>Llano River near Mason</i>	<i>08150700</i>	<i>USGS</i>	<i>32</i>	<i>70</i>	<i>1980-2009</i>	<i>312</i>
<i>Llano River near Junction</i>	<i>08150000</i>	<i>USGS</i>	<i>69</i>	<i>37</i>	<i>1980-2009</i>	<i>217</i>
North Llano River near Junction	08148500	USGS	61	18	2001-2009	46
<i>Sandy Creek near Kingsland</i>	<i>08152000</i>	<i>USGS</i>	<i>63</i>	<i>7</i>	<i>1980-2009</i>	<i>72</i>
Beaver Creek near Mason	08150800	USGS	37	4	1980-2009	21
James River near Mason	2399	Hydromet	40	7	1999-2009	22
Sandy Creek near Click	2878	Hydromet	64	6	2001-2009	53
Johnson Fork near Junction	2313	Hydromet	75	6	2000-2009	41
Hickory Creek near Castell	2498	Hydromet	19	3	2000-2009	24
Sandy Creek near Willow City	2851	Hydromet	54	3	1996-2009	38
San Fernando Creek near Llano	2616	Hydromet	8	3	1999-2009	29
Willow Creek near Mason	2443	Hydromet	12	1	1999-2009	5
Little Llano River near Llano	2669	Hydromet	1	1	1999-2009	7
Comanche Creek near Mason	2424	Hydromet	16	1	2000-2009	8
Honey Creek near Kingsland	2694	Hydromet	44	1	2002-2009	10
Walnut Creek near Kingsland	2897	Hydromet	68	<1	2001-2009	8

Note: Station names in bold italics indicate primary hydrology calibration stations.

3.2.2.2 Hydrology Calibration Approach

The hydrology calibration process focused on the two distinct geologic regions of the Lake LBJ watershed (Figure 3-3) due to their geographic location within the watershed and particular hydrogeologic behavior. Because soil type development is specific to a given parent rock (Section 3.2.1.1), model calibration could target each geologic region by applying parameter variations to their respective soil types. Soil type can be used in ArcSWAT to categorize calibration parameter variations because HRUs are partially defined by soil type. Therefore, the calibration process could target a specific geologic region and simultaneously maintain a basin-wide calibration approach.

The karst region of the watershed is upland of the crystalline rock area. As a result, the first step in the hydrology calibration process was to calibrate parameters in the karst region to data from the Llano at Junction gage, which has a contributing area composed entirely of karst area. Once the karst area of the watershed was calibrated to satisfaction, the karst area calibration parameter values were held static as the crystalline rock region parameters were calibrated to data from the Llano River near Mason, Llano River near Llano, and the Sandy Creek gages. These three gages have contributing areas composed of both karst and crystalline rock areas.

Table 3-5 lists the model parameters that were adjusted to calibrate the watershed hydrology in SWAT. The table briefly describes each parameter, identifies the major geologic region or sub-basin in which the parameters were changed, indicates the parameter location in the SWAT input files, and provides both the default and calibrated values. These values were derived through iterative runs of the model while implementing small changes in this suite of model parameters, based on both the graphical and statistical evaluations of the model's agreement with measured data. Discussion of these evaluations is presented in Section 3.2.3.1.

Several SWAT model groundwater calibration parameters proved particularly useful to improving model performance. Initial model simulations using the default values of the model calibration parameters overestimated total flow volumes by as much as 485% in a given month at the primary calibration gages (Figure 3-13). As a result, hydrologic sinks were needed in the model in order to reduce the amount of water available for runoff and baseflow. Losses to existing regional groundwater flow systems (calibration parameter RCHRG_DP) in both karst and crystalline rock areas were increased once the evapotranspiration parameters were set to values reasonable for the region's environmental conditions. The RCHRG_DP value represents the amount of water infiltrated to the subsurface that is lost to a groundwater system that transports water out of the watershed (i.e., regional or deep aquifer). RCHRG_DP was set at 55% in the karst area and 80% in the crystalline rock area. A localized groundwater flow component in the karst area contributes to spring discharge and baseflow within the watershed (Mace et al. 2004) and, therefore, the water loss in the karst area is less than that in the crystalline rock area.

Table 3-5 Lake LBJ SWAT Hydrologic Calibration Parameters

Parameter	Units	Description	Location in SWAT Input	Geologic Region or Sub-Basin	Calibrated Value	Default Value
CN2*	--	SCS curve number	**.mgt	Karst	RNGB-25%, Rest-15%	--
				Crystalline Rock	FRSE-22% (except no change to soil TX151), RNGB-30%, Rest-28%	--
GW_DELAY	day	Amount of time groundwater spends in the vadose zone	**.gw	Karst	365	31
				Crystalline Rock	0	31
RCHRG_DP	--	Percent of infiltrated water lost to a regional aquifer	**.gw	Karst	55%	5
				Crystalline Rock	80%	5
ALPHA_BF	day	Baseflow recession constant	**.gw	All	0.058	1
SOL_AWC*	mmH2O/ mmSoil	Soil available water content for plant uptake	**.sol	All	+0.04	--
SOL_K*	mm/hr	Soil saturated hydraulic conductivity	**.sol	All	-75%	--
ESCO	--	Evaporation coefficient	**.hru	All	0.5	1
EPCO	--	Uptake coefficient	**.hru	All	0.7	1
CH_K2	mm/hr	Channel effective hydraulic conductivity	**.rte	Llano at Junction	1.5	0
				Llano at Llano	1	0
				Sandy Creek	0.2	0

Notes:

'*' indicates that the value varies by HRU and was therefore increased or decreased by a percent or constant value.

'**' represents variable sub-watershed or HRU number contained in input file name.

Calibration parameters for open water land cover areas in .mgt, .sol, and .hru files were not changed from default values.

Another calibration parameter that proved useful was the channel hydraulic conductivity coefficient (CH_K2). The CH_K2 value is used to calculate simulated water loss from the stream channel. In this case, CH_K2 was used not only to simulate channel losses, but also to slow down the propagation of the water through the watershed when other parameters that perform that function – such as changes in slope, soil hydraulic conductivity, etc. – failed to slow the water enough. Without this function, the model stream network emptied during drier periods because the rainfall-produced surface runoff passed through the system too quickly. Increasing the CH_K2 value simulated water flow out of the channel and into the subsurface, at which point the model routed the water more slowly to a downstream location or was lost to the regional aquifer. Channel loss in karst areas is particularly common and recharged water may discharge back to the original stream, to a downstream water body, or to a regional aquifer system (Mace et al. 2004). CH_K2 was increased, but to a lesser degree, in the sub-basins underlain by crystalline rock (CH_K2 = 1 in sub-watersheds underlain by crystalline rock in the Llano River near Llano contributing area and CH_K2 = 0.2 in the Sandy Creek sub-basin) because the fracture system behaves like less efficient karst. Finally, CH_K2 was the only parameter for which the basin-wide calibration approach was not used because it is reasonable to assume that channel conditions vary by reach based on conditions particular to a given sub-watershed.

The process of channel water loss is illustrated in Figure 3-14, which shows Llano River flow data from Junction, Mason, and Llano (upstream to downstream) in 2006. Following storm events, the flow in the river increases from upstream to downstream, but during drier periods, the flow in the river can decrease from upstream to downstream. Also of note is that, even though the Llano River is a losing stream, the river is never dry. Conversely, smaller tributaries in both the karst and crystalline rock regions, as in many semi-arid environments, can be ephemeral (Mace et al. 2004).

By combining variations in the groundwater delay parameter (GW_DELAY) and the baseflow recession constant (ALPHA_BF) with the CH_K2 values, it was possible to provide constant baseflow to the larger stream networks.

3.2.2.3 Water Quality Calibration Data

CREMs and RSS water quality data collected from the early 1980s to 2008 near the four primary hydrology calibration gages were used for sediment and nutrient load calibrations (Figure 3-12). The stations, along with the nearby flow stations, are listed in Table 3-6.

Table 3-6 Lake LBJ Watershed Water Quality Calibration Stations

Station ID	Station Description	Proximal USGS Station Name	Approximate POR	Approximate Number of Days Sampled
12214	Sandy Creek at SH 71 South of Kingsland	Sandy Creek near Kingsland	1984-2008	299
12386	Llano River 0.4 miles downstream from bridge on SH 16 at Llano	Llano River near Llano	1984-2008	167
17470	Llano River 1.5 miles downstream of US 87 and 0.45 miles downstream of the confluence of Beaver Creek	Llano River near Mason	1999-2008	36
17471	Llano River at Hydromet station east of Junction	Llano River near Junction	1999-2008	36

Daily loads for each of the constituents were estimated for each of the four locations using the average, continuous daily flow data and the LOADEST rating curve predictions (Figure 3-15a-d). Table 3-7 presents the standard errors associated with the rating curve predictions for each station and constituent. These values are calculated in LOADEST and are provided in the LOADEST output file.

Table 3-7 Uncertainty Associated with Lake LBJ Watershed Rating Curve Predictions

Station	Parameter	Mean Load (kg/day)	Standard Error (kg/day)
Sandy Creek (12214)	TSS	17,756	2,597
	OrgN	165	22
	OrgP	30	3.8
	NO _x	22	1.8
	NH ₄	4	0.4
	PO ₄	4	0.5
	TP	32	4.1
Llano near Llano (12386)	TSS	42,133	14,455
	OrgN	596	121
	OrgP	119	46
	NO _x	2,334	1,190
	NH ₄	50	11
	PO ₄	19	5.9
	TP	94	25

Station	Parameter	Mean Load (kg/day)	Standard Error (kg/day)
Llano near Mason (17470)	TSS	37,282	28,539
	OrgN	226	79
	OrgP	35	0.8
	NO _x	6,115	7,537
	NH ₄	18	3.0
	PO ₄	--	--
	TP	41	0.6
Llano near Junction (17471)	TSS	15,565	12,965
	OrgN	363	267
	OrgP	16	8.5
	NO _x	3,527	2,000
	NH ₄	11	1.6
	PO ₄	--	--
	TP	19	9.0

Note:
 kg/day = kilograms per day

The water quality stations 12386 and 12214 were not co-located with flow gages but were near enough (within 1 mile) that flow proration was not required for generating LOADEST rating curves. A sufficient amount of PO₄ data for the LOADEST program to calculate a rating curve were only available near the Llano River near Llano and Sandy Creek near Kingsland stations.

3.2.2.4 Water Quality Calibration Approach

The sediment and nutrient load calibrations proceeded in much the same fashion as the hydrology calibration in that the karst area parameters were calibrated first followed by the crystalline rock area parameters. Table 3-8 lists the model parameters that were adjusted to calibrate the sediment and nutrient loads in SWAT. The parameter SLSUBBSN, which is the slope length for sheet flow, was adjusted during the sediment calibration process. Adjusting SLSUBBSN also affected the watershed hydrology but not to a degree that required hydrology recalibration. Mineralized P model output was used for PO₄ calibration because the majority of mineralized phosphorus is in the form of PO₄; NO₃+NO₂ model output was used for NO_x calibration; and the appropriate model species output were added together for TN (OrgN, NO_x, and NH₄) and TP (OrgP and PO₄) calibrations. OrgP, OrgN, and NH₄ are directly output from the model.

Table 3-8 Lake LBJ SWAT Water Quality Calibration Parameters

Calibration Type	Parameter	Units	Description	Location in SWAT Input	Calibration Value	Default Value
Sediment*	SPEXP	--	Sediment re-entrainment exponent	basins.bsn	1.5	1
	ADJ_PKR	--	Sub-basin peak rate factor	basins.bsn	1	1
	PRF	--	Channel peak rate factor	basins.bsn	0.6	1
	USLE_C	--	Land cover factor	crop.dat	0.001 for RNGB, RNGE	0.003
	HVSTI	--	Biomass harvest loss	crop.dat	0.1 for RNGB, RNGE, FRSE	0.9, 0.9, 0.76
	LAT_SED	mg/l	Discharge TSS Concentration	** .hru	Soils TX151 and TX327=5, Rest=10	0
	SLSUBBSN	m	Slope length for sheet flow	** .hru	SLSUBBSN*3	--
	USLE_K	Special	Soil erodibility factor	** .sol	0.1 for RNGB, FRSE	0.1-0.37
Nutrients	ISUBWQ	--	Subbasin water quality code	basins.bsn	0	0
	IWQ	--	In-stream water quality code	basins.bsn	0	0
	CMN	--	Humus mineralization factor	basins.bsn	0.0004	0.0003
	CDN	kg/ha	Denitrification exponential rate coefficient	basins.bsn	0.15	1.4
	SDNCO	--	Denitrification threshold water content	basins.bsn	0.6	1.10
	PSP	--	Phosphorus availability index	basins.bsn	0.69	0.4

Notes:

All parameter changes were made for the entire watershed.

DP - Dissolved phosphorus

'' indicates that the value is variable by HRU and was therefore increased or decreased by a percent or constant value.*

*'**' represents the variable sub-watershed or HRU number contained in input file name.*

SWAT allows for instream transformations and kinetics of algae growth, nitrogen and phosphorus cycling, CBOD, and DO to be performed on the basis of routines developed for the QUAL2E model (Brown and Barnwell 1987). This function can be turned on or off. Both options were tested, and turning off the instream processes provided the most appropriate model results for nearly all of the key parameters. In doing so, NH_4 is not modeled appropriately, and therefore model results for this parameter should not be used. As both modeled and real-world NH_4 levels are relatively small, the impact of NH_4 on the system is inconsequential.

3.2.2.5 Watershed Operations

As part of the constituent load calibration, watershed operations were added to the model in order to address land uses that can significantly impact watershed nutrient loads. Based on conversations with Dr. Raghavan Srinivasan, a professor at TAMU and one of the developers of ArcSWAT, appropriate grazing operations were added to grasslands of 0-10 slope (heat units = 0.45, consecutive grazing days = 180, consumed biomass = 5 (kg/ha)/day, and dry weight of daily deposited manure = 2 (kg/ha)/day) (Srinivasan 2009).

3.2.3 Lake LBJ SWAT Model Results

3.2.3.1 Hydrology Calibration Results

Figures 3-16a-d show the temporal average daily flow calibration results, Figures 3-17a-d show the average monthly flow calibration results, Figures 3-18a-d show the average annual flow calibration results, and Figure 3-19 shows crossplots of the average monthly flow calibration results for the primary Lake LBJ watershed calibration gages. The calibration was based on the average monthly values. The model performed well based on the graphical and statistical calibration metrics, particularly at the Llano River near Llano gage, whose drainage area accounts for 84% of the Lake LBJ watershed area. The Sandy Creek watershed hydrology calibration provided a good fit to the data, as well, but the model tended to over-predict lower flows. This minor shortcoming of the model hydrology is of little consequence considering how little of the total flow volume these low flows represent and most sediment and nutrient transport to the lake does not occur during low flow.

Table 3-9 includes statistical descriptors of the monthly hydrologic calibration for the primary calibration locations (NS, R^2 , and volume percent difference). The model performance is good based on the NS values ranging from 0.63 to 0.84 for the primary calibration stations. A percent difference comparison of the sum of the measured flow volumes to the sum of the simulated flow volumes also indicates the hydrology of the model is performing well with differences at the calibration stations ranging from 14% at the Sandy Creek gage to 13% at the Llano River near Mason gage.

Table 3-9 Lake LBJ SWAT Monthly Hydrologic Calibration Metrics for Primary Calibration Locations

Station Number and Name	Contributing Area to Total Lake LBJ Watershed Area (%)	Period of Record Used in Calibration	Monthly NS	Monthly R^2	Volume Percent Difference	Average Measured Monthly Flow (cfs)	Average Simulated Monthly Flow (cfs)
08151500 - Llano River near Llano	84	1984-2009	0.82	0.83	-0.4	424	422
08150700 - Llano River near Mason	70	1984-2009	0.84	0.85	13	311	350
08150000 - Llano River near Junction	37	1984-2009	0.82	0.83	-7	217	202
08152000 - Sandy Creek near Kingsland	7	1984-2009	0.63	0.68	-14	72	61

Table 3-10 includes statistical descriptors of the monthly hydrologic calibration at the secondary, smaller tributary locations. Traditionally, modeling small sub-watersheds is difficult when model adjustments are made at a basin-wide scale (Benaman et al. 2005). In this case, parameters were varied across the basin to fit the measured data at the primary stations, which have relatively large contributing areas. Consequently, the performance of the model at these secondary stations is not as consistently good as at the primary calibration stations.

Table 3-10 Lake LBJ SWAT Monthly Hydrologic Calibration Metrics for Secondary Calibration Locations

Station Name	Station Number	Source	POR	Contributing Area to Total Lake LBJ Watershed Area (%)	NS	R^2	Volume Percent Difference	Average Measured Monthly Flow (cfs)	Average Simulated Monthly Flow (cfs)
North Llano River near Junction	08148500	USGS	2001-2009	18	0.88	0.92	46	46	67
Beaver Creek near Mason	08150800	USGS	1980-2009	4	0.49	0.58	97	21	41
James River near Mason	2399	Hydromet	1999-2009	7	0.27	0.51	212	22	68
Sandy Creek near Click	2878	Hydromet	2001-2009	6	0.43	0.47	8	53	58
Johnson Fork near Junction	2313	Hydromet	2000-2009	6	-0.55	0.52	-12	41	35
Hickory Creek near Castell	2498	Hydromet	2000-2009	3	-0.11	0.27	18	24	28

Station Name	Station Number	Source	POR	Contributing Area to Total Lake LBJ Watershed Area (%)	NS	R ²	Volume Percent Difference	Average Measured Monthly Flow (cfs)	Average Simulated Monthly Flow (cfs)
Sandy Creek near Willow City	2851	Hydromet	1996-2009	3	-1.53	0.38	-43	38	22
San Fernando Creek near Llano	2616	Hydromet	1999-2009	3	-1.38	0.64	-58	29	12
Willow Creek near Mason	2443	Hydromet	1999-2009	1	0.67	0.71	32	5	6
Little Llano River near Llano	2669	Hydromet	1999-2009	1	0.21	0.53	-36	7	5
Comanche Creek near Mason	2424	Hydromet	2000-2009	1	0.36	0.59	-27	8	7
Honey Creek near Kingsland	2694	Hydromet	2002-2009	1	-19.9	0.05	-62	10	4
Walnut Creek near Kingsland	2897	Hydromet	2001-2009	<1	-1.59	0.05	-8	8	7

The Lake LBJ watershed SWAT hydrology calibration results compare to other SWAT applications, including the recent application of SWAT to the Lake Travis watershed (Anchor QEA and Parsons 2009), which reported NS values of 0.47 and 0.82. In a Northeastern study, Cho et al. (1995) reported monthly NS values ranging from 0.57 to 0.83 for a small forested watershed in the Delaware River basin. A previous study in the Trinity River watershed in Texas (Srinivasan et al. 1998) obtained monthly NS values of 0.87 and 0.84. A more recent modeling effort completed in the Bosque River watershed in Texas obtained flow volume monthly NS values of 0.80 and 0.89 for two sub-watersheds of 926 and 2997 km², respectively (Santhi et al. 2001). Also, a second Texas effort in the West Fork watershed of the Trinity River basin obtained NS values of 0.12 and 0.72 for two USGS flow stations in a 4552 km² watershed (Santhi et al. 2006). A recent review of many SWAT applications throughout the world, including many in Texas, show monthly NS values ranging from 0.3 to above 0.95 (Gassman et al. 2007). The Santhi et al. (2001) study assumed an “acceptable calibration” for hydrology as a monthly NS greater than 0.6. The NS values for Lake LBJ watershed primary calibration stations were all greater than 0.6 and, therefore, based on these NS values and the other calibration metrics, the hydrology calibration was deemed acceptable.

3.2.3.2 Sediment Calibration Results

Figure 3-20 shows crossplots of monthly average sediment load calibration results for the Lake LBJ watershed, and Table 3-11 includes statistical descriptors of the monthly sediment load calibration. The calibration was based on the average monthly values.

Table 3-11 Lake LBJ SWAT Monthly Sediment (TSS) Calibration Metrics

Station Name	Station Number	Contributing Area to Total Lake LBJ Watershed Area (%)	NS	R^2	Mass Percent Difference	Average LOADEST Monthly Load (metric tons/day)	Average Simulated Monthly Load (metric tons/day)
Llano River near Llano	12386	84	0.73	0.83	29	42	55
Llano River near Mason	17470	70	0.71	0.75	23	40	50
Llano River near Junction	17471	37	0.85	0.86	-9	18	16
Sandy Creek near Kingsland	12214	7	0.83	0.83	-4	28	26

NS values for TSS range from 0.71 to 0.85, and the model comes within a factor of 2 of the observed TSS, which is considered good performance for this constituent in watershed modeling (Benaman et al. 2005). The Lake LBJ SWAT model produces percent differences for TSS ranging from -9% to 29%. Santhi et al. (2001) considered SWAT's simulations of sediment loading acceptable with percent differences of -16% and -20%. Srinivasan et al. (1998) also performed a sediment calibration in Texas and came within 2% of the measured annual sediment loads. Although the review of 37 different SWAT applications across many different basins does not report percent differences in their summary, they indicate NS values that are negative up to above 0.8 (Gassman et al. 2007). Gassman et al. (2007) and Benaman et al. (2005) also document weaknesses in sediment erosion and transport simulation that make it difficult to simulate sediments in SWAT. The NS values for the Lake LBJ watershed calibration stations are good given the uncertainty in the TSS calibration record estimated by LOADEST.

3.2.3.3 Nutrient Calibration Results

Figures 3-21a-g shows crossplots of monthly average nutrient load calibration results for Lake LBJ and Table 3-12 includes statistical descriptors (NS, R^2 , and mass percent difference) of the monthly nutrient load calibration. The calibration was based on the average monthly values. Sufficient PO_4 calibration data for running LOADEST were only available at the Llano River near Llano and Sandy Creek stations. As the model is run with the kinetics off, NH_4 is not modeled appropriately, and therefore results are not provided here.

Table 3-12 Lake LBJ SWAT Monthly Nutrient Calibration Metrics

Parameter	Station Name	Station Number	Contributing Area to Total Lake LBJ Watershed Area (%)	NS	R ²	Mass Percent Difference	Average LOADEST Monthly Load (kg/day)	Average Simulated Monthly Load (kg/day)
OrgP	Llano River near Llano	12386	84	0.17	0.54	-34	120.90	80
	Llano River near Mason	17470	70	0.14	0.20	97	34.10	68
	Llano River near Junction	17471	37	0.61	0.62	15	19.00	22
	Sandy Creek near Kingsland	12214	7	0.14	0.66	-24	46.30	33
PO ₄	Llano River near Llano	12386	84	0.77	0.81	35	19.10	26
	Llano River near Mason	17470	70	--	--	--	--	--
	Llano River near Junction	17471	37	--	--	--	--	--
	Sandy Creek near Kingsland	12214	7	0.65	0.86	-39	6.00	4
TP	Llano River near Llano	12386	84	0.58	0.62	11	95.30	106
	Llano River near Mason	17470	70	0.17	0.28	128	40.3	93
	Llano River near Junction	17471	37	0.69	0.78	72	23	39
	Sandy Creek near Kingsland	12214	7	0.11	0.70	-22	50	37
OrgN	Llano River near Llano	12386	84	0.51	0.54	-5	608	581
	Llano River near Mason	17470	70	0.43	0.47	56	260	406
	Llano River near Junction	17471	37	-16	0.52	-62	412	155
	Sandy Creek near Kingsland	12214	7	0.67	0.69	2	248	240
NO _x	Llano River near Llano	12386	84	-165	0.23	-78	2315	507
	Llano River near Mason	17470	70	-2792	0.19	-92	6474	502

Parameter	Station Name	Station Number	Contributing Area to Total Lake LBJ Watershed Area (%)	NS	R ²	Mass Percent Difference	Average LOADEST Monthly Load (kg/day)	Average Simulated Monthly Load (kg/day)
	Llano River near Junction	17471	37	-2323	0.2	-92	3945	314
	Sandy Creek near Kingsland	12214	7	0.02	0.53	19	33	38
TN	Llano River near Llano	12386	84	0.64	0.65	7	1019	1094
	Llano River near Mason	17470	70	-1.22	0.45	-2	935	915
	Llano River near Junction	17471	37	-110	0.45	-73	1791	477
	Sandy Creek near Kingsland	12214	7	0.57	0.70	-6	312	278

Notes:

LOADEST uncertainty is illustrated by average monthly LOADEST TP values that are less than the sum of the average monthly LOADEST PO₄ + OrgP values.

For the nutrient series, the model fits are fair. Generally, the model tends to overestimate nutrient loads and phosphorus series calibration results are more reliable than nitrogen series calibration results. The model performs particularly well predicting TP, TN, and PO₄ for the Llano River near Llano (within a factor of 2 and NS values of 0.58, 0.64, and 0.77, respectively). PO₄ is the phosphorus available for algae growth and can be considered one of the most critical to calibrate (Anchor QEA and Parsons 2009). Additionally, the Lake LBJ watershed model at the Llano River near Llano station outperformed the Lake Travis watershed model for PO₄, TP, NH₄, and NO_x, but did not perform as well for OrgP or OrgN (Table 3-13).

Table 3-13 Comparison of Lake LBJ (Llano near Llano) and Lake Travis SWAT Monthly Nutrient Calibration Metrics

Parameter	Lake LBJ		Lake Travis ^a	
	Monthly NS	Mass Percent Difference	Monthly NS	Mass Percent Difference
OrgP	0.17	-34	0.31	-18.40
PO ₄	0.77	35	0.53	-44.60
TP	0.58	11	0.35	2.80
OrgN	0.5	-5	0.06	-69.00
NO _x	-165	-78	-20.17	640.00
TN	0.64	7	NA	NA

Notes:

^a As reported in the CREMs 2 Final Modeling Report (Anchor QEA and Parsons 2009)

Modeling the nutrient series in SWAT is challenging. Gassman et al. (2007) summarized SWAT model performance in nutrient simulations for various studies and found that SWAT performed “acceptably” to “poorly” in general. LOADEST rating curve uncertainties, which are illustrated by average monthly LOADEST TP values that are less than the sum of the average monthly LOADEST PO₄ + OrgP values, are propagated to the SWAT model calibration. Adjustment of multiple parameters that describe both land-side processes (including erosion and plant uptake) and instream kinetic processes are required. Little site-specific data are available to guide the modeler as to which parameters should be adjusted and, consequently, literature values and professional judgment are used to guide the calibration. Despite these limitations, the nutrient calibration of the Lake LBJ SWAT model, when compared to other nutrient calibration efforts, is considered acceptable. Santhi et al. (2001) and Santhi et al. (2006) show percent differences for the phosphorus series of -18% and -3% for orthophosphate, on average. Santhi et al. (2001) also reported a 7% over-prediction in organic phosphorus. In both studies, the mineral nitrogen (i.e., ammonia plus nitrite+nitrate) was over-predicted by about 45%. Another study in upstate New York showed phosphorus percent differences of about 6 to 41% (Tolson and Shoemaker 2007).

3.3 Lake Marble Falls Watershed

3.3.1 Lake Marble Falls Watershed Spatial Domain

The spatial extent of the Lake Marble Falls SWAT model is the drainage basin of the Colorado River from Alvin Wirtz Dam to Max Starcke Dam (Figure 3-22). Lake Marble Falls is a run-of-river reservoir impounded between these two dams. The Lake Marble Falls capacity volume is approximately 7,486 acre-feet at 738 ft above mean sea level with a capacity area of approximately 608 acres (TWDB 2007b). The SWAT model was only required to simulate the watershed of Lake Marble Falls that either drains directly to the lake or drains to one of the tributaries of the lake because observed data taken at Wirtz Dam served as the upstream input to the Lake Marble Falls CE-QUAL-W2 model. The modeled watershed is approximately 50,400 acres.

3.3.1.1 Geology

Geological features in the Lake Marble Falls watershed directly and indirectly impact watershed hydrology and constituent loading. The Llano Uplift underlies approximately 99% of the Lake Marble Falls watershed. Fracture systems in these crystalline rocks influence groundwater recharge and discharge patterns by providing preferential groundwater flow paths and, therefore, directly affect runoff and baseflow (Mace et al. 2004). The southern tip of the Lake Marble Falls watershed is underlain by karstified Cretaceous limestone. The karst area accounts for only 1% of the total watershed area.

The geology of the Lake Marble Falls watershed also indirectly impacts watershed hydrology and constituent loading in that soil formation, type, and distribution, which directly impact watershed hydrology and constituent loads, are uniquely derived from the parent rocks. Also, soil type and climate determine the vegetative cover of a region. Vegetative cover, in turn, directly impacts watershed hydrology and constituent loads.

3.3.1.2 Climate

The Lake Marble Falls watershed is in a semi-arid environment. Average annual precipitation is approximately 30 to 32 inches (TWDB 1998). Rainfall in the region generally occurs as intense convective or frontal thunderstorms followed by extended dry periods (Asquith et al. 2006). These thunderstorms result in ‘flashy’ hydrographs including many ephemeral streams that only flow in response to storm events (Asquith et al. 2006).

Precipitation data were available for input to the Lake Marble Falls SWAT model from three nearby meteorological stations (two NCDC stations and one TAMU station) and temperature data were available from two TAMU stations (Table 3-14, Figure 3-23).

Table 3-14 Meteorological Stations Used for the Lake Marble Falls SWAT Model

Station ID	Station Name	Source	Data Types
414605	Johnson City	TAMU	T
417787	Round MTN 4WNW	NCDC	P
418531	Spicewood	NCDC	P
411250	Burnet	TAMU	P, T

Notes: P = precipitation, T = temperature

3.3.1.3 Topography

The Lake Marble Falls watershed features rolling hills, which are the result of the variable erodibility of Llano Uplift formations (Figure 3-24).

3.3.1.4 Soils

Soil formation, type, and distribution are directly related to parent rock type (Figure 3-25). Soil types cross-cut topography in the Llano Uplift area due to the inherent heterogeneity of crystalline rock formations.

3.3.1.5 Land Cover

The Lake Marble Falls watershed is predominately rural. About 50% of the watershed land cover is range brush and grassland and about 38% is forested (evergreen and deciduous) (Figure 3-26, Table 3-15). There is significant development in and around the city of Marble Falls, which makes up about 9% of the watershed.

Table 3-15 Lake Marble Falls Watershed Land Cover

Name	Code	Area (acre)	Percent of Total Watershed Area
Open Water	WATR	690	1.4
Developed, Open Space	URLD	2693	5.3
Developed, Low Intensity	URMD	1142	2.3
Developed, Medium Intensity	URHD	412	0.8
Developed, High Intensity	UIDU	285	0.6
Barren Land	SWRN	14	0.03
Deciduous Forest	FRSD	7015	14.0
Evergreen Forest	FRSE	12271	24.3
Scrub/Shrub	RNGB	15053	30.0
Grassland/Herbaceous	RNGE	10427	20.7
Pasture/Hay	HAY	121	0.2
Cultivated Crops	AGRR	65	0.1
Wood Wetlands	WETF	250	0.5
Emergent Herbaceous Wetland	WETN	2	0.005

3.3.1.6 Watershed Ordinance

Approximately 90% of the Lake Marble Falls watershed is covered by the HLWO (Figure 3-27). The HLWO controls storm water runoff and enforces erosion controls to reduce pollution to the Highland Lakes (LCRA 2006). Changes to HLWO regulations may be considered in the future and, therefore, model scenario runs that address alternative watershed conditions can accommodate these changes.

3.3.1.7 Point Sources

There are no active permitted domestic discharges in the Lake Marble Falls watershed.

3.3.1.8 Sub-watershed Delineation

The Lake Marble Falls sub-watershed delineation accounted for the location of one calibration station, which had limited data (Backbone Creek), the HLWO, and the Lake Marble Falls lake model segmentation. An attempt was made to locate pour points so that the majority of a defined sub-watershed area was either contained within or outside of the HLWO. As a result, specific sub-watersheds can be targeted in future scenario simulations that may involve

changes to the HLWO. Also, pour points were added in order to facilitate the spatial linkage between output from the watershed model and input to the lake model (Figure 3-28). Finally, additional pour points were added, as needed, in order to break larger sub-watersheds into more manageable parcels. The sub-watershed delineation resulted in 35 sub-watersheds (Figure 3-29), and the intersection of the slope, land cover, and soil type resulted in 991 HRUs.

3.3.1.9 Lake Marble Falls SWAT Model Calibration

Due to the small watershed size and absence of water quality stations in the Lake Marble Falls watershed, calibrated parameters from the Lake LBJ watershed model were used for the sediment and nutrient loading calibration of the Lake Marble Falls SWAT model. As with the LBJ model, all three calibration steps, unless noted otherwise, followed a ‘lumped’ approach. In other words, identical flow and water quality calibration parameters were applied to identical HRUs (i.e., areas of the same soil type, land cover, and slope) regardless of the sub-watershed in which they were located.

3.3.1.10 Hydrology Calibration Data

Flow data from Backbone Creek Hydromet gage were available for the Lake Marble Falls watershed model hydrology calibration. The gage had limited data from 1998 through 2008 (Figure 3-29, Table 3-16).

Table 3-16 Lake Marble Falls Watershed Hydrologic Calibration Stations

Station Name	Station Number	Source	SWAT Sub-watershed Number	Contributing Area to Total Lake Marble Falls Watershed Area (%)	POR during Model Simulation Period	Average Monthly Flow Rate (cfs)
Backbone Creek	2992	Hydromet	7	40	1998 - 2008	8

3.3.1.11 Hydrology Calibration Approach

Because data for calibration in the Lake Marble Falls watershed were limited, calibrated hydrologic parameters determined for the Lake LBJ SWAT model were directly applied to the Lake Marble Falls SWAT model within the soil types and land uses that were applicable to the Lake Marble Falls basin. Slight modifications were made to the LBJ calibrated parameters to better fit the data available at the Backbone Creek gage. Table 3-17 lists the model parameters that were adjusted to calibrate the Lake Marble Falls watershed hydrology in SWAT. The table briefly describes each parameter, indicates the location in the SWAT input, and provides both the default and calibrated values. The following parameters were modified from the original LBJ calibration for Lake Marble Falls: CN2, RCHRG_DP and CH_K2. These values were derived through iterative runs of the model while implementing small changes in this suite of model parameters based on both graphical and statistical evaluations of the model’s agreement with measured data. Results from the valuations are presented below in Section 3.3.2

Table 3-17 Lake Marble Falls SWAT Hydrologic Calibration Parameters

Parameter	Units	Description	Location in SWAT Input	Sub-basin	Calibrated Value	SWAT Default Value
CN2	--	SCS Curve Number	*.mgt	All	*90%	--
RCHRG_DP	--	Percent of infiltrated water lost to a regional aquifer	*.gw	All	60%	5
ALPHA_BF	day	Baseflow recession constant	*.gw	All	0.1	1
SOL_AWC	mmH2O/mmSoil	Soil Available Water Content for Plant Uptake	*.sol	All	+0.04	--
SOL_K	mm/hr	Saturated hydraulic conductivity	*.sol	All	-75%	--
ESCO	--	Evap Coefficient	*.hru	All	0.5	1
EPCO	--	Uptake Coefficient	*.hru	All	0.7	1
CH_K2	mm/hr	Effective river channel hydraulic conductivity	*.rte	All	0.5	0

Notes:

'--' indicates that the value varies by HRU and was therefore increased or decreased by a percent or constant value

'*' represents variable sub-watershed or HRU number contained in input file name

Calibration parameters for open water land cover areas in .mgt, .sol, and .hru files were not changed from default values

3.3.1.12 Water Quality Calibration Data

There are no water quality stations within the Lake Marble Falls watershed.

3.3.1.13 Water Quality Calibration Approach

Due to the lack of water quality stations within the modeled Lake Marble Falls watershed, Lake LBJ watershed sediment and nutrient load calibration parameter values were directly applied to the Lake Marble Falls SWAT model, with one exception discussed below. Table 3-8 (in the LBJ section) identifies the model parameters that were adjusted to calibrate the sediment and nutrient loads in SWAT, except for the sediment parameters ADJ_PKR, PRF, and SPCON. These three parameters were adjusted to achieve a reasonable long term average TSS concentration (approximately 60 mg/L) based on professional judgment.

Table 3-18 Lake Marble Falls SWAT Water Quality Calibration Parameters

Parameter	Units	Description	Location in SWAT Input	Sub-basin	Calibrated Value	SWAT Default Value
ADJ_PKR	--	Peak rate adjustment factor for sediment routing in the subbasin (tributary channels)	*.bsn	All	0.5	1.0
PRF	--	Peak rate adjustment factor for sediment routing in main channel	*.bsn	All	0.5	1.0
SPCON	kg/L	Linear parameter for calculating the maximum amount of sediment that can be reentrained during channel sediment routing	*.bsn	All	0.00008	0.0001

3.3.1.14 Watershed Operations

As part of the constituent load calibration, watershed operations were added to the model in order to address land uses that can significantly impact watershed nutrient loads. Based on conversations with Dr. Srinivasan, one of the developers of ArcSWAT, appropriate grazing operations were added to grasslands of 0-10 slope (heat units = 0.45, consecutive grazing days = 180, consumed biomass = 5 (kg/ha)/day, and dry weight of daily deposited manure = 2 (kg/ha)/day) (Srinivasan 2009).

3.3.2 Lake Marble Falls SWAT Model Results

3.3.2.1 Hydrology Calibration Results

Figures 3-30 to 3-32 show the temporal daily, monthly, and annual average flow calibration for Backbone Creek (Reach 7). A satisfactory calibration was difficult to accomplish due to the low flows at this gage. In general, the model is biased high at low flows (less than 0.1 cfs) but reproduces higher flows well. Because high flows carry constituents to the lake, the calibration was focused on the model performance at flows greater than 0.1 cfs. Table 3-19 lists statistical descriptors of the monthly hydrologic calibration for Backbone Creek for flows greater than 0.1 cfs.

Table 3-19 Lake Marble Falls SWAT Hydrologic Calibration Metrics for Backbone Creek

Station Name	POR	Measured Average Monthly Flow (cfs)	Modeled Average Monthly Flow (cfs)	Contributing Area to Total Lake Marble Falls Watershed Area (%)	Monthly NS	Monthly R ²	Volume Percent Difference
Backbone Creek <i>(Calibration metrics are for flows greater than 0.1 cfs.)</i>	1998-2008	9.39	10.33	40	0.06	0.5	1.34
Backbone Creek <i>(All flows)</i>	1998-2008	7.69	8.22	40	-0.34	0.52	7.03

Notes:
 Calibration metrics are for flows greater than 0.1 cfs.

3.3.2.2 Water Quality Calibration Results

No sediment or nutrient calibration results are available due to the lack of water quality data in the Lake Marble Falls watershed. A summary for the full simulation periods of the average daily flows and average daily loads for sediment, TP, PO₄, and TN at the Backbone Creek gage are provided in Table 3-20.

Table 3-20 Lake Marble Falls SWAT Water Quality Calibration Metrics for Backbone Creek

Station Name	Simulation Period	Modeled Daily Average Flow (cfs)	Modeled Daily Average Sediment Load (kg/d)	Modeled Daily Average TP Load (kg/d)	Modeled Daily Average PO ₄ Load (kg/d)	Modeled Daily Average TN Load (kg/d)
Backbone Creek <i>(All Flows)</i>	1984-2008	8.12	1,190	1.20	0.21	10.74

3.4 Inks Lake Watershed

3.4.1 Inks Lake Watershed Spatial Domain

The spatial extent of the Inks Lake SWAT model is the drainage basin of the Colorado River from Buchanan Dam upstream to Roy Inks Dam (Figure 3-33). Inks Lake is a run-of-river reservoir impounded between these two dams. There are no floodgates on Inks Dam so the bulk of the floodwater passes over an uncontrolled spillway, although a small amount of water is released through turbines for hydroelectric power generation (TWDB 2007a). The surface area of Inks Lake at full elevation (888.22 ft NGVD 29) is approximately 837 acres and its corresponding volume is close to 15,000 acre-ft (LCRA 2009). The upstream input to the Inks Lake CE-QUAL-W2 model was derived from observed data taken at Buchanan Dam;

therefore, the SWAT model is only required to simulate the watershed of Inks Lake that either drains directly to the lake or drains to one of its tributaries.

The watershed draining to Inks Lake is about 24,600 acres (approximately 100 km²) and is located mainly in Burnet County (94% of the total area). The remaining 6% of the watershed is located in Llano County. The bulk of the modeled watershed comprises the Spring Creek and Clear Creek watersheds, with both tributaries entering Inks Lake from the northeast (see Figure 3-33). The Spring Creek watershed is 46% of the total Inks Lake watershed area, the Clear Creek watershed is 31%, and the remaining 23% of the watershed area drains either through small tributaries or directly into Inks Lake.

3.4.1.1 Geology

Sixty-four percent of the Inks Lake watershed is underlain by Precambrian igneous and sedimentary rocks of the Llano Uplift (Figure 3-34). Fracture systems in these rocks influence groundwater recharge and discharge patterns by providing preferential groundwater flow paths and, therefore, directly affect runoff and baseflow. Carbonate-platform (limestone and dolomite) sediments from the Cambrian and Ordovician periods underlay the uppermost and southeast portions of the watershed (approximately 25% of the total watershed) as shown in Figure 3-34.

3.4.1.2 Climate

The Inks Lake watershed is in a semi-arid environment. Average annual precipitation ranges from approximately 28 inches in the western reaches of the watershed to approximately 32 inches in the east (TWDB 1998) (Figure 3-35). Precipitation data from two proximal meteorological towers (one NCDC station and one TAMU station) were input to the Inks Lake SWAT model. Temperature data were available from TAMU station 411250 at Burnet (Table 3-21). These time-series precipitation data were imported into the SWAT model along with the station coordinates and SWAT subsequently assigned the precipitation to the various subbasins using the nearest station (Neitsch et al. 2005).

Table 3-21 Meteorological Stations used for the Inks Lake SWAT Model

Station ID	Station Name	Source	County	Data Types
419099	Tow	NCDC	Llano	P
411250	Burnet	TAMU	Burnet	P, T

Notes: P = precipitation; T = temperature

3.4.1.3 Topography

Ground elevations on the watershed range from 251 to 489 m above mean sea level (Figure 3-36). The Inks Lake watershed features gently sloping to steep uplands with most of the area exhibiting moderately steep (rolling) hills. Slopes vary from 1% to more than 60%, with about 80% of the watershed exhibiting slopes lower than 10%.

3.4.1.4 Soil

Soil formation, type, and distribution are directly related to parent rock type. The distribution of soil types within the Inks Lake watershed is shown in Figure 3-37. Most of the watershed is underlain by Keese series soil, which is shallow, well-drained, moderately permeable, and formed in weathered granite or gneiss (NRCS 2009). A summary of soil distribution is provided in Table 3-22.

Table 3-22 Soil Distribution within the Inks Lake Watershed

Soil Series	STATSGO Soil Group	Area (acre)	Percent of Total Watershed Area
Brackett	TX071	1,066	4
Keese	TX089	14,696	60
	TX592	959	4
Eckert	TX151	209	1
Hensley	TX227	4,424	18
Nebgen	TX360	2,441	10
-	TXW	805	3

3.4.1.5 Land Cover

The Inks Lake watershed is predominately rural. About 50 percent of the watershed land cover is forest and 42 percent is shrub and grass (Figure 3-38, Table 3-23). Less than 6% of the watershed is developed and most of the developed area is open space. The medium and high intensity residential areas are in the vicinity of the lake. Development around the lake is of importance because runoff from direct drainage sub-watersheds can deliver urban pollution directly to the lake.

Table 3-23 Inks Lake Watershed Land Cover

Name	Code	Area (acre)	Percent of Total Watershed Area
Water	WATR	833	3
Developed, Open Space	URLD	1,134	5
Developed, Low Density	URLD	80	0.3
Developed, Medium Density	URMD	28	0.1
Developed, High Density	URHD	6	<0.1
Deciduous Forest	FRSD	2,933	12
Evergreen Forest	FRSE	9,360	38
Shrubland	RRGB	7,510	31
Grassland/Herbaceous	RNGE	2,707	11
Woody Wetlands	WETF	9	<0.1

3.4.1.6 Watershed Ordinance

Most of the Inks Lake watershed is in Region C of the HLWO with a small area in Region A (Figure 3-39). The HLWO controls storm water runoff and enforces erosion controls to reduce pollution to the Highland Lakes (LCRA 2006).

3.4.1.7 Point Sources

Three permitted point sources are located in the Inks Lake watershed (Figure 3-40). One of the point sources is on a direct drainage sub-watershed, while the remaining two are on tributary reaches. Permitted discharge flow rates range from 0.006 to 0.05 MGD. However, they are all land application permits (i.e., no direct discharge). Thus, the outfalls were included in the SWAT model with flows and concentrations equal to zero.

3.4.1.8 Sub-watershed Delineation

Figure 3-41 shows the subwatersheds into which the Inks Lake watershed was divided. These subwatersheds were derived from the available digital elevation models of the area along with the USGS National Hydrography Dataset that provided information of the stream network required by SWAT. The Inks Lake sub-watershed delineation accounted for the Inks Lake model segmentation. Pour points were added in order to intersect the output from the watershed model to the segmented input of the lake model (Figure 3-41). Finally, additional pour points were added, as needed, to break larger subwatersheds into more manageable parcels. The subwatershed delineation resulted in 47 subwatersheds and the intersection of the slope, land cover, and soil type resulted in 1,085 HRUs. The average HRU area was approximately 23 acres.

3.4.2 Inks Lake SWAT Model Results

Due to the lack of gage stations and water quality data on the Inks Lake watershed, it was not possible to complete a calibration. Rather, the calibrated parameters for the Sandy Creek subwatershed of the LBJ watershed model were used. This was done due to the similarity of the geology and soil of the Sandy Creek subwatershed (basin 63) to the Inks Lake watershed. A summary of the parameters and values used for the base scenario run is presented in Table 3-24.

Table 3-24 Parameters Changed for Base Run of the Inks Lake SWAT Model (same as calibration parameters for basin 63 of the LBJ SWAT model)

Calibration Type	Parameter	Units	Description	Location in SWAT Input	LBJ SWAT Value	SWAT Default Value
Hydrology	CN*	-	SCS Curve Number	** .mgt	FRSE-22% (except no change to soil), RRGB-30%, Rest-28%	-

Calibration Type	Parameter	Units	Description	Location in SWAT Input	LBJ SWAT Value	SWAT Default Value
	GW_DELAY	day	Amount of time groundwater spends in the vadose zone	** .gw	0	31
	RCH_DP	-	Percent of infiltrated water lost to a regional aquifer	** .gw	80%	5
	SOL_AWC*	mm H2O/mm soil	Soil available water content for plant uptake	** .sol	+0.04	-
	ESCO	-	Evaporation coefficient	** .hru	0.5	1
	EPCO	-	Uptake coefficient	** . hru	0.7	1
	ALPHA_BF	day	Baseflow recession constant	** .gw	0.058	1
	SOL_K*	mm/hr	Soil saturated hydraulic conductivity	** .sol	-75%	-
	CH_K2	mm/hr	Channel effective hydraulic conductivity	** .rte	0.2	0
Sediment*	SPEXP	-	Sediment re-entrainment exponent	basins.bs n	1.5	1
	LAT SED	mg/L	Discharge TSS concentration	** .hru	Soils TX151 and TX327=5, Rest=10	0
	USLE_K	Special	Soil erodibility factor	** .sol	0.1 for RNGB, FRSE	0.1-0.37
	ADJ_PKR	-	Sub-basin peak rate factor	basins.bs n	1	1
	PRF	-	Channel peak rate factor	basins.bs n	0.5	1

Calibration Type	Parameter	Units	Description	Location in SWAT Input	LBJ SWAT Value	SWAT Default Value
	SPCON	-	Sediment re-entrainment linear parameter	basins.bs n	0.00008	0.0001
	SLSUBBSN	m	Slope length for sheet flow	** .hru	SLSUBBSN*3	-
	USLE_C	-	Land cover factor	crop.dat	0.001 for RNGB, RNGE	0.003
	HVSTI	-	Biomass harvest loss	crop.dat	0.1 for RNGB, RNGE, FRSE	0.9,0.9, 0.76
Nutrients	ISUBWQ	-	Subbasin water quality code	basins.bs n	0	0
	IWQ	-	In-stream water quality code	basins.bs n	0 (do not model in-stream transformations)	0
	CMN	-	Humus mineralization factor	basins.bs n	0.0004	0.0003
	PSP	-	Phosphorus availability index	basins.bs n	0.69	0.4
	CDN	-	Denitrification Exponential rate coefficient	basins.bs n	0.15	1.4
	SDNCO	-	Denitrification threshold water content	basins.bs n	0.6	1.1
Management Operations	Grazing	-	Add operation	** .mgt	RNGE, 0-10 slope, HUS=0.45, GRZ_DAYS=180, EAT=5, MAN=2	N/A

Notes:

'*' indicates that the value varies by HRU and was therefore increased or decreased by a percent or constant value.

'**' represents variable sub-watershed or HRU number contained in input file name.

Calibration parameters for open water land cover areas in .mgt, .sol, and .hru files were not changed from default values.

Figures 3-42 and 3-43 show the base scenario resulting time series for flow, sediment, total phosphorus, and total nitrogen, for the downstream most reaches of Spring Creek and Clear Creek, respectively. A summary of average daily values over the 1984-2008 period is presented in Table 3-25.

Table 3-25 Summary of SWAT Results for the Two Major Tributaries of Inks Lake

Tributary	Downstream SWAT Reach	Daily Average Flow (cfs)	Daily Average Sediment Load (kg/day)	Daily Average Total Phosphorus Load (kg/day)	Daily Average Total Nitrogen Load (kg/day)
Clear Creek	10	1.35	113	0.23	1.71
Spring Creek	29	2.08	381	1.40	3.92

3.5 Sensitivity Analysis

Sensitivity analysis relates how the variation (uncertainty) in the output of a mathematical model can be apportioned, qualitatively or quantitatively, to different sources of variation in both model input data and, more commonly, the various parameters in the model that affect the performance or calibration of the model. In general, both uncertainty and sensitivity analyses investigate the robustness of a model. While uncertainty analysis evaluates the overall uncertainty in the conclusions of the model, sensitivity analysis tries to identify what source of uncertainty weighs more on the model output or conclusions.

Choosing the appropriate uncertainty analysis/sensitivity analysis method is often a matter of trading off between the amount of information one wants from the analyses and the computational difficulties of the analyses. These computational difficulties are often inversely related to the number of assumptions one is willing or able to make about the shape of a model's response surface (Pascual et al. 2003).

Considering the computational difficulty of running the SWAT models in an iterative or Monte Carlo fashion to facilitate uncertainty analysis, a one-at-a-time sensitivity analysis was performed in three steps. The initial step was to select the parameters and their ranges to test in the one-at-a-time sensitivity analysis. Table 3-26 lists the eight parameters chosen for sensitivity analysis. The table shows the calibrated value for the parameter and the range evaluated in the sensitivity analysis. Ranges were developed using professional judgment, taking into account information available in the literature pertaining to the ranges for these parameters where possible.

Table 3-26 SWAT Parameters Selected for Sensitivity Analysis

Parameter	Description	Location in SWAT Input	Calibrated Value	Sensitivity Range
ESCO	Soil evaporation compensation factor	** .hru	0.5	0.01-1
EPCO	Plant uptake compensation factor	** .hru	0.7	0.01-1
SPCON ¹	Linear parameter to determine maximum amount of sediment reentrainment	basins.bsn	0.00008	0-0.01
PSP	Phosphorus availability index	basins.bsn	0.69	0.1-0.9
CDN	Denitrification exponential rate coefficient	basins.bsn	0.15	0.01-3
SDNCO	Denitrification threshold water coefficient	basins.bsn	0.6	0.01-1
PRF ²	Peak rate adjustment factor for sediment routing	basins.bsn	0.5	0.1-2
SLSUBBSN	Average slope length (m)	** .hru	SLSUBBSN*3	SLSUBBSN*1- SLSUBBSN*5

Notes:

¹ SPCON was calibrated at 0.0001 for Lake LBJ and 0.00008 for Lake Marble Falls and Inks.

² PRF was calibrated at 0.6 for Lake LBJ and 0.5 for Lake Marble Falls and Inks.

For each parameter selected, step 2 of the procedure involved changing the model input to the low value of the range specified in Table 3-26 and running the model. This was repeated using the high value of the range. In this one-at-a-time manner, the two results are used in step 3 in the presentation and evaluation of the sensitivity analysis for each of the seven major state variables of the model including:

- flow (m³/s);
- total suspended solids (tons/d);
- orthophosphate² (kg/d);
- organic phosphorus (kg/d);
- nitrate + nitrite (kg/d);
- ammonia nitrogen (kg/d); and
- organic nitrogen (kg/d).

Changing parameters one-at-a-time ignores correlations between parameters and, consequently, introduces a limitation of this approach. However, given the desired study outcomes and the restricted time and resources, a one-at-a-time sensitivity approach aided in

² Based on the state variable mineral phosphorus (minP) in SWAT

narrowing down the list of parameters efficiently. Results from this approach should not supersede professional judgment or previous analyses.

To evaluate the sensitivity of the SWAT models to the selected variables, a sensitivity index (SI) was computed in step 3:

$$SI = \text{Max} \left(\left| \frac{\overline{Param}_{low} - \overline{Param}_{base}}{P_{low}} \right|, \left| \frac{\overline{Param}_{high} - \overline{Param}_{base}}{P_{high}} \right| \right)$$

where:

Param = average concentration for a given state variable

P_{low} = percent reduction from base parameter value

P_{high} = percent increase from base parameter value

The main function of the SWAT model is to generate nutrient loadings for the CE-QUAL-W2 lake models. As a result, the main focus of the sensitivity analyses centered on the nitrogen and phosphorus series. Results of the sensitivity analyses are summarized in Table 3-27 for Lake LBJ, Table 3-28 for Lake Marble Falls, and Table 3-29 for Inks Lake. The tables show the difference between the high run and the low run for each parameter for each state variable along with the sensitivity index. The sensitivity indices are sorted in descending order so that the most sensitive parameter for a given state variable is listed first.

Table 3-27 Sensitivity Results for the Lake LBJ SWAT Model

Output Variable	Parameter	Sensitivity Index	Parameter Values			Results for Output Variable of Concern ^a		
			Base	Min	Max	Base	Min Param	Max Param
Flow (m ³ /s)	ESCO	12.078	0.5	0.01	1	11.89	9.97	23.97
	PRF	2.644	0.6	0.1	2	11.89	11.94	5.72
	SLSUBBSN	1.805	3	1	5	11.89	13.10	11.66
	EPCO	0.960	0.7	0.01	1	11.89	12.84	11.84
	PSP	0.171	0.69	0.1	0.9	11.89	11.95	11.95
	SDNCO	0.164	0.6	0.01	1	11.89	11.95	12.00
	CDN	0.050	0.15	0.01	3	11.89	11.94	12.20
	SPCON	0.001	0.0001	0	0.01	11.89	11.89	11.94
TSS (ton/day)	PRF	60.718	0.6	0.1	2	55.00	4.40	155.75
	ESCO	60.604	0.5	0.01	1	55.00	44.39	115.60
	SDNCO	12.376	0.6	0.01	1	55.00	57.17	46.75
	CDN	8.336	0.15	0.01	3	55.00	47.22	61.42
	EPCO	8.076	0.7	0.01	1	55.00	62.96	54.95
	SPCON	2.458	0.0001	0	0.01	55.00	55.00	298.33
	SLSUBBSN	1.007	3	1	5	55.00	54.33	55.49

Output Variable	Parameter	Sensitivity Index	Parameter Values			Results for Output Variable of Concern ^a		
			Base	Min	Max	Base	Min Param	Max Param
	PSP	0.111	0.69	0.1	0.9	55.00	54.96	54.97
PO4 (kg/day)	PSP	33.184	0.69	0.1	0.9	26.00	54.37	26.92
	ESCO	18.928	0.5	0.01	1	26.00	22.17	44.93
	SDNCO	13.242	0.6	0.01	1	26.00	24.60	34.83
	CDN	7.543	0.15	0.01	3	26.00	33.04	24.09
	EPCO	1.992	0.7	0.01	1	26.00	27.96	25.47
	PRF	0.296	0.6	0.1	2	26.00	25.75	25.75
	SLSUBBSN	0.291	3	1	5	26.00	25.92	25.81
	SPCON	0.002	0.0001	0	0.01	26.00	26.00	25.75
Organic P (kg/day)	PSP	162.748	0.69	0.1	0.9	80.00	219.16	74.70
	ESCO	56.390	0.5	0.01	1	80.00	68.55	136.39
	SDNCO	56.252	0.6	0.01	1	80.00	103.94	42.50
	CDN	38.979	0.15	0.01	3	80.00	43.62	184.79
	SLSUBBSN	35.819	3	1	5	80.00	56.12	93.35
	EPCO	6.118	0.7	0.01	1	80.00	86.03	79.64
	PRF	0.339	0.6	0.1	2	80.00	80.28	80.28
	SPCON	0.003	0.0001	0	0.01	80.00	80.00	80.28
Nitrate+ Nitrite (kg/day)	SDNCO	3623.299	0.6	0.01	1	507.00	372.09	2922.53
	CDN	1541.786	0.15	0.01	3	507.00	1946.00	163.61
	ESCO	398.045	0.5	0.01	1	507.00	443.77	905.05
	SLSUBBSN	19.880	3	1	5	507.00	520.25	504.44
	EPCO	18.738	0.7	0.01	1	507.00	525.47	504.13
	PSP	6.302	0.69	0.1	0.9	507.00	512.39	506.54
	PRF	0.062	0.6	0.1	2	507.00	506.95	506.95
	SPCON	0.001	0.0001	0	0.01	507.00	507.00	506.95
Ammonium (kg/day)	ESCO	1.654	0.5	0.01	1	5.70	5.32	7.35
	SLSUBBSN	0.251	3	1	5	5.70	5.87	5.70
	EPCO	0.136	0.7	0.01	1	5.70	5.83	5.72
	PSP	0.102	0.69	0.1	0.9	5.70	5.73	5.73
	SDNCO	0.099	0.6	0.01	1	5.70	5.73	5.77
	CDN	0.056	0.15	0.01	3	5.70	5.75	5.76
	PRF	0.037	0.6	0.1	2	5.70	5.73	5.73
	SPCON	0.000	0.0001	0	0.01	5.70	5.70	5.73
Organic N (kg/day)	SDNCO	419.370	0.6	0.01	1	580.00	760.97	300.42
	ESCO	401.943	0.5	0.01	1	580.00	499.91	981.94

Output Variable	Parameter	Sensitivity Index	Parameter Values			Results for Output Variable of Concern ^a		
			Base	Min	Max	Base	Min Param	Max Param
	CDN	290.475	0.15	0.01	3	580.00	308.89	1359.31
	SLSUBBSN	271.075	3	1	5	580.00	399.28	679.27
	EPCO	43.351	0.7	0.01	1	580.00	622.73	577.63
	PSP	2.849	0.69	0.1	0.9	580.00	581.28	580.87
	PRF	1.157	0.6	0.1	2	580.00	580.96	580.96
	SPCON	0.010	0.0001	0	0.01	580.00	580.00	580.96

Table 3-28 Sensitivity Results for the Lake Marble Falls SWAT Model

Output Variable	Parameter	Sensitivity Index	Parameter Values			Results for Output Variable of Concern ^a		
			Base	Min	Max	Base	Min Param	Max Param
Flow (m ³ /s)	ESCO	0.256	0.5	0.01	1	0.230	0.184	0.486
	EPCO	0.039	0.7	0.01	1	0.230	0.269	0.229
	CDN	0.011	0.15	0.01	3	0.230	0.220	0.242
	SDNCO	0.008	0.6	0.01	1	0.230	0.230	0.224
	SLSUBBSN	0.002	3	1	5	0.230	0.230	0.229
	PSP	0.001	0.69	0.1	0.9	0.230	0.230	0.230
	PRF	0.000	0.5	0.1	2	0.230	0.230	0.230
	SPCON	0.000	0.00008	0	0.01	0.230	0.230	0.230
TSS (ton/day)	SLSUBBSN	1.580	3	1	5	1.190	0.137	1.184
	PRF	1.316	0.5	0.1	2	1.190	0.137	5.098
	ESCO	1.221	0.5	0.01	1	1.190	0.901	2.411
	SPCON	0.243	0.00008	0	0.01	1.190	1.433	8.495
	EPCO	0.228	0.7	0.01	1	1.190	1.415	1.181
	SDNCO	0.156	0.6	0.01	1	1.190	1.220	1.086
	CDN	0.129	0.15	0.01	3	1.190	1.070	1.434
	PSP	0.004	0.69	0.1	0.9	1.190	1.189	1.189
PO4 (kg/day)	PSP	1.240	0.69	0.1	0.9	0.210	1.271	0.180
	ESCO	0.228	0.5	0.01	1	0.210	0.163	0.438
	EPCO	0.058	0.7	0.01	1	0.210	0.267	0.213
	SDNCO	0.023	0.6	0.01	1	0.210	0.216	0.225
	CDN	0.017	0.15	0.01	3	0.210	0.226	0.246
	SLSUBBSN	0.011	3	1	5	0.210	0.214	0.217

Output Variable	Parameter	Sensitivity Index	Parameter Values			Results for Output Variable of Concern ^a		
			Base	Min	Max	Base	Min Param	Max Param
	PRF	0.005	0.5	0.1	2	0.210	0.214	0.214
	SPCON	0.004	0.00008	0	0.01	0.210	0.214	0.214
Organic P (kg/day)	PSP	4.719	0.69	0.1	0.9	0.990	5.025	0.834
	ESCO	0.952	0.5	0.01	1	0.990	0.771	1.942
	SDNCO	0.435	0.6	0.01	1	0.990	1.120	0.700
	CDN	0.319	0.15	0.01	3	0.990	0.692	1.879
	SLSUBBSN	0.195	3	1	5	0.990	0.988	1.120
	EPCO	0.087	0.7	0.01	1	0.990	1.075	0.992
	PRF	0.003	0.5	0.1	2	0.990	0.988	0.988
	SPCON	0.002	0.00008	0	0.01	0.990	0.988	0.988
Nitrate+ Nitrite (kg/day)	ESCO	4.679	0.5	0.01	1	4.480	3.738	9.159
	SDNCO	3.463	0.6	0.01	1	4.480	4.020	6.789
	CDN	2.989	0.15	0.01	3	4.480	7.270	1.507
	EPCO	0.405	0.7	0.01	1	4.480	4.880	4.452
	PSP	0.012	0.69	0.1	0.9	4.480	4.484	4.484
	SLSUBBSN	0.007	3	1	5	4.480	4.479	4.485
	PRF	0.001	0.5	0.1	2	4.480	4.479	4.479
	SPCON	0.001	0.00008	0	0.01	4.480	4.479	4.479
Ammonium (kg/day)	ESCO	0.000	0.5	0.01	1	0.000	0.000	0.000
	EPCO	0.000	0.7	0.01	1	0.000	0.000	0.000
	SPCON	0.000	0.00008	0	0.01	0.000	0.000	0.000
	PSP	0.000	0.69	0.1	0.9	0.000	0.000	0.000
	CDN	0.000	0.15	0.01	3	0.000	0.000	0.000
	SDNCO	0.000	0.6	0.01	1	0.000	0.000	0.000
	PRF	0.000	0.5	0.1	2	0.000	0.000	0.000
	SLSUBBSN	0.000	3	1	5	0.000	0.000	0.000
Organic N (kg/day)	ESCO	6.097	0.5	0.01	1	6.260	4.885	12.357
	SDNCO	2.797	0.6	0.01	1	6.260	7.130	4.395
	CDN	2.057	0.15	0.01	3	6.260	4.340	12.070
	SLSUBBSN	1.263	3	1	5	6.260	6.259	7.102
	EPCO	0.637	0.7	0.01	1	6.260	6.888	6.287
	PSP	0.005	0.69	0.1	0.9	6.260	6.259	6.258
	PRF	0.002	0.5	0.1	2	6.260	6.259	6.259
	SPCON	0.001	0.00008	0	0.01	6.260	6.259	6.259

Table 3-29 Sensitivity Results for the Inks Lake SWAT Model

Output Variable	Parameter	Sensitivity Index	Parameter Values			Results for Output Variable of Concern ^a		
			Base	Min	Max	Base	Min Param	Max Param
Flow (m ³ /s)	ESCO	0.035	0.5	0.01	1	0.0383	0.0329	0.0731
	SLSUBBSN	0.015	3	1	5	0.0383	0.0482	0.0359
	EPCO	0.003	0.7	0.01	1	0.0383	0.0414	0.0382
	SDNCO	0.000	0.6	0.01	1	0.0383	0.0383	0.0382
	CDN	0.000	0.15	0.01	3	0.0383	0.0382	0.0388
	PSP	0.000	0.69	0.1	0.9	0.0383	0.0383	0.0383
	SPCON	0.000	0.00008	0	0.01	0.0383	0.0383	0.0383
	PRF	0.000	0.5	0.1	2	0.0383	0.0383	0.0383
TSS (ton/day)	PRF	0.232	0.5	0.1	2	0.1133	0.0103	0.8097
	ESCO	0.099	0.5	0.01	1	0.1133	0.1003	0.2120
	SLSUBBSN	0.039	3	1	5	0.1133	0.1390	0.1080
	SPCON	0.027	0.00008	0	0.01	0.1133	0.1406	2.3881
	EPCO	0.014	0.7	0.01	1	0.1133	0.1266	0.1131
	SDNCO	0.001	0.6	0.01	1	0.1133	0.1136	0.1126
	CDN	0.001	0.15	0.01	3	0.1133	0.1126	0.1161
	PSP	0.000	0.69	0.1	0.9	0.1133	0.1133	0.1133
PO4 (kg/day)	PSP	0.287	0.69	0.1	0.9	0.0319	0.2774	0.0263
	ESCO	0.032	0.5	0.01	1	0.0319	0.0269	0.0636
	SDNCO	0.011	0.6	0.01	1	0.0319	0.0310	0.0394
	CDN	0.008	0.15	0.01	3	0.0319	0.0392	0.0334
	EPCO	0.001	0.7	0.01	1	0.0319	0.0333	0.0316
	SLSUBBSN	0.001	3	1	5	0.0319	0.0314	0.0322
	SPCON	0.000	0.00008	0	0.01	0.0319	0.0319	0.0319
	PRF	0.000	0.5	0.1	2	0.0319	0.0319	0.0319
Organic P (kg/day)	PSP	1.235	0.69	0.1	0.9	0.1949	1.2509	0.1551
	ESCO	0.222	0.5	0.01	1	0.1949	0.1564	0.4168
	SLSUBBSN	0.093	3	1	5	0.1949	0.1328	0.2304
	SDNCO	0.036	0.6	0.01	1	0.1949	0.2049	0.1709
	CDN	0.026	0.15	0.01	3	0.1949	0.1711	0.2986
	EPCO	0.015	0.7	0.01	1	0.1949	0.2099	0.1950
	SPCON	0.000	0.00008	0	0.01	0.1949	0.1949	0.1949
	PRF	0.000	0.5	0.1	2	0.1949	0.1949	0.1949
Nitrate+ Nitrite (kg/day)	ESCO	0.515	0.5	0.01	1	0.6501	0.5700	1.1647
	SDNCO	0.319	0.6	0.01	1	0.6501	0.6126	0.8629
	CDN	0.230	0.15	0.01	3	0.6501	0.8650	0.3211

Output Variable	Parameter	Sensitivity Index	Parameter Values			Results for Output Variable of Concern ^a		
			Base	Min	Max	Base	Min Param	Max Param
	SLSUBBSN	0.120	3	1	5	0.6501	0.7299	0.6198
	EPCO	0.051	0.7	0.01	1	0.6501	0.7002	0.6483
	PSP	0.000	0.69	0.1	0.9	0.6501	0.6501	0.6501
	SPCON	0.000	0.00008	0	0.01	0.6501	0.6501	0.6501
	PRF	0.000	0.5	0.1	2	0.6501	0.6501	0.6501
Ammonium (kg/day)	ESCO	0.008	0.5	0.01	1	0.0100	0.0088	0.0184
	SLSUBBSN	0.002	3	1	5	0.0100	0.0112	0.0090
	EPCO	0.001	0.7	0.01	1	0.0100	0.0107	0.0099
	SDNCO	0.000	0.6	0.01	1	0.0100	0.0100	0.0099
	CDN	0.000	0.15	0.01	3	0.0100	0.0099	0.0100
	SPCON	0.000	0.00008	0	0.01	0.0100	0.0100	0.0100
	PSP	0.000	0.69	0.1	0.9	0.0100	0.0100	0.0100
	PRF	0.000	0.5	0.1	2	0.0100	0.0100	0.0100
Organic N (kg/day)	ESCO	1.239	0.5	0.01	1	1.0486	0.8366	2.2874
	SLSUBBSN	0.542	3	1	5	1.0486	0.6875	1.2524
	SDNCO	0.204	0.6	0.01	1	1.0486	1.1056	0.9125
	CDN	0.144	0.15	0.01	3	1.0486	0.9138	1.6419
	EPCO	0.100	0.7	0.01	1	1.0486	1.1472	1.0491
	SPCON	0.000	0.00008	0	0.01	1.0486	1.0486	1.0486
	PSP	0.000	0.69	0.1	0.9	1.0486	1.0486	1.0486
	PRF	0.000	0.5	0.1	2	1.0486	1.0486	1.0486

^a Average of the results for the entire simulation period (1984-2008) for Clear Creek (Reach 10)

For all three models, it was found that phosphorus concentrations are most sensitive to the phosphorus availability index (PSP) and the soil evaporation compensation factor (ESCO). The equilibration between the soluble and active mineral pool for phosphorus is governed by the PSP. This index specifies the fraction of fertilizer P that is in solution after an incubation period or the rapid reaction period. This factor relate to the amount of phosphorus available especially in the upper layers of the soil. The ESCO coefficient modifies the depth distribution used to meet the soil evaporative demand to account for the effect of capillary action, crusting and cracks and is related to soil nutrient availability.

Nitrogen concentrations are sensitive to ESCO, SLSUBBSN, and SDNCO. As explained above, ESCO is related to soil nutrient availability. Regarding SLSUBBSN, the average slope length, this is the distance that sheet flow is the dominant surface runoff flow process and is also directly related to erosive potential. SDNCO represents the fraction of field capacity water content above which denitrification takes place.

THIS PAGE INTENTIONALLY LEFT BLANK

SECTION 4 LAKE MODEL

4.1 Introduction

The lake model selected for Phase 3 of CREMs is CE-QUAL-W2 (version 3.6), a two-dimensional laterally averaged hydrodynamic and water quality model developed and maintained by the USACE Waterways Experiment Station. Model selection was based on the model evaluation section in the Master Plan (CH2M Hill 2002), results from the Phase 1 work, and discussions within the project team. Selection of CE-QUAL-W2 version 3.6 also maintains compatibility with the model used for CREMs Phase 2 modeling of Lake Travis (CE-QUAL-W2 version 3.5), while incorporating recent improvements to the model code. CE-QUAL-W2 is best suited for relatively long and narrow water bodies, such as Lakes Travis, LBJ, Inks, and Marble Falls, that exhibit longitudinal and vertical water quality gradients. The model has been applied to rivers, lakes, reservoirs, and estuaries across the United States (Cole and Wells 2008). In addition, the SWAT and CE-QUAL-W2 models have been successfully linked for other sites such as the Cedar Creek Reservoir, Texas (Debele et al. 2006). This section describes the development and calibration of the CE-QUAL-W2 model for Lakes Inks, LBJ, and Marble Falls.

Three separate reservoir models were developed: one for each of Lakes Inks, LBJ, and Marble Falls. Although the models were developed independently, and designed to run in stand-alone mode, there were some flow and water quality linkages among outputs from the upstream lake and inputs to the next reservoir downstream. Most modeling procedures and data inputs were the same for all three models, and a single description adequately describes all three. In other parts of this section, separate descriptions of each model will be required.

4.1.1 Spatial Domain, Model Segmentation, and Bathymetry

The lakes are modeled in CE-QUAL-W2 in two dimensions, in the longitudinal direction (i.e., spatially, in the direction of flow) and in the vertical direction (i.e., at depth). The CE-QUAL-W2 models divided the lakes longitudinally into multiple segments of varying length, and vertically into layers of fixed height. In addition to the main Colorado River channel of the lakes, inundated channels of tributary streams and other coves are included in the models as “branches” off the main channel, composed of one or more segments. Each longitudinal segment extends from “bank to bank” and therefore, the model predicts average concentrations for each segment in the direction transverse to flow. CE-QUAL-W2 predicts average concentrations for each vertical model layer. During a model simulation, the number and thickness of vertical segments remain fixed and the vertical segments become variably wet (i.e., active) or dry (i.e., inactive) depending on the water surface elevation of the lake.

The widths of each of the model computational elements, formed by the longitudinal and vertical segmentation of the model domain, was determined from bathymetric surveys performed on each lake in 2007 (TWDB 2007a,b; 2009). A Triangulated Irregular Network developed from the bathymetric surveys was queried in ArcGIS™ to provide the widths of each longitudinal segment at elevations corresponding to the top and bottom of each vertical layer. These widths served as the primary input to the CE-QUAL-W2 bathymetry file. The lengths and orientation of each longitudinal segment were also determined using ArcGIS. The

widths of some cells were manually adjusted in cases where they caused numerical instability in the model or to improve computational efficiency. This typically occurred when segments widths were less than 5 m (10 m for Lake Marble Falls). The adequacy of the CE-QUAL-W2 model bathymetry was evaluated by comparing its elevation-volume relationship to that measured during the bathymetric survey.

4.1.1.1 Inks Lake

Inks Lake is a 4.3 mile long run-of-the-river reservoir formed by the impoundment of the Colorado River by Roy Inks Dam. Releases from Lake Buchanan through Buchanan Dam comprise almost all of the inflows to Inks Lake; the local contributing watershed covers only approximately 100 km². The lake forms a sideways “J” shape, progressively widening from 160 m in the upstream reaches to 640 m near Inks Dam. When full, the lake surface area covers 788 acres (3.19 km²) and impounds 14,074 acre-feet (1.74x10⁷ m³) of water. The deepest point, near Inks dam, is more than 18 m below the surface. Inks Lake is the second smallest of the Highland Lakes in terms of volume. Except during periodic lowerings for dam or dock maintenance, the lake elevation seldom varies by more than a foot from its standard operating level of 887.6 feet NAVD88 (270.34 m). The historical elevation range since 1980 is 877.1 to 896.1 ft.

The longitudinal segmentation for the main body of the Lake begins below Buchanan Dam and ends at Roy Inks Dam (Figure 4-1). The model domain also includes two coves on the north and east sides of the lake formed by Clear Creek and Spring Creek. Table 4-1 summarizes the longitudinal segmentation and dimensions of the CE-QUAL-W2 model representing Inks Lake. The entire model domain consists of 24 longitudinal divisions, called segments, in three branches. Six of the longitudinal segments are “dummy” segments required at the upstream and downstream boundaries of each branch.

Table 4-1 Summary of Longitudinal Segmentation for Inks Lake CE-QUAL-W2 Model

Branch	Number of Active Longitudinal Model Segments	Average Length (m)	Average Width (m) at Surface Elevation of		
			267 m	270 m	273 m
Inks Lake (Main Branch)	14	494	250	367	506
Clear Creek Cove	2	679	15	121	276
Spring Creek Cove	2	625	38	163	296
Total	18	529	200	317	457

The lake model was segmented vertically into 24 layers, including “dummy” layers on the top and bottom. Each layer was one meter thick. The computational grid in the longitudinal/vertical plane is shown in Figure 4-2.

Figure 4-3 compares the measured and model elevation-volume relationship. The percent difference in volume was less than 1% for all elevations.

4.1.1.2 Lake LBJ

Lake LBJ is a 21 mile long reservoir formed by the impoundment of the Colorado River by Alvin Wirtz Dam. Releases and spillage from Inks Lake comprise roughly half of the inflows to Lake LBJ. The Llano River, draining a watershed of roughly 11,000 km², makes up the majority of the balance. It enters the main channel of Lake LBJ from the west approximately nine river miles downstream of Inks Dam. The lake is somewhat sinuous, progressively widening from as narrow as 50 m in the upstream reaches to more than 1 km near Wirtz Dam. When full, the lake surface area covers 6,273 acres (25.4 km²) and impounds 133,090 acre-feet (1.64x10⁸ m³) of water. The deepest point, near Wirtz Dam, is more than 22 m below the surface. Lake LBJ is considered full at an elevation of 251.67 m (NAVD88), and its normal operating range is from 251.48 to 251.67 m.

The lake model domain consists of the main Colorado River channel of Lake LBJ, the inundated channels of the Llano River and Sandy Creek, and eight other coves formed by smaller tributaries (Figure 4-4). The longitudinal segmentation for the main body of Lake LBJ begins below Roy Inks Dam and ends at Alvin Wirtz Dam. Table 4-2 summarizes the longitudinal segmentation and dimensions of the CE-QUAL-W2 model representing Lake LBJ. The entire model domain consists of 107 longitudinal segments, in eleven branches, although 22 of the longitudinal segments are “dummy” segments required at the upstream and downstream boundaries of each branch. The Lake LBJ model was segmented vertically into 26 layers, including “dummy” layers on the top and bottom. Each layer was one meter thick. The computational grid in the longitudinal/vertical plane is shown in Figure 4-5.

The adequacy of the CE-QUAL-W2 model bathymetry was evaluated by comparing its elevation-volume relationship to that measured during the bathymetric survey. Figure 4-6 compares the measured and model elevation-volume relationship. The percent difference in volume was less than 1% for all elevations.

Table 4-2 Summary of Longitudinal Segmentation for Lake LBJ CE-QUAL-W2 Model

Branch	Number of Active Longitudinal Model Segments	Average Length (m)	Average Width (m) at Surface Elevation of		
			250.8 m	251.8 m	252.8 m
Lake LBJ (Main Branch)	53	637	466	506	569
Llano River Arm	9	598	205	248	287
Dry Creek Cove	3	685	221	299	363
Spring Branch Cove	2	475	547	640	748
Sandy Creek Cove	3	497	350	477	578
Pecan Creek Cove	2	449	262	344	424
Unnamed Cove	2	463	254	298	345

Branch	Number of Active Longitudinal Model Segments	Average Length (m)	Average Width (m) at Surface Elevation of		
			250.8 m	251.8 m	252.8 m
Elm Creek Cove	2	627	318	400	468
Unnamed Cove	2	498	372	430	493
Slickrock Creek Cove	5	665	477	512	567
Horseshoe Creek Cove	2	699	385	432	490
Total	85	617	412	460	521

4.1.1.3 Lake Marble Falls

Lake Marble Falls is a 5.75 mile long run-of-the-river reservoir formed by the impoundment of the Colorado River by Max Starcke Dam. Releases from Lake LBJ comprise almost all of the inflows to Lake Marble Falls; the local contributing watershed covers only approximately 204 km². The lake is long and narrow, with widths ranging from about 90 to 330 meters. When full, the lake surface area covers 608 acres (2.46 km²) and impounds 7,486 acre-feet (9.23 x 10⁶ m³) of water. The deepest point, near Max Starcke Dam, is more than 18 m below the surface. Lake Marble Falls is the smallest of the Highland Lakes in terms of volume. Except during periodic lowerings for dam or dock maintenance, the lake elevation seldom varies by more than a foot from its standard operating level of 738.19 ft NAVD88 (225.04 m). The normal operating range is 736.39 to 737.19 ft.

The longitudinal segmentation for the main body of the Lake Marble Falls begins below Wirtz Dam and ends at Max Starcke Dam (Figure 4-7). Table 4-3 summarizes the longitudinal segmentation and dimensions of the CE-QUAL-W2 model representing Lake Marble Falls. The model domain consists of 27 longitudinal segments in one branch. Two of the longitudinal segments are “dummy” segments required at the upstream and downstream boundaries of each branch.

Table 4-3 Summary of Longitudinal Segmentation for Lake Marble Falls CE-QUAL-W2 Model

Waterbody	Number of Active Longitudinal Model Segments	Average Length (m)	Average Width (m) at Surface Elevation of		
			224 m	225 m	226 m
Lake Marble Falls	25	410	168	213	250

The lake model was segmented vertically into 24 layers, including “dummy” layers on the top and bottom. Each layer had a fixed thickness of one meter. The computational grid in the longitudinal/vertical plane is shown in Figure 4-8. Adjustments to bottom-most layers were necessary in the shallow upstream half of the lake due to model stability issues; the minimum width allowed for bottom active segments was five meters and several widths of bottom active cells were increased from zero at certain locations for simulation stability.

Figure 4-9 compares the measured and model elevation-volume relationship. The percent difference in volume ranged from 1.7 to 2.4% for elevations within the normal lake operating range.

4.1.2 Model Time Period

The lake models were developed and calibrated using data from January 1, 1984 through December 31, 2008, matching the time period of the output from the watershed model calibration (Section 3). CE-QUAL-W2 internally calculates the time step necessary for the model to maintain hydrodynamic numerical stability. The minimum time step specified was one second (0.1 second for Lake Marble Falls) and the maximum time step allowed was set to 360 seconds. The models were specified to output values for each day simulated.

4.1.3 General Processes Modeled

CE-QUAL-W2 contains both hydrodynamic and water quality components. For hydrodynamics and associated constituent transport, CE-QUAL-W2 uses laterally averaged equations of fluid motion, namely equations for continuity and for conservation of momentum. Included in these equations are velocity, acceleration, gravity, pressure, and turbulent shear stresses. Additional governing equations incorporated are the equation of state, which relates density to temperature and concentration of dissolved substances, and the equation of free water surface, which integrates continuity over the depth of the water column. For details on the hydrodynamic and constituent transport processes that CE-QUAL-W2 simulates, see Appendix A of the user manual (Cole and Wells 2008).

For water quality, CE-QUAL-W2 computes the concentrations of user-specified state variables such as algae, dissolved oxygen, organic matter, and sediment for each model segment and each time step using constituent-specific rate equations that account for sources and sinks associated with biological and chemical processes. The user can specify any number of generic constituents, suspended solids groups, CBOD groups, algal groups, macrophyte groups, zooplankton groups, and epiphyton groups. The full list of state variables available in CE-QUAL-W2 version 3.6 is given in Table 4-5. Numerous processes are associated with these variables (e.g., algal dynamics include photosynthesis, respiration, settling, mortality, and excretion). For detailed descriptions of all water quality processes simulated by CE-QUAL-W2, see Appendix B of the CE-QUAL-W2 user manual (Cole and Wells 2008).

4.1.4 Calibration Metrics and Goals

The CE-QUAL-W2 models were manually calibrated to observed water quality measurements from January 1, 1984 through December 31, 2008. To evaluate model goodness of fit (GOF) to observed data, it is typical to identify quantitative calibration metrics that compare simulated constituents with measured data. GOF measures should quantify 1) model bias, 2) absolute error, and 3) relative error. GOF metrics are described in detail in Appendix C. Throughout Section 4, various model-to-data GOF measures are provided with the calibration results. The absolute mean error (AME) is an indicator of model accuracy, and is the primary indicator of model GOF, as recommended by Cole and Wells (2002). The AME is simply calculated and directly interpretable, i.e., it is in the same units as the measurement. The mean error (ME) is used as a measure of the bias of model predictions. The Reliability

Index (RI) of Leggett and Williams (1981) is applied as a measure of relative error. The RI indicates the average factor by which model predictions differ from observations. A RI of 1.0 indicates a perfect fit. If all predicted values are one-half order of magnitude apart, a RI of 5 will result. RI values of less than 3 are generally considered to be acceptable for most parameters. RI values of greater than 10 usually indicate extremely low values near detection limits, as often found with some nutrient species, or highly variable parameters, such as algae biomass. One of the weaknesses of the RI is that the values are difficult to interpret since they are unitless and their range is expected to vary by parameter.

Cole and Wells (2002) do not provide guidelines regarding *a priori* acceptable levels of error for CE-QUAL-W2. Ultimately, acceptable levels of error should be based on model uncertainty versus water quality prediction requirements of lake managers. However, based on a review of reported model calibration metrics in other systems, calibration goals for AME were identified for some parameters that were optimistically considered potentially achievable (Table 4.4). These calibration goals are not considered strict criteria, but rather as guidelines or objectives. It is worth noting that most of the reports used much shorter data collection periods for calibration data, and had fewer monitoring sites. By calibrating to twenty-five years of data, the CREMS model calibration addresses a very broad range of environmental conditions, enhancing its utility for predicting future water quality. However, in addition to natural variation, calibration to a dataset collected over 25 years incorporates concomitant data uncertainty due to changes in analytical methods, sampling procedures, and data quality objectives that may contribute to inflation of the overall AME metric relative to that reported in short-term modeling efforts. An artificial contribution to AME inflation occurs for parameters that sometimes occur below analytical detection limits. As an example, if an orthophosphate phosphorus concentration was reported as less than a detection limit of 0.040 mg/L, and the model predicted a concentration of 0.001 mg/L, the error was calculated as 0.039 mg/L, though the error may have been 0. For these reasons, the AME calibration goals were applied only as objectives and guidelines, not as strict criteria. The ultimate determination of model calibration is better judged based on the spatial-temporal calibration plots included as figures later in Section 4.

Table 4-4. Calibration Goals† for Absolute Mean Error

Parameter	Units	Absolute Mean Error
Water level	meters	0.2
Water temperature	°C	1
Total organic carbon	mg/l	0.6
Chlorophyll a	µg/l	4
Total Kjeldahl nitrogen	mg/l	0.4
Ammonia nitrogen	mg/l	0.03
Nitrate+nitrite nitrogen	mg/l	0.1
Total phosphorus	mg/l	0.02
Orthophosphate phosphorus	mg/l	0.01

†these are average AME goals for the system as a whole

4.2 Model Overview

The modeling of Lakes Inks, LBJ, and Marble Falls was divided into two major steps. The hydrodynamic portions of the models were simulated first to predict water transport including flows, depths, velocities, water surface elevations, temperature, and conservative constituents such as chloride. The water quality portions of the models were then applied to simulate the major processes of eutrophication kinetics. After water quality calibration, hydrodynamics were checked again as parameters such as suspended solids affect light penetration and therefore potentially affect water temperature, density, and movement.

4.2.1 State Variables of Concern

The CE-QUAL-W2 model includes a variety of optional state variables to simulate aquatic systems using models of varying complexity. The state variables chosen for water quality simulation are listed in Table 4-5.

Table 4-5 List of Water Quality State Variables in CE-QUAL-W2 Version 3.6

Constituent Name	Include in Phase 3 Models?	Comments
Generic constituents	Yes	Included chloride, specific conductivity, total dissolved solids, water age
Inorganic suspended solids (ISS)	Yes	One class included
Algae	Yes	Four groups included
Epiphyton	No	Insufficient ambient data for simulation
CBOD	No	Modeled as organic matter groups
Ammonium (NH ₄)	Yes	
Nitrite+nitrate (NO ₂ +NO ₃)	Yes	
Bioavailable phosphorus (e.g., PO ₄)	Yes	
Labile dissolved organic matter (LDOM)	Yes	
Refractory dissolved organic matter (RDOM)	Yes	
Labile particulate organic matter (LPOM)	Yes	
Refractory particulate organic matter (RPOM)	Yes	
Dissolved silica	No	Insufficient ambient data for simulation
Particulate biogenic silica	No	Insufficient ambient data for simulation
Total inorganic carbon	No	Total inorganic carbon is not an issue of management concern and does not significantly impact other state variables.
Alkalinity	No	Alkalinity is not an issue of management concern and does not significantly impact other state variables.

Constituent Name	Include in Phase 3 Models?	Comments
Total iron	No	Iron is included in CE-QUAL-W2 primarily as a sorption site for PO ₄ . This mechanism is not expected to be significant in the Highland Lakes; thus it was not simulated.
DO	Yes	
Organic sediments	No	Organic sediments were not specified because the method selected for simulation uses a constant release and demand instead of using a sediment compartment to accumulate organic sediments and allow their decay.
Macrophytes	No	Insufficient ambient data for simulation
Zooplankton	No	Parameterized as mortality rate of phytoplankton
Labile dissolved organic matter-phosphorus (LDOM-P)	Yes	
Refractory dissolved organic matter-phosphorus (RDOM-P)	Yes	
Labile particulate organic matter-phosphorus (LPOM-P)	Yes	
Refractory particulate organic matter-phosphorus (RPOM-P)	Yes	
Labile dissolved organic matter-nitrogen (LDOM-N)	Yes	
Refractory dissolved organic matter-nitrogen (RDOM-N)	Yes	
Labile particulate organic matter-nitrogen (LPOM-N)	Yes	
Refractory particulate organic matter-nitrogen (RPOM-N)	Yes	

4.3 Water Balance

A water balance was developed for the Colorado River system from Buchanan Dam to Max Starcke Dam. The objective of this effort was to achieve daily water balances for the three lake system (Inks, LBJ, and Marble Falls) while minimizing any required adjustments (in terms of frequency and magnitude) from the reported water release time series. Attempts were also made to link the water balance for the Phase 3 lakes to the existing water balance of the Lake Travis model. A linked water balance time series facilitates linking of the lake models.

The numerical stability of CE-QUAL-W2 is highly sensitive to the water balance. Given the model requirement for mass balance, an imbalance between inflows and outflows will result in changes in lake volume and surface elevation in the model.

The water balance was based on the available data on water releases from lakes (including hydroelectric generation, releases through floodgates, and spillage [Inks Lake]), lake elevations, evaporation, precipitation, point source discharges, and tributary and watershed runoff inflow estimates from the three calibrated SWAT models (see Section 3). The data sources used are described in Appendix A.

The water balance was calculated on a daily time step, and compared to measured water surface elevations for each lake at the dam. While small deviations from measured elevations were expected, large daily deviations or systematic discrepancies between inflows and outflows are not physically realistic for small lakes such as Inks Lake and Lake Marble Falls, and quickly resulted in unrealistic lake elevations and volumes in the CE-QUAL-W2 models. When adjustments to inflows and/or outflows were required to achieve a daily water balance, it was typically necessary to adjust the inflows and/or outflows at the dams. While there is significant uncertainty in the watershed and tributary inflows predicted by the SWAT watershed models, these inflows were small compared to the total inflow and often insufficient to make up the required volume. The water balance procedure is described in detail in Appendix A.

4.4 Hydrodynamics and Temperature Model Development and Calibration

4.4.1 Model Inputs

Hydrodynamic and temperature inputs to the lake models include initial conditions, flows, boundary temperatures, and meteorological data. Each of these is described in more detail below.

4.4.1.1 Initial Conditions

For each model element (longitudinal and vertical), the initial water temperature on January 1, 1984 was set to 10 °C. This temperature was estimated based on interpolation between average temperatures in the lakes (all depths and locations) on December 12, 1983, January 12, 1984, and January 17, 1984. The lakes were not thermally stratified at that time.

4.4.1.2 Flows

4.4.1.2.1 Inks Lake

Table 4-6 describes the inflows and outflows to/from the Inks Lake model. These same flows were used in development of the water balance (Section 4.3). Tributary and watershed runoff inflow estimates were derived from the output of the calibrated SWAT models. There are no direct point source wastewater discharges to the lake.

Precipitation and evaporation were simulated as a net distributed tributary discharge spread evenly across the main branch (branch 1). The evaporation and precipitation data sets are described in Appendix A. Because evaporation typically exceeded precipitation, these

distributed tributary discharges were negative on most days, corresponding to a net withdrawal of water.

Each of the inflows and outflows was specified as a daily time series in units of cubic meters per second (cms).

Table 4-6 Inks Lake Model Flows: Tributaries, Outflows and Directly Connected Watersheds

Branch	Segment	Inflow/Outflow Name
1	2	Buchanan Dam (Colorado River)
1	2	SWAT sub-basin 25
1	4	SWAT sub-basin 27
1	5	SWAT sub-basin 33
1	6	SWAT sub-basin 32 and reach 26
1	7	SWAT sub-basin 34
1	8	SWAT sub-basin 35
1	10	SWAT sub-basin 39
1	12	SWAT sub-basin 41
1	13	SWAT sub-basin 43
1	14	SWAT sub-basins 44 and 46, and reach 45
1	15	SWAT sub-basin 47
1	15	Outflow (Inks Dam)
2	18	Clear Creek
2	18	SWAT sub-basin 16
2	19	SWAT sub-basins 30 and 24, and reach 23
3	22	Spring Creek
3	22	SWAT sub-basin 38
3	23	SWAT sub-basin 40

4.4.1.2.2 Lake LBJ

Table 4-7 describes the inflows and outflows to/from the Lake LBJ model. These same flows were used in development of the water balance (Section 4.3). Tributary and watershed runoff inflow estimates were derived from the output of the calibrated SWAT models. Point source discharges were derived from monthly DMRs for periods for which DMRs were available, or estimated as the long-term average discharge flows for periods when DMR data was not available. There were few point source discharges to the lakes, and most were very minor in terms of flow. The largest discharge is that from the LCRA Thomas C. Ferguson power plant, which discharges to the downstream reaches of Lake LBJ. However, this discharge is almost completely composed of once-through cooling water withdrawn from Lake

LBJ a short distance upstream. Evaporative losses during use for cooling were calculated according to a formula provided by the LCRA:

$$\text{Evaporative loss (mgd)} = (T_{\text{out}} - T_{\text{in}}) * \text{Circulating Water (mgd)} * 0.00181029$$

where T_{in} and T_{out} represent the measured water temperatures at the Ferguson Plant's intake and discharge, respectively. Measured daily water temperatures at the intake and discharge, as well as water circulation rate, were provided by the LCRA.

Precipitation and evaporation were simulated as a net distributed tributary discharge spread evenly across the main branch (branch 1) of each model. The evaporation and precipitation data sets are described in Appendix A. Because evaporation typically exceeded precipitation, these distributed tributary discharges were negative on most days, corresponding to a net withdrawal of water.

Each of the inflows and outflows was specified as a daily time series in units of cms.

Table 4-7 Lake LBJ Model Inflows: Tributaries, Discharges, Outflows, Withdrawals, and Directly Connected Watersheds

Branch	Segment	Inflow/Outflow Name
1	2	Inks Dam (Colorado River)
1	4	Peters Creek (SWAT sub-basin 30)
1	15	Williams Creek (SWAT sub-basin 36)
1	26	AquaSource Utilities discharge
1	28	Mill Creek (SWAT sub-basin 43)
1	32	SWAT sub-basin 46
1	38	SWAT sub-basin 50
1	46	Ferguson Power Plant intake (withdrawal)
1	54	Wirtz Dam (outflow)
2	57	Llano River (SWAT reach 41)
2	59	Moss Creek (SWAT sub-basin 42)
2	79	Kingsland MUD discharge
3	68	Dry Creek (SWAT sub-basin 52)
4	73	SWAT sub-basin 47
5	77	Sandy Creek and Walnut Creek (SWAT reach 55)
6	82	Pecan Creek (SWAT reach 59)
7	86	SWAT sub-basin 51
8	91	Elm Creek (SWAT reach 49 and 57)
9	94	SWAT sub-basin 60
10	98	Slickrock Creek (SWAT reach 58)

Branch	Segment	Inflow/Outflow Name
10	100	Ferguson Power Plant discharge
11	105	Horseshoe Creek (SWAT reach 65)

4.4.1.2.3 Lake Marble Falls

Inflows and outflows to/from the Lake Marble Falls model are listed in Table 4-8. These same flows were used in development of the water balance (Section 4.3). Tributary and watershed runoff inflow estimates were derived from the output of the calibrated SWAT models. There are no direct point source wastewater discharges to the lake.

Precipitation and evaporation were simulated as a net distributed tributary discharge spread evenly across the main branch (branch 1). The evaporation and precipitation data sets are described in Appendix A. Because evaporation typically exceeded precipitation, these distributed tributary discharges were negative on most days, corresponding to a net withdrawal of water.

Each of the inflows and outflows was specified primarily as a daily time series in units of cms. During high flow events, however, it was necessary to interpolate flows to sub-daily values (0.1 day) in order to maintain numerical stability.

Table 4-8 Lake Marble Falls Model Flows: Outflows and Directly Connected Watersheds

Branch	Segment	Inflow/Outflow Name
1	2	Wirtz Dam (Colorado River)
1	2	SWAT sub-basin 18
1	4	SWAT reach 15
1	5	SWAT sub-basin 13
1	6	SWAT reach 11 and sub-basin 14
1	7	SWAT reach 12
1	8	SWAT sub-basin 19
1	10	SWAT sub-basin 21
1	11	SWAT reach 24 and sub-basin 26
1	14	SWAT reach 28 and sub-basin 25
1	15	SWAT reach 27
1	16	SWAT sub-basin 20
1	18	SWAT reach 16
1	19	SWAT sub-basin 17
1	23	SWAT sub-basin 23
1	26	SWAT reach 22
1	26	Outflow (Max Starcke Dam)

4.4.1.3 Boundary Temperatures

Boundary water temperatures for flows from upstream lakes, tributaries and non-point sources, as well as temperature of the sediment bed, were needed as model inputs. Boundary temperatures were estimated as described below.

4.4.1.3.1 Upstream Water Temperatures

Daily water temperatures for flow to each lake from upstream were linearly interpolated from depth-averaged measurements taken typically on a monthly or weekly basis at the following LCRA water quality monitoring sites:

- Inks Lake model: Site 12344 (Lake Buchanan near Buchanan Dam),
- Lake LBJ model: Site 12336 (Inks Lake near Inks Dam),
- Lake Marble Falls model: Site 12323 (Marble Falls at the headwaters).

From March 2007 through 2008, these measurements were supplemented for the Lake LBJ model by twice daily measurements using an automated profiler at site 12324 (see Section 2.4).

4.4.1.3.2 Tributary Water Temperatures

Daily water temperatures for inflows from the Llano River and Sandy Creek were linearly interpolated from data collected at LCRA sites 12383 (Llano River at County Road 6.5 miles upstream from Kingsland) and 12214 (Sandy Creek at State Highway [SH] 71 south of Kingsland). Measurements at these stations were made monthly from 1984 through mid-1989, every two months from mid-1989 to 2006, and weekly from 2007 through 2008. Linear interpolation between measurements was performed to obtain temperature values for days without data.

Water temperatures for model inflows from Walnut Creek were derived from hourly measurements recorded by thermistors deployed at LCRA site LC917 (Walnut Creek at SH 71) from May 15, 2007 through November 2008. Similarly, water temperatures for inflows from Slickrock Creek were derived from hourly measurements recorded by thermistors deployed at LCRA site LC916 (Slickrock Creek at FM 2147) from March 12, 2007 through May 29, 2008. For other time periods during 2007 and 2008, water temperatures in these tributaries were linearly interpolated from data collected on a monthly basis at these sites. No water temperature measurements were available on these tributaries prior to 2007. Thus, a water temperature time series for the model was calculated from the average of the Llano River and Sandy Creek temperature time series on each date.

Water temperature data for other tributaries to Lake LBJ were not available. Thus, a water temperature time series for the model was calculated from the average of the Llano River and Sandy Creek temperature time series on each date.

For Inks Lake and Lake Marble Falls, temperature data from Sandy Creek only were used as model input for tributary temperature.

4.4.1.4 Direct Drainage Water Temperature

Water temperature data for direct drainage to the lakes were not available. Thus, a water temperature time series for the model was calculated from the average of the Llano River and Sandy Creek temperature time series on each date. For direct drainage to Inks Lake and Lake Marble Falls, water temperature data from Sandy Creek (site 12214) were used.

4.4.1.5 Meteorological Data

Hourly cloud cover, wind speed and direction, and air and dew point temperature data were obtained from the NCDC for Austin Mueller Municipal Airport (January 1, 1984 to May 23, 1999) and Austin Bergstrom International Airport (May 24, 1999 to December 31, 2008). These meteorological stations are located between 37 and 58 miles from the modeled lakes. Model performance could potentially be improved by meteorological data from a more proximate station, which would be expected to be more representative of local weather conditions. However, the more nearby stations reported data for only a subset of the required parameters, and only for portions of the modeled period.

Model inputs were created using hourly values. For cloud cover, the values in the NCDC dataset range from 0 to 8 oktas representing eighths of the total celestial dome covered by clouds (i.e., 0 oktas for clear to 8 oktas for fully overcast). The input to the lake model required cloud cover on a scale of 0 to 10 rather than 0 to 8; therefore, each NCDC value was multiplied by 1.25. For times with no data, the value from the previous observation was used. NCDC values of 9 or 10 were reported to represent partial but indeterminate obscuration; model values for these times were interpolated from observations with quantified cloud cover, imposing a minimum value of 5. Because many consecutive days were missing data between July 1995 and August 1996, interpolation was not performed for this time period; instead, historical monthly averages for cloud cover were used. Daily solar radiation was computed internally in the model from cloud cover for the lakes and their position on the earth (i.e., latitude: 30.60 degrees, longitude: -98.40 degrees for Lake LBJ).

4.4.2 Model Parameterization

Model parameter values considered during the hydrodynamic and thermal calibration process were primarily the default, recommended values cited in the CE-QUAL-W2 manual (Table 4-9). The equilibrium temperature calculation of surface heat exchange was used in lieu of the default term-by-term approach, and the Manning equation for bottom surface roughness was used instead of the default Chezy formulation.

Table 4-9 Model Parameters Affecting Hydrodynamic and Thermal Calibration

Parameter	Calibration Value	Default Value	Units	Description
SLHTC	ET	TERM	---	Specifies either equilibrium temperature (ET) or term-by-term surface heat exchange calculations
AFW	9.2	9.2	---	Coefficients in wind speed effects on heat exchange
BFW	0.46	0.46	---	

Parameter	Calibration Value	Default Value	Units	Description
CFW	2.0	2.0	---	
SLTRC	ULTIMATE	ULTIMATE	---	Transport solution scheme, ULTIMATE, QUICKEST, or UPWIND
THETA	0.55	0.55	---	Time weighting for vertical advection scheme
AX	1.0	1.0	m ² sec ⁻¹	Longitudinal eddy viscosity
DX	1.0	1.0	m ² sec ⁻¹	Longitudinal eddy diffusivity
CBHE	0.3	0.3	Watts m ⁻² sec ⁻¹	Coefficient of bottom heat exchange
TSED	12.0 (Inks) 16.5 (LBJ) 19.6 (MF)	---	deg C	Sediment temperature
FI	0.01 (Inks) 0.01 (LBJ) 0.01 (MF)	0.01	---	Interfacial friction factor
TSEDF	1.0 (Inks) 1.0 (LBJ) 1.0 (MF)	1.0	---	Heat lost to sediments that is added back to water column
FRICC	MANN	CHEZY	---	Bottom friction solution, MANNING or CHEZY
FRICT	0.02 – 0.04 (Inks) 0.035 (LBJ) 0.035 (MF)	---	---	Manning's N coefficient for bottom friction
Z0	0.001	0.001	m	Water surface roughness height
AZC	W2	W2	---	Form of vertical turbulence closure algorithm, NICK, PARAB, RNG, W2, W2N, or TKE
AZSLC	EXP	EXP	---	Specified either implicit, IMP, or explicit, EXP, treatment of the vertical eddy viscosity in the longitudinal momentum equation
AZMAX	1.0E-3	1.0E-3 (lakes)	m ² s ⁻¹	Maximum value for vertical eddy viscosity
WSC	0.95 (Inks) 0.55 - 0.95 (LBJ) 0.50 - 0.95 (MF)	---	---	Wind sheltering coefficient
EXH20	0.35	0.25 or 0.45	m ⁻¹	Extinction coefficient for pure water
EXSS	0.01	0.1	m ⁻¹ / g m ⁻³	Extinction coefficient for inorganic solids

Parameter	Calibration Value	Default Value	Units	Description
EXOM	0.2 (Inks) 0.2 (LBJ) 0.2 (MF)	0.1	$m^{-1} / g m^{-3}$	Extinction coefficient for organic solids
EXA	0.2	0.2	$m^{-1} / g m^{-3}$	Extinction coefficient for algae
BETA	0.45	0.45		Fraction of incident solar radiation absorbed at the water surface

4.4.3 Hydrodynamic and Temperature Calibration Approach

The calibration of the hydrodynamics portion of the lake models involved adjusting the model prediction of water surface elevation to data collected at the dams, and temperature to data collected at various stations throughout the lakes for the time period from January 1, 1984 to December 31, 2008.

The calibration objective was for the model water surface elevation to be within 0.2 m of the measured water surface elevation at the dam. This calibration objective was based on the observed intra-day variation in water surface elevation, the variation in lake elevation from upstream to downstream, and uncertainty in the timing of daily inflows and outflows. Modeled water surface elevations were allowed to deviate more than 0.2 m from the measured elevation for a single day, but not more. The calibration method involved manual adjustments to the water release time series at dams from the water balance.

The calibration objective for water temperature was an absolute mean error of 1.0 °C. Temperature calibration was performed by varying the sediment bed temperature (TSED) and by varying the wind sheltering coefficient (WSC).

4.4.4 Calibration Data

Water surface elevation was recorded daily at midnight by the LCRA River Operations Center at Inks, Wirtz, and Starcke Dams for the entire simulation period. Water temperatures were measured by the LCRA at several locations in each reservoir from 1984 to 2008. From May 1984 through June 1989 and in 2004 through 2006 (for Lake LBJ), temperatures were recorded every month. From July 1989 through December 2004 for Lake LBJ and July 1989 through 2006 for Lake Marble Falls, water temperatures were measured every other month. In 2007 and 2008, temperatures were measured on a weekly basis for Lake LBJ and as frequently as bi-monthly for Lake Marble Falls. For each sampling event, measurements were taken at the surface (approx. 0.3 m below the surface) and at depth at generally two meter intervals for the entire depth of the water column. From March 2007 through 2008, these measurements were supplemented by twice-daily measurements using an automated profiler at site 12324 (Lake LBJ near Wirtz Dam), and with hourly temperature measurements by thermistors and chains of thermistor at several other sites, as described in Section 2.4.

4.4.5 Calibration Results

4.4.5.1 Inks Lake

The calibration of predicted water surface elevation to measured data at Inks Dam (model segment 15) is shown in Figure 4-10. The model predicted elevation tracks the measured data very well. Comparing the modeled daily water surface elevation to measured elevations, the average absolute mean error was 0.094 m.

During temperature calibration of the Inks Lake model, the temperature of the sediment bed was adjusted to 12 °C, while the WSC was held at 0.95. Also, the fraction of heat lost to sediments added back to the water column was set to 0 throughout the model. Figure 4-11 compares predicted and measured water temperatures at Inks Dam (Inks Lake model segment 15). Vertical profiles of simulated temperatures are provided in Appendix B. The model prediction agrees well with the data both seasonally and at depth, with an AME of 0.99 °C, meeting the calibration objective of 1 °C. Model fit statistics are summarized in Table 4-10.

Table 4-10 Inks Lake Model Performance Metrics for Water Temperature

Station ID (Segment)	Depth	Mean Error (°C)	Absolute Mean Error (°C)	Reliability Index	Number of Samples
12336 (15)	Upper Third	-0.02	0.89	1.08	870
12336 (15)	Middle Third	-0.25	0.94	1.08	940
12336 (15)	Lower Third	-0.49	1.14	1.10	942
12336 (15)	All Depths	-0.26	0.99	1.09	2,752

4.4.5.2 Lake LBJ

The calibration of predicted water surface elevation to measured data at Wirtz Dam (model segment 54) is shown in Figure 4-12. The model predicted elevation tracks the measured data very well. Comparing the modeled daily water surface elevation to measured elevations, the absolute mean error was 0.085 m.

The temperature of the Lake LBJ sediment bed throughout the modeled domain was adjusted to 16.5 °C. This coincided with the average temperature measured at Site 12324 (Lake LBJ near Alvin Wirtz Dam) at depths of 20 m or greater. Temperature calibration of the Lake LBJ model consisted primarily of adjustment of the WSC. The WSC was varied spatially between 0.55 and 0.95, but held constant with time. Figures 4-13 to 4-22 show model-predicted and measured temporal profiles of water temperature at the ten sites at which temperatures have historically been recorded. Vertical profiles of water temperature are provided in Appendix B. Model predictions agree well with the observed data both seasonally and at depth. Overall, the AME of model-predicted temperature was 1.14 °C, which is slightly greater than the calibration objective of 1 °C. However, the model AME for the upper third of the water column was 0.89 °C. Complete model fit statistics are summarized in Table 4-11 for the period 1984 through 2008.

Table 4-11 Lake LBJ Model Performance Metrics for Water Temperature

Station ID (Segment)	Depth	Mean Error (°C)	Absolute Mean Error (°C)	Reliability Index	Number of Samples
12335 (2)	All Depths*	0.85	1.11	1.08	872
12333 (24)	Upper Third	0.95	1.18	1.08	602
12333 (24)	Middle Third	1.0	1.24	1.09	476
12333 (24)	Lower Third	1.89	1.99	1.15	599
12333 (24)	All Depths	1.30	1.49	1.11	1,677
12332 (26)	Upper Third	1.08	1.25	1.09	75
12332 (26)	Middle Third	1.21	1.37	1.09	70
12332 (26)	Lower Third	1.22	1.44	1.11	80
12332 (26)	All Depths	1.17	1.35	1.10	225
12330 (30)	Upper Third	0.53	1.02	1.08	620
12330 (30)	Middle Third	0.88	1.35	1.1	440
12330 (30)	Lower Third	1.58	1.84	1.14	387
12330 (30)	All Depths	0.92	1.34	1.11	1,447
12327 (41)	Upper Third	-0.04	0.72	1.09	617
12327 (41)	Middle Third	0.19	0.85	1.08	583
12327 (41)	Lower Third	0.86	1.2	1.11	652
12327 (41)	All Depths	0.35	0.93	1.09	1,852
12325 (53)	Upper Third	-0.83	0.94	1.06	187
12325 (53)	Middle Third	0.11	1.12	1.1	168
12325 (53)	Lower Third	0.7	1.32	1.15	44
12325 (53)	All Depths	-0.26	1.06	1.09	399
12324 (54)	Upper Third	-0.57	0.89	1.05	4,293
12324 (54)	Middle Third	0.3	1.11	1.08	4,253
12324 (54)	Lower Third	1.56	1.85	1.17	2,401
12324 (54)	All Depths	0.24	1.19	1.1	10,947
12331 (62)	Upper Third	0.82	1.46	1.16	206
12331 (62)	Middle Third	0.79	1.62	1.15	341
12331 (62)	Lower Third	1.17	1.9	1.15	181
12331 (62)	All Depths	0.89	1.64	1.15	728
12328 (78)	Upper Third	0.94	1.05	1.07	32
12328 (78)	Middle Third	0.72	1.01	1.06	29
12328 (78)	Lower Third	0.57	0.87	1.05	53

Station ID (Segment)	Depth	Mean Error (°C)	Absolute Mean Error (°C)	Reliability Index	Number of Samples
12328 (78)	All Depths	0.71	0.95	1.06	114
LC915 (100)	Upper Third	-0.14	0.59	1.04	1,320
LC915 (100)	Middle Third	-0.41	0.88	1.05	1,401
LC915 (100)	Lower Third	0.31	0.93	1.06	1,246
LC915 (100)	All Depths	-0.09	0.8	1.05	3,967
Overall	Upper Third	-0.16	0.89	1.06	8,222
Overall	Middle Third	0.3	1.09	1.08	8,331
Overall	Lower Third	1.2	1.57	1.14	5,675
Overall	All Depths	0.36	1.14	1.09	22,228

*Statistics for all layers combined due to shallowness of lake at this station

4.4.5.3 Lake Marble Falls

The calibration of predicted water surface elevation to measured data at Max Starcke Dam (model segment 26) is shown in Figure 4-23. The model predicted elevation tracks the measured data very well, even during lake draw-downs. The exceptions occurred during high flow events, when the model over-predicts water surface elevation by up to 3 m despite reducing the model time step and interpolating the high inflows and outflows into sub-daily intervals. The high flow events happened infrequently and for short durations; daily flows greater than 1,000 cms occurred less than 3% of modeled days. Comparing the model-predicted daily water surface elevation to measured elevations, the average absolute mean error was 0.136 m.

The temperature of the Lake Marble Falls sediment bed throughout the modeled domain was set to 19.6 °C, based on the average temperature measured at Site 12319 (Lake Marble Falls at Max Starcke Dam) at depths of 14 m or greater. The WSC was held constant with time and space at 0.95. Figure 4-24 compares predicted and measured water temperatures at Max Starcke Dam (model segment 26). Vertical profiles of water temperature are provided in Appendix B. The model prediction agrees well with the data both seasonally and at depth, with an AME of 0.7 °C, meeting the calibration objective of 1 °C. Model fit statistics are summarized in Table 4-12. For Lake Marble Falls, model performance metrics were computed by aligning the average data in the top, middle, and bottom thirds of the water column with the average model predictions in the top, middle, and bottom thirds of the water column prior to calculation.

Table 4-12 Lake Marble Falls Model Performance Metrics for Water Temperature

Station ID (Segment)	Depth	Mean Error (°C)	Absolute Mean Error (°C)	Reliability Index	Number of Samples
12319 (26)	Upper Third	0.06	0.71	1.06	207
12319 (26)	Middle Third	0.06	0.67	1.06	206
12319 (26)	Lower Third	-0.18	0.80	1.08	206

Station ID (Segment)	Depth	Mean Error (°C)	Absolute Mean Error (°C)	Reliability Index	Number of Samples
12319 (26)	All Depths	-0.02	0.73	1.07	619

4.5 Water Quality Model Development and Calibration

4.5.1 Model Inputs

Water quality inputs to the lake model include initial conditions, boundary conditions, tributary and direct drainage loadings, point source loadings, and sediment fluxes. Each of these is described in more detail below.

4.5.1.1 Upstream Boundary Water Column Concentrations

For the Lake LBJ model, water quality constituent concentrations in inflows from Inks Lake were extracted from the most downstream segment of the calibrated Inks Lake water quality model. Similarly, for the Lake Marble Falls model the water quality constituent concentrations in inflows from Lake LBJ were extracted from the most downstream segment of the calibrated Lake LBJ water quality model; LBJ predictions from the surface layer (top 1 m) were used because they most closely matched the measured data at the most upstream station in Lake Marble Falls. In this manner, the lake water quality models were directly linked.

Because a water quality model of Lake Buchanan has not yet been developed as part of CREMs, ambient water quality measured from station 12343 (Inks Lake at the headwaters) were used to represent water quality constituent concentrations in inflows from Lake Buchanan to the Inks Lake model. The measured water quality parameters at station 12343 are shown in Table 4-13. Some of the input parameters required by CE-QUAL-W2 have been directly measured at one or more depths at station 12343 throughout the modeled period. In this case the preparation of Inks Lake model input data sets involved simple daily interpolation between average concentrations measured at all depths³. These parameters include DO, chloride, specific conductance (SPCOND), NH₄-N, NO_x-N, and PO₄-P. Other parameters that were routinely measured over the full modeled period, but which are not used directly as input for CE-QUAL-W2, include TOC, chlorophyll-a, pheophytin-a, total Kjeldahl nitrogen (TKN), pH, TP, and TSS. TKN is the sum of OrgN and NH₄-N. TP is the sum of OrgP, PO₄-P, and inorganic polyphosphate phosphorus. Pheophytin-a is a degradation product of chlorophyll-a, and the relative abundance of chlorophyll-a and pheophytin-a may indicate the photosynthetic activity of algae; however, it is not directly used.

Water quality in the lakes under study is very strongly influenced by the quality of the water entering upstream from Lake Buchanan. The monthly monitoring frequency available at this upstream boundary from 1984 through 2006 may introduce significant uncertainty throughout the models and limit their ability to predict short-term variations in water quality.

³ Prior to processing, data below detection were set to half of the detection limit.

Table 4-13 Measured Water Quality Parameters at Inks Lake Upstream Boundary Site

Abbreviation	Description	Years Available
DO	Dissolved Oxygen	1984-2008
TOC	Total Organic Carbon	1984-2008
CHLA	Chlorophyll-a	1984-2008
PHEO	Pheophytin-a	1984-2008
NOX-N	Nitrite + Nitrate Nitrogen	1984-2008
NH4-N	Ammonia Nitrogen	1984-2008
TKN	Total Kjeldahl Nitrogen	1984-2008
TP	Total Phosphorus	1984-2008
PO4-P	Dissolved Orthophosphorus	1984-2008
TSS	Total Suspended Solids (Total Non-filterable Residue)	1984-2008
TDS	Total Dissolved Solids (Total Filterable Residue)	1984-1992, 2003-2007
VSS	Volatile Suspended Solids (Volatile Non-filterable Residue)	1984-1992
ALK	Total Alkalinity	1984-2008
BOD	Biochemical oxygen demand	1984-1992
COD	Chemical oxygen demand	1984-1992
Cl	Chloride	1984-2008
SPCOND	Specific Conductance	1984-2008
SO4	Sulfate	1984-2008
TURB	Turbidity	1990-2008
SECCHI	Transparency, Secchi Depth	1984-2008
FC	Fecal Coliform	1984-2001
ORP	Oxidation-Reduction Potential	1990-1997
EC	E. Coli	1994-2008
TEMP	Water Temperature	1984-2008
pH	pH	1984-2008

**Parameters in bold represent primary state variables in CE-QUAL-W2, or those needed for deconvolution to state variables*

Other data required some additional processing or assumptions for deconvolution to the state variables required by CE-QUAL-W2.

4.5.1.1.1 Total Dissolved Solids

Total dissolved solids were measured from 1984 through 1990, on a limited basis in 1999 and 2000, and then from 2003 to 2007. For other periods, TDS was estimated based on a strong relationship ($R^2 = 0.979$) with SPCOND at the boundary sites:

$$\text{TDS (mg/L)} = 0.614 * \text{SPCOND } (\mu\text{S/cm}) - 38.1$$

4.5.1.1.2 Algae

Chlorophyll-a is the primary photosynthetic pigment of algae and is present in all oxygen-evolving photosynthetic organisms except for photosynthetic bacteria. In CE-QUAL-W2, algal abundances are indicated by chlorophyll-a concentration; the two are linked by a fixed stoichiometric ratio ACHLA.

$$\text{ALG} = \text{CHLA} * \text{ACHLA}$$

where:

ALG = algal biomass in mg/L

CHLA = chlorophyll-a concentration in $\mu\text{g/L}$

ACHLA = stoichiometric ratio algal biomass to chlorophyll-a, in mg per μg

The chlorophyll-a content of algae is variable in natural systems. Chlorophyll-a can comprise from 0.1 to 9.7% of algal mass (Wetzel 1983). In 56 paired samples from three sites in Lake LBJ and one in Inks Lake, the mass ratio of chlorophyll-a to particulate carbon ranged from 0.3 to 2.2%, with an average of 0.7%. Assuming an algal carbon content of 45%, the chlorophyll-a content of algae could be calculated to range from 0.14% to 0.99%, with an average of 0.33%. Based on these measurements, the ACHLA ratio as used in CE-QUAL-W2 would then range from 0.10 to 0.73 mg algae per μg chlorophyll-a, with an average of 0.30. However, the particulate carbon pool is not entirely composed of living algae, but also includes non-living organic solids (detritus), zooplankton, and other organisms which have no chlorophyll-a. Thus, it was concluded that the minimum ACHLA calculated from measured data (ACHLA = 0.10 mg algae per μg chlorophyll-a, equivalent to 1% chlorophyll-a content of algae) was a better estimate of ACHLA, as it may represent a time when living algae dominated the particulate carbon pool. Other investigators have used ACHLA values of 0.025 to 0.22 in CE-QUAL-W2 models of other systems.

The total algae concentration was then divided into four taxa (diatoms, blue-green, green, and flagellates). No data were available on the algal speciation in Lake Buchanan. The division was based on the average monthly relative abundance of these taxa measured by the USGS in 2007 and 2008 in Lakes Inks, LBJ, and Marble Falls (Table 4-14), after normalizing to mass using the taxa-specific biovolume estimates (Table 4-15) from McFarland et al. (2001) and assuming an identical density.

Table 4-14 Relative Abundance (%) of Algal Cells by Class

Month	Diatom	Blue-Green	Green	Flagellates
January	9	41	23	26
February	9	24	9	58
March	30	27	10	33
April	10	22	18	49
May	11	48	12	29
June	19	52	16	14
July	7	71	8	14
August	6	82	6	7
September	5	76	5	14
October	5	73	4	19
November	6	64	8	22
December	10	65	10	16
Grand Total	10	57	10	23

Table 4-15 Estimated Algal Biovolume by Major Group†

Group	Mean Biovolume (µm ³ /cell)
Diatoms	2,826
Blue-green algae - filamentous - coccoid	281.5 508.9
Green algae	1,766
Flagellates	81.8

† data from McFarland et al. (2001)

4.5.1.1.3 Organic Matter

Based on paired measurements, it was observed that dissolved organic carbon comprised, on average, 96% of the TOC concentration at the Inks Lake headwaters. The ratio of carbon in organic matter (both particulate and dissolved) was assumed to be 0.45. Thus particulate organic matter (POM) and dissolved organic matter (DOM) were calculated as:

$$\text{POM} = \text{TOC} * 0.04 / 0.45$$

$$\text{DOM} = \text{TOC} * 0.96 / 0.45$$

In some cases the total algae concentration, calculated more directly from chlorophyll-a (as described above), exceeded the POM concentration estimated from TOC. In these cases, POM

was assumed equal to the calculated total algae concentration and the DOM was adjusted accordingly. Also in a few cases, the calculated POM concentration exceeded the measured TSS concentration. In these cases, the POM concentration was limited to match the measured TSS level, or the analytical quantitation limit, whichever was greater.

The particulate and dissolved pools of organic matter were further split into labile and refractory fractions by assuming a constant 25% labile: 75% refractory ratio. There is no analytical method for specifically quantifying these fractions. The ratio of biochemical oxygen demand at five days (BOD5) to chemical oxygen demand (COD) may provide an indication of the labile fraction, although these parameters include oxidation of inorganic substances. Both of these parameters were measured in all three modeled reservoirs from 1984 to 1990, and on average the BOD5/COD ratio was approximately 20%. A similar modeling effort on the Bosque River (Flowers et al. 2001) assumed a labile fraction of 25%; however, no data were presented to support this assumption.

$$LPOM = 0.25 * POM$$

$$RPOM = 0.75 * POM$$

$$LDOM = 0.25 * DOM$$

$$RDOM = 0.75 * DOM$$

4.5.1.1.4 Organic Nitrogen

Total organic nitrogen was calculated as TKN minus ammonia nitrogen (NH₄-N). Dissolved organic nitrogen (DON) was similarly calculated as dissolved Kjeldahl nitrogen (DKN) minus NH₄-N when DKN was measured, mostly in 2007 and 2008. Particulate organic nitrogen (PON) was then calculated as the difference between TON and DON. When DKN was not measured, DON was calculated as 60% of TON, which was the average calculated from 1,038 sets of TKN, DKN, and NH₄-N measurements in Inks Lake, Lake LBJ, Lake Marble Falls, and their tributaries.

$$TON = TKN - NH_4-N$$

$$DON = DKN - NH_4-N \quad \text{or} \quad DON = 0.60 * TON$$

$$PON = TON - DON$$

The dissolved and particulate organic nitrogen concentrations were further partitioned into labile and refractory pools based on a fixed ratio of 25% labile: 75% refractory, as described above for bulk organic matter.

$$LDOM_N = DON * 0.25$$

$$RDOM_N = DON * 0.75$$

$$LPOM_N = PON * 0.25$$

$$\text{RPOM_N} = \text{PON} * 0.75$$

4.5.1.1.5 Organic Phosphorus

Total organic phosphorus (TOP) was calculated as measured total phosphorus minus measured $\text{PO}_4\text{-P}$. When dissolved phosphorus (DP) was measured, dissolved organic phosphorus (DOP) was calculated as DP minus PO_4P , and particulate organic phosphorus (POP) was then calculated as $\text{TOP} - \text{DOP}$. However, DP was seldom measured prior to 2007. When DP was not measured TOP was fractionated into particulate and dissolved pools by assuming that the DOP composed 28% of TOP. This was the average of 1,171 sets of TP, DP, and $\text{PO}_4\text{-P}$ measurements in Inks Lake, Lake LBJ, Lake Marble Falls, and their tributaries.

$$\text{TOP} = \text{TP} - \text{PO}_4\text{-P}$$

$$\text{DOP} = \text{DP} - \text{PO}_4\text{-P} \quad \text{or} \quad \text{DOP} = 0.28 * \text{TOP}$$

$$\text{POP} = \text{TOP} - \text{DOP}$$

The DOP and POP concentrations were further partitioned into labile and refractory pools based on a fixed ratio of 25% labile: 75% refractory, as described above for bulk organic matter.

$$\text{LDOM_P} = \text{DOP} * 0.25$$

$$\text{RDOM_P} = \text{DOP} * 0.75$$

$$\text{LPOM_P} = \text{POP} * 0.25$$

$$\text{RPOM_P} = \text{POP} * 0.75$$

4.5.1.1.6 Inorganic Suspended Solids

The ISS concentration was calculated as $\text{TSS} - \text{POM}$.

$$\text{ISS} = \text{TSS} - \text{POM}$$

4.5.1.2 Initial Conditions

For each reservoir, initial conditions for CE-QUAL-W2 state variables were estimated from ambient data from the first sampling event in January 1984. Measurements from all depths at the monitoring site nearest to the dam in each reservoir were averaged. Some measured water quality parameters needed to be deconvoluted, as described above, into state variables because the measured parameters did not directly correspond to the input variables required by the model.

4.5.1.3 Tributary and Runoff Water Quality Concentrations

Water quality constituent concentrations in inflows to the three lakes from tributaries as well as runoff (direct drainage) from each of the directly connected watershed sub-basins were derived from the calibrated SWAT watershed model. The results from the SWAT model were

output on a daily basis for either a) sub-basins, for small watersheds draining directly to the lakes, or b) reaches. The SWAT reach output was used for larger watersheds draining to the lakes primarily through tributaries, including those draining multiple SWAT sub-basins such as the Llano River or Sandy Creek. In general, the reach file output was used for tributaries draining two or more sub-basins in SWAT (i.e., containing two or more outlet points), or for tributaries draining single sub-basin watersheds when a drainage outlet was located off of the main Colorado River channel. If the outlet point was located on the main Colorado channel, the reach output consisted of flows and loads from the sub-basin of interest, plus loads from all upstream sub-basins, minus any in-channel loss or transformation processes. Using the sub-basin output provided a more accurate way to quantify the loads from each sub-basin.

4.5.1.3.1 Flow

For direct runoff, the SWAT sub-basin outputs provide water yield (WYLD) as a depth in millimeters (mm). This depth was then multiplied by the sub-basin area and divided by a unit conversion factor to obtain an estimated flow from the sub-basin in cms. For tributaries, the SWAT reach output file directly provided the flow in cms.

$$\text{Flow (m}^3\text{/s)} = \text{WYLD (mm/day)} * \text{Area (m}^2\text{)} \div \text{Conv. Factor}$$

4.5.1.3.2 Organic Matter, Organic Nitrogen, and Organic Phosphorus

Organic nitrogen and phosphorus loads were calculated from SWAT sub-basin output daily loads by dividing by areal water yield and watershed area, or from SWAT reach output loads by dividing by outflow.

$$\text{OrgN (mg/L)} = \text{ORGN (kg/ha*day)} \div \text{WYLD} * \text{Conv. Factor}$$

$$\text{OrgP (mg/L)} = \text{ORGP (kg/ha*day)} \div \text{WYLD} * \text{Conv. Factor}$$

$$\text{OrgN (mg/L)} = \text{ORGN_OUT (kg/day)} \div \text{FLOWOUT (m}^3\text{/s)} * \text{Conv. Factor}$$

$$\text{OrgP (mg/L)} = \text{ORGP_OUT (kg/day)} \div \text{FLOWOUT (m}^3\text{/s)} * \text{Conv. Factor}$$

These concentrations were then partitioned into dissolved and particulate labile and refractory pools assuming a 60%:40% dissolved:particulate proportion and a 25%:75% labile:refractory split. The basis for these proportions was described above under the upstream boundary concentrations. Similarly, OrgP loads from SWAT were converted to inflow concentrations, then partitioned into dissolved and particulate labile and refractory pools assuming a 28%:72% dissolved:particulate proportion and a 25%:75% labile:refractory split.

$$\text{LDOM_N} = \text{OrgN} * 0.25 * 0.60$$

$$\text{RDOM_N} = \text{OrgN} * 0.75 * 0.60$$

$$\text{LPOM_N} = \text{OrgN} * 0.25 * 0.40$$

$$\text{RPOM_N} = \text{OrgN} * 0.75 * 0.40$$

$$\text{LDOM_P} = \text{OrgP} * 0.25 * 0.28$$

$$\text{RDOM_P} = \text{OrgP} * 0.75 * 0.28$$

$$\text{LPOM_P} = \text{OrgP} * 0.25 * 0.72$$

$$\text{RPOM_P} = \text{OrgP} * 0.75 * 0.72$$

Organic matter concentrations in inflows were estimated from the OrgN loads output by SWAT, using a carbon:nitrogen ratio in organic matter of 9.8 and a carbon content of 0.45 in OM. The carbon:nitrogen ratio was estimated as the median of 894 samples collected from Lake LBJ tributaries since 1984, where TOC was directly measured and TON was calculated as TKN minus NH₄-N. These OM loads were converted to inflow concentrations, then partitioned into dissolved and particulate labile and refractory pools assuming a 67%:33% dissolved:particulate proportion and a 25%:75% labile:refractory split.

$$\text{OM (mg/L)} = \text{OrgN (mg/L)} * 9.8 / 0.45$$

$$\text{LDOM} = \text{OM} * 0.67 * 0.25$$

$$\text{RDOM} = \text{OM} * 0.67 * 0.75$$

$$\text{LPOM} = \text{OM} * 0.33 * 0.25$$

$$\text{RPOM} = \text{OM} * 0.33 * 0.75$$

4.5.1.3.3 Bioavailable Orthophosphorus

Orthophosphorus concentrations in inflows from SWAT sub-basin outputs were calculated from the areal WYLD and loads of PO₄-P transported with water (SOLP) and sorbed to eroded sediment (SEDP).

$$\text{PO}_4\text{-P (mg/L)} = (\text{SOLP} + \text{SEDP}) \div \text{WYLD} * \text{Conv. Factor}$$

For inflows from SWAT reach file output, PO₄-P concentrations were calculated from daily loads of PO₄-P (MINP_OUT) divided by daily outflow volume (FLOW_OUT).

$$\text{PO}_4\text{-P (mg/L)} = \text{MINP_OUT} \div \text{FLOW_OUT} * \text{Conv. Factor}$$

4.5.1.3.4 Nitrate/Nitrite Nitrogen

Concentrations of NO_x-N in inflows from SWAT sub-basin outputs were calculated from the sum of areal NO₃-N loads in 1) surface runoff, 2) groundwater, and 3) lateral inflows, divided by the areal WYLD.

$$\text{NO}_3\text{-N (mg/L)} = (\text{LATNO3} + \text{GWNO3} + \text{NSURQ}) \div \text{WYLD} * \text{Conv. Factor}$$

For inflows from SWAT reach file output, NO_x-N concentrations were calculated from the sum of NO₂-N and NO₃-N daily loads divided by daily flow volume.

$$\text{NO}_3\text{-N (mg/L)} = (\text{NO}_3_OUT + \text{NO}_2_OUT) \div \text{FLOW_OUT} * \text{Conv. Factor}$$

4.5.1.3.5 Ammonia Nitrogen

Ammonia nitrogen inflow concentrations were not output in the SWAT sub-basin file and were assumed equal to zero. For inflows from SWAT reach file output, $\text{NH}_4\text{-N}$ concentrations were calculated from $\text{NH}_4\text{-N}$ daily loads (NH_4_OUT) divided by daily flow volume.

$$\text{NH}_4\text{-N (mg/L)} = \text{NH}_4_OUT \div \text{FLOW_OUT} * \text{Conv. Factor}$$

4.5.1.3.6 Dissolved Oxygen

Dissolved oxygen was assumed to be 100% saturated in tributaries and runoff. Saturation DO concentrations were calculated via a temperature-dependent formula provided in Standard Methods 20th Edition (APHA 1998) at an atmospheric pressure of 101.3 kPa and using water temperatures measured at Sandy Creek at SH 71 south of Kingsland (Station 12214).

4.5.1.3.7 Suspended Sediments

SWAT sub-basin output provided daily areal yields of sediment (SYLD), on a mass per day per hectare basis. These were divided by the runoff water yield (in m^3) and multiplied by a conversion factor to obtain an estimated TSS concentration in runoff from the sub-basin in g/m^3 . The TSS concentration was directly reported in the SWAT reach file and used as provided. The POM concentration was subtracted from TSS to obtain the estimate of the ISS concentration.

$$\text{TSS} = \text{SYLD} \div \text{WYLD} * \text{Conv. Factor}$$

4.5.1.3.8 Generic Constituents

Total dissolved solids, chloride, and specific conductance were not simulated by SWAT. Instead, inflow time series concentrations of these constituents were set equal to that interpolated from measured concentrations at Station 12214.

4.5.1.3.9 Algae

Algae inflow concentrations were not output in the SWAT sub-basin file and were assumed equal to zero. For inflows from SWAT reach file output, total algal biomass daily loads were divided by daily flow volume and an algal stoichiometric ratio of 0.1 mg algae per μg chlorophyll-a to derive a total algal concentration, then partitioned into the four algal taxa as described above under Section 4.5.1.1.2.

4.5.1.4 Direct Wastewater Discharges

Only three facilities hold permits discharge water to the three reservoirs, all to Lake LBJ. Two of these discharges are minor domestic wastewater treatment facilities, with permitted wastewater flows of less than 1 MGD. These two facilities report monthly average and maximum discharge rate, pH, and concentrations of DO, TSS, BOD5, TP, and residual chlorine. Records are available on the concentrations of these parameters since approximately 1998. The reported average DO, TSS, and TP concentrations (Table 3.3) were used as model input directly. Concentrations of dissolved, labile organic matter were estimated from average

reported BOD5 concentrations assuming a carbon:oxygen stoichiometric ratio of 12:32 for oxidation of organic matter and a carbon content of 0.45 in organic matter. Concentrations of dissolved, labile organic nitrogen, and phosphorus were then estimated based on an assumption that nitrogen and phosphorus comprised 8% and 0.5%, respectively, of the mass of organic matter. These ratios were based on the average elemental ratios in particulate matter as measured by the USGS in the three lakes from 2007 to 2009. The PO₄-P concentration was then calculated as the difference between reported TP and the estimated organic phosphorus concentration. NO_x-N and NH₃-N concentrations in discharges were estimated to be 20 and 2 mg/L, respectively, based on typical concentrations from the Low-Flow Survey (Section 3.1.2.3). Finally, TDS, chloride, and specific conductance concentrations in discharges were estimated to be 250 mg/L, 50 mg/L, and 500 µS/cm, respectively, based on typical concentrations.

4.5.1.5 Utility Water Discharge

The third discharge to Lake LBJ is composed almost exclusively of cooling waters used in steam electric power generation at the Ferguson Power Plant. While there are very minor low volume wastes, metal cleaning wastes, and storm water associated with this discharge, the overwhelming majority is once-through cooling water withdrawn from Lake LBJ. Thus, concentrations of water quality constituents in the discharge were estimated to be 101% of the simulated concentrations withdrawn from Lake LBJ (segment 41), to account for the 1% evaporative loss of circulating water associated with the average 5 °F temperature increase. The water quality calibration was then performed in an iterative process to account for the feedback effects of changes in simulated in-lake constituent concentrations on discharge concentrations.

4.5.1.6 Sediment Fluxes

CE-QUAL-W2 allows for sediment fluxes of NH₄-N (source), PO₄-P (source), NO_x-N (sink) and DO (sink). The parameterization of these fluxes was determined through calibration.

4.5.2 Loading Summaries

Figures 4-28 to 4-30 illustrate the proportion of overall loads to Inks Lake, Lake LBJ, and Lake Marble Falls of major water quality parameters over the period 1984 to 2008. These sources are grouped into 1) releases from directly upstream reservoirs on the Colorado River, 2) specific major tributaries, 3) the sum of runoff inflows from local watershed plus minor tributaries, and 4) the sum of direct point source discharges.

Releases from Lake Buchanan constitute the majority of loads of all water quality constituents other than inorganic suspended solids to Inks Lake. Runoff from the local watershed was responsible for the majority of the loading of inorganic suspended solids to Inks Lake. There were no direct point source discharges to Inks Lake.

In Lake LBJ, the sources of loading of water quality constituents were more varied. Releases from Inks Lake constituted the largest sources of chloride, NH₄-N, organic nitrogen, and organic carbon. As in Inks Lake, runoff from the local watershed through many minor tributaries was the largest single source of inorganic suspended solids. The Llano River was the largest source of NO₃-N, organic phosphorus, and orthophosphorus, as well as the largest

source of total nitrogen and phosphorus. Point sources and Sandy Creek contribute approximately 10% each of the loading of organic carbon, nitrogen, and phosphorus.

Similar to Inks Lake, the majority of the loads of all water quality constituents other than ISS comes from the releases from the upstream lake. Runoff from the local watershed constitutes almost all of the loading of ISS to Lake Marble Falls. There are no direct point source discharges to Lake Marble Falls.

4.5.3 Water Quality Parameterization

4.5.3.1 Light Extinction

In addition to nutrients, light is a factor that limits algal growth in lakes. In CE-QUAL-W2, light attenuation is simulated based on the formula:

$$I = (1 - \beta) * I_0 * e^{-\alpha * z}$$

where:

I = light intensity

I_0 = light intensity incident at water surface

β = Beta, fraction of light adsorbed at water surface

α = attenuation coefficient, m^{-1}

z = depth, m

Measured attenuation coefficients in the three lakes, calculated from the slope of the $\ln(I/I_0)$:depth relationship, ranged from 0.54 to 12.5 m^{-1} , with an average of 1.03 m^{-1} . In CE-QUAL-W2, the attenuation coefficient is calculated as the sum of a baseline attenuation due to water (EXH2O) and additional concentration-dependent attenuation by inorganic suspended solids (EXSS), algae (EXA), macrophytes (EXM), zooplankton (EXZ), and organic suspended solids (EXOM). Light extinction due to macrophytes and zooplankton were considered negligible. Values of Beta and EXH2O were set to 0.45 and 0.35 m^{-1} , respectively, consistent with literature values. Based on ambient vertical light extinction profile and water quality measurements in all three lakes, the following attenuation coefficients were then estimated by iterative minimization of the deviation from observed light levels at all sites:

$$\text{EXSS: } 0.01 \text{ m}^{-1}/(\text{g}/\text{m}^3)$$

$$\text{EXA: } 0.20 \text{ m}^{-1}/(\text{g}/\text{m}^3)$$

$$\text{EXOM: } 0.20 \text{ m}^{-1}/(\text{g}/\text{m}^3)$$

4.5.3.2 Algae

Four groups of algae were simulated, corresponding to the four taxa enumerated by the USGS basis in 2007 and 2008: diatoms, cyanophytes (blue-green algae), green algae, and flagellates. These four taxa are modeled in CE-QUAL-W2 as groups 1, 2, 3, and 4, respectively. There is ample evidence of seasonal changes in relative abundance of algal taxa in Lake LBJ (Davenport et al 1976; Fruh et al. 1977; Wallace 2009). Although it was not a project objective to simulate the individual taxa, it was believed that utilization of more than one class of algae was necessary to simulate the observed seasonal trends in chlorophyll-a. In particular, some species of blue-green algae are able to fix dissolved nitrogen gas from the atmosphere, and their growth is less limited by a nitrogen deficit (Fogg et al. 1973). Thus, blue-green algae may thrive relative to other algal taxa under seasonal low nitrogen conditions, which often occur in summer. Some blue-green algae can also utilize gas vacuoles to reduce the rate at which they settle from the water column (Fogg and Walsby 1971).

Unlike most other algal taxa, diatoms are enclosed in cell walls composed of silica, which makes the diatoms denser than water and other algal taxa (Sommer 1988). This density and their relatively large size causes them to settle more rapidly from the water column than other algal taxa, particularly as it warms in the summertime (Sommer 1988; Cole and Wells 2008). Rapid diatom growth can also deplete the water column of silica, leading to a diatom growth limitation (Egge and Aksnes 1992). However, silica has not been routinely measured in Lake LBJ or its tributaries, and thus was not simulated in the model.

Because zooplankton were not simulated, algal grazing by zooplankton was incorporated into algal mortality rates. The USGS measured zooplankton grazing rates in samples collected from five sites (12319, 12324, 12327, 12330, and 12336) in the three lakes on six to eight dates each during 2007 and 2008 (see Appendix B of the CREMs Phase 2 final report [Anchor QEA and Parsons 2009]). In these measurements, zooplankton populations were supplemented and the resulting algal chlorophyll-a levels were monitored over time. The algal grazing rates by zooplankton, quantified as the excess mortality rate of algae, ranged from 0.05 to 0.52 day⁻¹, with an overall average value of 0.16 day⁻¹ for all three lakes. No systematic temporal or spatial trends were apparent in the grazing data, and the average rate of 0.16 day⁻¹ was used as the algal mortality rate due to grazing in the model.

4.5.4 Water Quality Calibration Approach

The calibration of the water quality portion of the lake models involved fitting the model prediction of nutrients, chlorophyll-a, and DO to data collected at monitoring stations in each lake for the time period from 1/1/1984 through 12/31/2008. Model parameters were adjusted to match observed water quality concentrations, generally following the sequence:

- specific conductance and chloride
- TOC and DO
- TP and TKN
- chlorophyll-a and inorganic nutrients

This approach is useful as it targets the water quality parameters with the simplest kinetics first, proceeding to those with greater complexity. Using this approach as a guide, model calibration required iteration of the above steps until final parameterization was reached.

The majority of water quality parameters were measured near the surface (often at a depth of one foot) and similarly near the bottom of the lake. For these parameters, calibration focused on matching temporal trends in surface concentrations with secondary consideration to bottom concentrations. Samples collected near the bottom can be less representative of typical water column concentrations due to stirred-up sediments or the presence of a benthic nepheloid layer of high solids concentration. For DO and specific conductance, measurements were available at multiple depths throughout the water column, so calibration focused on matching observed vertical profiles.

A number of different model parameters were varied from their default values in an effort to better calibrate the model to observed data. In addition to the default values, the CE-QUAL-W2 User Manual (Cole and Wells 2008) provides guidance on the range of values that have been measured in many aquatic systems for most parameters. Additional guidance on the expected range of parameter values was obtained from Bowie et al. (1985) and references therein, Wetzel (1983) and references therein, the Phase 2 Lake Travis model calibration (Anchor QEA and Parsons 2009), and numerous other published reports on application of CE-QUAL-W2 to reservoirs.

Among the key parameters that were varied significantly from model default values was ANPR, the algal half-saturation constant for ammonia preference over nitrate as a source of nitrogen. This parameter allows algae to use ammonia preferentially and switch to nitrate as ammonia concentrations decrease. The model formulation is based upon Thomann and Fitzpatrick (1982):

$$P_{NH4} = C_{NH4} \frac{C_{NOx}}{(K_{NH4} + C_{NH4})(K_{NH4} + C_{NOx})} + C_{NH4} \frac{K_{NH4}}{(C_{NH4} + C_{NOx})(K_{NH4} + C_{NOx})}$$

where:

P_{NH4} = ammonium preference factor

K_{NH4} = ammonia preference half-saturation coefficient, mg/L (ANPR)

C_{NH4} = ammonia concentration, mg/L

C_{NOx} = nitrate+nitrite concentration, mg/L

In these reservoirs, algal preference for ammonium over nitrate was not as evident as predicted by the model default value for ANPR of 0.001. However, other modelers have recommended ANPR values in the range of 0.005 to 0.05 mg/L (Thomann et al. 1974; Cerco 2000). Setting ANPR to 0.03 mg/L allowed the model to better simulate the observed relative abundance of ammonia and nitrate+nitrite nitrogen. The simulated algal production was relatively insensitive to changes in the parameter ANPR, as will be discussed in Section 4.6.

The primary model parameters adjusted to achieve the observed seasonal succession of algal taxa were the temperature coefficients for algal growth (AT1 – AT4). Cole and Wells (2008) state:

“When including multiple algal groups, the temperature rate coefficients are one of the most important parameters determining algal succession. Diatoms would have much lower temperatures for AT1-AT4 and cyanobacteria would have higher values.”

In addition to temperature parameters, calibration to observed chlorophyll-a levels was significantly improved by reducing the settling rate and the nitrogen half-saturation coefficient of blue-green algae, which is supported by observations that some blue-green algae are able to fix dissolved nitrogen gas and enhance their flotation with gas vacuoles (see Section 4.5.3.2).

Other key calibration parameters included organic matter decay rates, sediment oxygen demand (SOD), and sediment release rates of phosphorus and ammonia nitrogen.

4.5.5 Calibration Data

The lake model was calibrated to water quality data collected between 1984 and 2008 as part of the LCRA RSS program and CREMs Phase 3 sampling (see Section 2 for details). The primary calibration stations in Lake LBJ were:

- Station 12336 – Inks Lake near Inks Dam (Inks model segment 15)
- Station 12330 – Lake LBJ below confluence with Llano River Arm (LBJ model segment 30)
- Station 12327 – Lake LBJ at confluence with Sandy Creek (LBJ model segment 41)
- Station 12324 - Lake LBJ near Wirtz Dam (LBJ Model Segment 54)
- Station 12319 - Lake Marble Falls near Starcke Dam (Lake Marble Falls model segment 26)

Additionally, the following monitoring stations were considered in calibrating a sub-set of parameters or time periods:

- Station 12335 – Lake LBJ near headwaters (LBJ model segment 2)
- Station 12333 – Lake LBJ at Kingsland cove (LBJ model segment 24)
- Station 12332 – Lake LBJ at FM 1431 (LBJ model segment 26)
- Station 12325 – Lake LBJ at the Narrows near T.C. Ferguson Power Plant (LBJ model segment 53)
- Station 12331 – Lake LBJ at FM 2900 bridge in Llano River Arm (LBJ model segment 62)
- Station 12328 – Lake LBJ near Lake Shore Dr in Sandy Creek Arm (LBJ model segment 78)
- Station LC915 – Lake LBJ near Horseshoe Bay Cove (LBJ model segment 100)
- Station 12323 – Lake Marble Falls at the headwaters (Lake Marble Falls model segment 2)
- Station 12322 - Lake Marble Falls at Hefner Ranch (Lake Marble Falls model segment 11)
- Station 12320 – Lake Marble Falls near US 281 bridge (Lake Marble Falls model segment 20)

4.5.6 Calibration Results for the Inks Lake Model

4.5.6.1 Conservatives (Specific Conductance and Chloride)

Figures 4-31 and 4-32 show the temporal plots of specific conductance and chloride in the upper, middle, and lower third of the water column at Station 12336. Overall, the model does a very good job in reproducing the specific conductance and chloride concentrations. Model performance metrics are provided in Table 4-16. The model accurately tracks the lake response to the large salt pulses that occurred during 1988 to 1990, as well as other peaks and dips in concentration. The overall AMEs were 21.1 $\mu\text{S}/\text{cm}$ for specific conductance, and 4.9 for chloride. Vertical profiles of specific conductance and chloride are provided in Appendix B.

Table 4-16 Model Performance Metrics for Specific Conductance and Chloride at Station 12336 of Inks Lake

Parameter	Depth	Mean Error	Absolute Mean Error	Reliability Index	Number of Samples
Specific Conductance, $\mu\text{S}/\text{cm}$	Upper Third	0.4	21.6	1.06	865
Specific Conductance, $\mu\text{S}/\text{cm}$	Middle Third	5.1	20.1	1.06	934
Specific Conductance, $\mu\text{S}/\text{cm}$	Lower Third	10.5	21.6	1.05	936
Specific Conductance, $\mu\text{S}/\text{cm}$	All Depths	5.5	21.1	1.06	2,735
Chloride, mg/L	Upper Third	1.97	5.28	1.13	224
Chloride, mg/L	Middle Third	0.02	5.68	1.07	25
Chloride, mg/L	Lower Third	0.88	4.26	1.08	165
Chloride, mg/L	All Depths	1.42	4.89	1.11	414

4.5.6.2 Dissolved Oxygen

The main drivers of oxygen levels in the lake are surface reaeration, sediment oxygen demand, and to a somewhat lesser degree, algal growth/respiration and organic matter decay. Figure 4-33 compares model-predicted DO concentrations to observed concentrations at Station 12336. Inspection of the temporal plots shows that the model does a good job of capturing the seasonal dynamics of oxygen at surface, middle, and bottom depths. Note that to facilitate display, the model results are grouped and averaged by depth in thirds. Measured data are not averaged, and often are collected at a depth of one foot in the upper third, and 1 m above the sediments in the bottom third. This may help explain some measurements in the upper third where the model appears to under-predict DO concentrations, and in the lower third where the model appears to over-predict some very low DO measurements. However, model performance statistics for DO (Table 4-17) indicate that the model does indeed under-predict DO in the surface third by 0.45 mg/L on average, over-predict DO by 0.49 mg/L in the middle layer, and over-predict DO by 0.22 mg/L in the bottom layer. The model does capture well the onset and duration of bottom hypoxia. Vertical profiles of DO are provided in Appendix B.

Table 4-17 Model Performance Metrics for DO at Station 12336 of Inks Lake

Parameter	Depth	Mean Error	Absolute Mean Error	Reliability Index	Number of Samples
DO, mg/L	Upper Third	0.47	1.34	1.45	870
DO, mg/L	Middle Third	-0.48	1.32	2.28	940
DO, mg/L	Lower Third	-0.21	1.26	3.35	942
DO, mg/L	All Depths	-0.09	1.31	2.35	2,752

4.5.6.3 Organic Matter (Total Organic Carbon)

Figure 4-34 compares model-predicted TOC concentrations to observed concentrations at Station 12336. Ambient data indicate a small but apparently significant increase in TOC with time, and the model reflects this increase. Model performance statistics for TOC are provided in Table 4-18. The overall AME was 0.67 mg/L, near the calibration goal of 0.6 mg/L. Almost all TOC concentrations fall within a somewhat narrow range of 3 to 6 mg/L.

Table 4-18 Model Performance Metrics for TOC at Station 12336 of Inks Lake

Parameter	Depth	Mean Error	Absolute Mean Error	Reliability Index	Number of Samples
TOC, mg/L	Upper Third	0.39	0.69	1.25	216
TOC, mg/L	Middle Third	0.43	0.74	1.28	25
TOC, mg/L	Lower Third	0.31	0.63	1.24	164
TOC, mg/L	All Depths	0.36	0.67	1.25	405

4.5.6.4 Nitrogen

Figures 4-35 to 4-37 compare model-predicted and measured temporal profiles of TKN, NH₄-N, and NO_x-N at Station 12336 of Inks Lake. Model performance statistics are provided in Table 4-19. The overall AME for TKN was 0.23 mg/L, significantly better than the 0.4 mg/L calibration objective.

Table 4-19 Model Performance Metrics for Nitrogen Species at Station 12336 of Inks Lake

Parameter	Depth	Mean Error	Absolute Mean Error	Reliability Index	Number of Samples
TKN, mg/L	Upper Third	0.04	0.21	1.59	216
TKN, mg/L	Middle Third	0.16	0.37	1.80	25
TKN, mg/L	Lower Third	0.03	0.24	1.55	165
TKN, mg/L	All Depths	0.05	0.23	1.59	406
NH ₄ -N, µg/L	Upper Third	4.5	30.4	2.46	213
NH ₄ -N, µg/L	Middle Third	-30.9	46.7	3.00	25

Parameter	Depth	Mean Error	Absolute Mean Error	Reliability Index	Number of Samples
NH ₄ -N, µg/L	Lower Third	6.4	131.3	2.52	163
NH ₄ -N, µg/L	All Depths	3.1	72.4	2.51	401
NO _x -N, µg/L	Upper Third	-54.2	74.7	4.01	220
NO _x -N, µg/L	Middle Third	-82.1	107.2	4.19	25
NO _x -N, µg/L	Lower Third	-41.8	57.8	2.83	161
NO _x -N, µg/L	All Depths	-51.0	70.0	3.51	406

Ammonia levels were often less than the analytical detection limit in Inks Lake, but exhibited pronounced seasonal peaks. In the hypolimnion, NH₄-N tended to increase during the summer due to fluxes from sediments, then declined in the late fall as stratification diminishes. Although the model predicted the occurrence of this seasonal variation, it did not accurately predict the magnitude of some of the hypolimnetic concentrations. Similar but smaller seasonal variations were often observed in the upper water column. The overall AME of model predicted NH₄-N was 71.7 µg/L, substantially greater than the calibration goal of 30 µg/L. The model performed poorly in simulating the variability in NH₄-N flux from sediments. However, the model did meet the AME calibration goal for the upper third of the water column.

Observed NO_x-N levels are generally low (< 0.5 mg/L). The model tends to over-predict NO_x-N levels. The model does reproduce the NO_x-N depletion that typically occurs in late summer. The overall AME is 0.07 mg/L, which is less than the calibration objective of 0.1 mg/L.

4.5.6.5 Phosphorus

Figures 4-38 and 4-39 compare the observed levels of TP and PO₄-P with model predictions over time. Table 4-20 summarizes model performance statistics for phosphorus species. TP is generally low throughout the lake, with a large number of samples below a detection limit that varied with time. Model-predicted concentrations were similar in magnitude and variance to measured concentrations. The overall model AME is 0.025 mg/L, slightly worse than the calibration goal. However, the AME was lower in the upper and middle depths.

Surface PO₄-P concentrations are typically below detection limits. Consequently, no observable patterns are visible. The model predicts surface PO₄-P levels that generally remain below detection limits, consistent with observed data. The model simulates very low limiting values of PO₄-P during the summer, but it cannot be verified against observations as the detection limit for the majority of calibration is greater than typical half-saturation values for PO₄ limitation. As with ammonia, PO₄-P levels in deeper layers tend to increase following thermal stratification due to the accumulation of PO₄-P released from the sediments under hypoxic condition. The overall model AME is 11.4 µg/L, though this quantification is very uncertain due to the large number of non-detected concentrations.

Table 4-20 Model Performance Metrics for Phosphorus Species at Station 12336 of Inks Lake

Parameter	Depth	Mean Error	Absolute Mean Error	Reliability Index	Number of Samples
TP, µg/L	Upper Third	-4.2	21.7	1.93	210
TP, µg/L	Middle Third	-9.1	11.0	1.82	25
TP, µg/L	Lower Third	6.0	32.5	1.91	164
TP, µg/L	All Depths	-0.3	25.5	1.91	399
PO ₄ -P, µg/L	Upper Third	6.3	9.2	4.29	213
PO ₄ -P, µg/L	Middle Third	2.3	6.5	2.95	25
PO ₄ -P, µg/L	Lower Third	2.8	15.4	2.26	157
PO ₄ -P, µg/L	All Depths	4.7	11.5	3.28	395

4.5.6.6 Algae and Chlorophyll-a

Figure 4-40 shows measured and model-predicted temporal variations of chlorophyll-a at Station 12336 of Inks Lake. The median measured chlorophyll-a concentration in the upper water column for the period 1984-2008 was 7.6 µg/L, while the model-predicted median concentration was 6.1 µg/L. Thus, the model somewhat under-predicted chlorophyll-a concentrations. Observed chlorophyll-a concentrations exhibited an increasing trend with time in the upper water column. The trend was reflected in model predictions. Model performance statistics are summarized in Table 4-21. The overall AME was 4.7 µg/L, higher than the calibration goal of 4 µg/L.

Table 4-21 Model Performance Metrics for Chlorophyll-a at Station 12336 of Inks Lake

Parameter	Depth	Mean Error	Absolute Mean Error	Reliability Index	Number of Samples
Chlorophyll-a, µg/L	Upper Third	2.7	4.8	1.96	215
Chlorophyll-a, µg/L	Middle Third	4.0	4.2	2.44	20
Chlorophyll-a, µg/L	Lower Third	3.9	4.3	3.72	29
Chlorophyll-a, µg/L	All Depths	3.0	4.7	2.16	264

The model predicted dominance of diatoms in March and April, of cyanobacteria from June to December, and a mixture of green algae, diatoms, and cyanobacteria in January, February, and May (Figure 4-41). This predicted seasonal succession was similar to what was measured *in situ* over a one-year period, although there were significant differences between absolute measured and model-predicted taxa dominance at times. Model performance may be

limited because diatom growth can be limited by availability of silica, and silica was not measured or simulated.

The model predicted that, overall, light was the primary algal limiting growth factor. However, considering only the limiting factor at noon in the uppermost 1-meter model layer, phosphorus was the primary model-predicted algal limiting growth factor (Figure 4-42) for most of the modeled period. However, the model predicts that due to an increasing phosphorus concentration, nitrogen has increasingly limited algal growth in recent years. It is not clear to what extent these model predictions may be influenced by an increase in reported detection limits for phosphorus in recent years, and use of half of the detection limits in lieu of non-detected values for input data sets. The model predicts that nitrogen limitation on algal growth peaked in the summer months (Figure 4-43).

4.5.6.7 Model Parameters

The parameters of the calibrated Inks Lake CE-QUAL-W2 model are provided in Table 4-22.

Table 4-22 Default and Calibrated Parameter Values for the Inks Lake Model

Parameter	Description	Default Value	Calibration Value	Units	Basis
AG	Maximum algal growth rate	2.0	2.0 (all groups)	day ⁻¹	model default
AR	Maximum algal respiration rate	0.04	0.04 (all groups)	day ⁻¹	model default
AE	Maximum algal excretion	0.04	0.04 (all groups)	day ⁻¹	model default
AM	Maximum algal mortality	0.1	0.16 (all groups)	day ⁻¹	USGS grazing measurements
AS	Algal settling rate	0.1	Group 1: 0.1 Group 2: 0.005 Group 3: 0.1 Group 4: 0.1	m day ⁻¹	calibration parameter
AHSP	Algal half-saturation for phosphorus-limited growth	0.003	0.003 (all groups)	g m ⁻³	model default
AHSN	Algal half-saturation for nitrogen-limited growth	0.014	Group 1: 0.014 Group 2: 0.007 Group 3: 0.014 Group 4: 0.014	g m ⁻³	calibration parameter
ASAT	Light saturation intensity at maximum photosynthetic rate	75	70 (all groups)	W m ⁻²	calibration parameter
AT1	Lower temperature for algal growth	5	Group 1: 7 Group 2: 15 Group 3: 10 Group 4: 10	°C	calibration parameter

Parameter	Description	Default Value	Calibration Value	Units	Basis
AT2	Lower temperature for maximum algal growth	25	Group 1: 17 Group 2: 20 Group 3: 20 Group 4: 20	°C	calibration parameter
AT3	Upper temperature for maximum algal growth	35	Group 1: 20 Group 2: 35 Group 3: 25 Group 4: 25	°C	calibration parameter
AT4	Upper temperature for algal growth	40	Group 1: 25 Group 2: 40 Group 3: 35 Group 4: 35	°C	calibration parameter
AK1	Fraction of algal growth at AT1	0.1	0.1 (all groups)	---	model default
AK2	Fraction of maximum algal growth at AT2	0.99	0.99 (all groups)	---	model default
AK3	Fraction of maximum algal growth at AT3	0.99	0.99 (all groups)	---	model default
AK4	Fraction of algal growth at AT4	0.1	0.1 (all groups)	---	model default
ALGP	Stoichiometric equivalent between algal biomass and phosphorus	0.005	0.007 (all groups)	---	USGS particulate C, total and dissolved P data
ALGN	Stoichiometric equivalent between algal biomass and nitrogen	0.08	0.07 (all groups)	---	USGS particulate C and N data
ALGC	Stoichiometric equivalent between algal biomass and carbon	0.45	0.45 (all groups)	---	model default
ACHLA	Stoichiometric ratio between algal biomass and chlorophyll-a	0.05	0.1 (all groups)	---	USGS particulate C, LCRA chlorophyll-a data
ALPOM	Fraction of algal biomass that is converted to POM when algae die	0.8	0.8 (all groups)	---	model default
ANEQN	Equation number for algal ammonia preference	2	2 (all groups)	---	model default
ANPR	Algal half-saturation constant for ammonia preference	0.001	0.03 (all groups)	g m ⁻³	calibration parameter
LDOMDK	Labile dissolved organic matter (LDOM) decay rate, day ⁻¹	0.1	0.08	day ⁻¹	calibration parameter

Parameter	Description	Default Value	Calibration Value	Units	Basis
RDOMDK	Refractory dissolved organic matter (LDOM) decay rate	0.001	0.001	day ⁻¹	model default
LRDDK	Labile to refractory conversion rate	0.01	0.01	day ⁻¹	model default
LPOMDK	Labile particulate organic matter (LPOM) decay rate	0.08	0.05	day ⁻¹	calibration parameter
RPOMDK	Refractory particulate organic matter (RPOM) decay rate	0.001	0.001	day ⁻¹	model default
LRPDK	Labile to refractory conversion rate	0.01	0.02	day ⁻¹	calibration parameter
POMS	particulate organic matter settling rate	0.1	0.05	m day ⁻¹	calibration parameter
OMT1	Lower temperature for organic matter decay	4	4	°C	model default
OMT2	Upper temperature for organic matter decay	25	25	°C	model default
OMK1	Fraction of organic matter decay at OMT1	0.1	0.1	---	model default
OMK2	Fraction of organic matter decay at OMT2	0.99	0.99	---	model default
ORGP	Stoichiometric equivalent between organic matter and phosphorus	0.005	0.004	---	calibration parameter
ORGN	Stoichiometric equivalent between organic matter and nitrogen	0.08	0.06	---	calibration parameter
ORGC	Stoichiometric equivalent between organic matter and carbon	0.45	0.45	---	model default
PO4R	Sediment release rate of phosphorus, fraction of SOD	0.001	0.001	fraction of SOD as g/m ² /day	model default
PARTP	Phosphorus partitioning coefficient for suspended solids	0.0	0.0	---	model default
NH4R	Sediment release rate of ammonium, fraction of SOD	0.001	0.011	fraction of SOD as g/m ² /day	calibration parameter
NH4DK	Ammonium decay rate	0.12	0.1	day ⁻¹	calibration parameter
NH4T1	Lower temperature for ammonia decay	5	5	°C	model default

Parameter	Description	Default Value	Calibration Value	Units	Basis
NH4T2	Lower temperature for maximum ammonia decay	25	25	°C	model default
NH4K1	Fraction of nitrification rate at NH4T1	0.1	0.1	---	model default
NH4K2	Fraction of nitrification rate at NH4T2	0.99	0.99	---	model default
NO3DK	Nitrate decay rate	0.03	0.03	day ⁻¹	model default
NO3S	Denitrification rate from sediments	0.001	0.001	m day ⁻¹	model default
FNO3SED	Fraction of NO3N diffused into the sediments that becomes part of organic N in the sediments	0.0	0.0	---	model default
NO3T1	Lower temperature for nitrate decay, °C	5	5	°C	model default
NO3T2	Lower temperature for maximum nitrate decay	25	25	°C	model default
NO3K1	Fraction of denitrification at NO3T1	0.1	0.1	---	model default
NO3K2	Fraction of denitrification at NO3T2	0.99	0.99	---	model default
O2NH4	Oxygen stoichiometry for nitrification	4.57	4.57	---	model default
O2OM	Oxygen stoichiometry for organic matter decay	1.4	1.4	---	model default
O2AR	Oxygen stoichiometry for algal respiration	1.1	1.1	---	model default
O2AG	Oxygen stoichiometry for algal primary production	1.4	1.4	---	model default
KDO	Dissolved oxygen half-saturation constant	0.1	0.2	g m ⁻³	calibration parameter
SOD	Sediment oxygen demand, zero-order	---	2.2	g O ₂ m ⁻² day ⁻¹	calibration parameter
SODT1	Lower temperature for zero-order SOD or first-order sediment decay	4	4	°C	model default
SODT2	Upper temperature for zero-order SOD or first-order sediment decay	25	25	°C	model default
SODK1	Fraction of SOD at SODT1	0.1	0.1	---	model default
SODK2	Fraction of SOD at SODT2	0.99	0.99	---	model default

Parameter	Description	Default Value	Calibration Value	Units	Basis
FSOD	Fraction of the zero-order SOD used	1	1	---	model default

4.5.7 Calibration Results for the Lake LBJ Model

4.5.7.1 Conservatives (Specific Conductance and Chloride)

Specific conductance ranged between approximately 250 and 1,300 $\mu\text{S}/\text{cm}$ during the model period, and chloride concentrations varied between approximately 10 and 240 mg/L. Figures 4-44 to 4-53 show temporal plots of specific conductance in the upper, middle, and lower third of the water column at ten monitoring stations in Lake LBJ where it has been measured. Figures 4-54 to 4-61 show temporal plots for chloride at eight monitoring stations where it has been measured. Please refer to Figure 2-1 for the locations of monitoring stations.

Overall, the model does a good job in reproducing the temporal variation in specific conductance and chloride concentrations. Model performance metrics are provided in Table 4-23. The model accurately tracks Lake LBJ's response to the large salt pulses that occurred during 1988 to 1990.

It is interesting to compare the model-predicted chloride concentrations in Segment 62, at FM 2900 in the Llano River Arm (Figure 4-59), to Segment 2, in the headwaters of the main (Colorado River) Arm (Figure 4-58). The salt pulse of 1988 to 1990 is pronounced in Segment 2, but in Segment 62 the chloride concentrations in this period were extremely dynamic. The salt pulse is only apparent during low flow periods when water from the main channel mixed back upstream in the Llano Arm. Also note that in Segment 62 the chloride concentrations increase with depth, implying that the lower chloride waters flowing in from the Llano River flow over the top of the denser, high chloride waters from downstream. Unfortunately, there were no chloride measurements at Segment 62 during this dynamic period, but specific conductance measurements (Figure 4-51) support model predictions. At most stations there was little vertical variation in specific conductance and chloride concentration. Vertical profiles of specific conductance and chloride are provided in Appendix B.

Table 4-23 Overall Model Performance Metrics for Specific Conductance and Chloride at Lake LBJ Monitoring Stations

Parameter	Depth	Mean Error	Absolute Mean Error	Reliability Index	Number of Samples
Specific Conductance, $\mu\text{S}/\text{cm}$	Upper Third	2.2	55.9	1.16	3,739
Specific Conductance, $\mu\text{S}/\text{cm}$	Middle Third	4.7	51.8	1.15	3,674
Specific Conductance, $\mu\text{S}/\text{cm}$	Lower Third	6.4	56.9	1.17	3,340
Specific Conductance, $\mu\text{S}/\text{cm}$	All Depths	4.4	54.8	1.16	10,753

Parameter	Depth	Mean Error	Absolute Mean Error	Reliability Index	Number of Samples
Chloride, mg/L	Upper Third	1.55	9.57	1.30	813
Chloride, mg/L	Middle Third	-0.57	9.05	1.25	325
Chloride, mg/L	Lower Third	-1.73	11.88	1.37	433
Chloride, mg/L	All Depths	0.21	10.10	1.31	1,571

4.5.7.2 Dissolved Oxygen

Excluding inflow and outflow, the main drivers of oxygen levels in the lake are algal growth, organic matter decay, SOD, and surface re-aeration. Algal respiration and ammonia nitrification also consume DO, to a lesser degree. Figures 4-62 to 4-71 compare model-predicted DO concentrations to observed concentrations at ten stations. Vertical profiles of DO are compared in Appendix B. Inspection of the temporal plots shows that the model does a good job of capturing the seasonal dynamics of oxygen at surface, middle, and lower depths. Model performance statistics for DO are provided in Table 4-24. One important feature that the model captures very well is the onset and duration of the bottom hypoxia. The model tends to over-predict some observed oxygen levels at the surface and middle depths during the summer months.

Table 4-24 Overall Model Performance Metrics for DO at Lake LBJ Monitoring Stations

Parameter	Depth	Mean Error	Absolute Mean Error	Reliability Index	Number of Samples
DO, mg/L	Upper Third	-0.19	0.87	1.24	3,718
DO, mg/L	Middle Third	-0.66	1.25	1.85	3,657
DO, mg/L	Lower Third	-0.56	1.38	2.89	3,326
DO, mg/L	All Depths	-0.46	1.16	1.98	10,701

4.5.7.3 Organic Matter (Total Organic Carbon)

Figures 4-72 to 4-79 compare model-predicted TOC concentrations to observed concentrations at eight stations. The model does well at capturing the average TOC concentrations, but tends to over-predict the range of observed variations. This may imply that the organic carbon content of algae and organic matter is not constant, as assumed by the model. Other than inflow and outflow, the main factors controlling TOC levels in the lake are algal mortality, labile OM decay, particulate settling, and labile to refractory conversion. The AME of 1.31 is substantially inflated by deviations in model predictions on just a few dates when high TOC loads from the Llano River occur on high flow days. However, the reliability indices of 1.4-1.7 imply that the model performs relatively well at explaining variations in TOC. Model performance statistics for TOC are provided in Table 4-25.

Table 4-25 Overall Model Performance Metrics for TOC at Lake LBJ Stations

Parameter	Depth	Mean Error	Absolute Mean Error	Reliability Index	Number of Samples
TOC, mg/L	Upper Third	0.21	1.47	1.63	810
TOC, mg/L	Middle Third	0.17	1.00	1.40	324
TOC, mg/L	Lower Third	0.69	1.25	1.68	432
TOC, mg/L	All Depths	0.34	1.31	1.60	1,566

4.5.7.4 Nitrogen

Figures 4-80 to 4-87 compare model-predicted and measured temporal profiles of TKN at eight stations in Lake LBJ. Model performance statistics are provided in Table 4-26. The model reproduces well the average and range of TKN levels. The overall model AME is 0.27 mg/L, which is significantly better than the calibration goal of 0.4 mg/L. The data exhibit greater variability in the bottom depths, particularly near Wirtz Dam where ammonia flux from sediments is higher.

Table 4-26 Overall Model Performance Metrics for Nitrogen Species at Lake LBJ Stations

Parameter	Depth	Mean Error	Absolute Mean Error	Reliability Index	Number of Samples
TKN, mg/L	Upper Third	0.08	0.25	1.85	781
TKN, mg/L	Middle Third	0.08	0.25	1.72	321
TKN, mg/L	Lower Third	0.13	0.34	1.91	421
TKN, mg/L	All Depths	0.09	0.27	1.84	1,523
NH ₄ -N, µg/L	Upper Third	21.8	33.9	2.86	804
NH ₄ -N, µg/L	Middle Third	14.0	37.9	2.64	324
NH ₄ -N, µg/L	Lower Third	38.3	200	3.22	430
NH ₄ -N, µg/L	All Depths	24.8	80.7	2.91	1,558
NO _x -N, µg/L	Upper Third	-108.8	147	4.32	778
NO _x -N, µg/L	Middle Third	-72.6	105	4.11	315
NO _x -N, µg/L	Lower Third	-79.1	129	3.49	417
NO _x -N, µg/L	All Depths	-93.0	133	4.03	1,510

Ammonia nitrogen levels in Lake LBJ are typically very low (0.05 mg/L or less), but are also extremely variable (Figures 4-88 to 4-95). The model also generates low NH₄-N concentrations comparable to the measured median values, but fails to predict many of the higher observed NH₄-N levels. Some of the deeper parts of the lake accumulate NH₄-N levels up to 1 mg/L during stratified periods due to releases from the sediment. The model does well to simulate the timing and magnitude of some, but not all, of these releases. Overall, the model

AME is 0.081 mg/L for $\text{NH}_4\text{-N}$. However, much of the error is in the deeper layers. The AME is 0.034 mg/L $\text{NH}_4\text{-N}$ in the upper layers, similar to the calibration goal of 0.03 mg/L.

Observed $\text{NO}_x\text{-N}$ levels are quite variable, responding to the impacts of runoff, algal growth, ammonia nitrification, and to a much lesser extent, denitrification. Figures 4-96 to 4-103 compare measured and model-predicted concentrations at eight stations in Lake LBJ. The model does well to reproduce the surface $\text{NO}_x\text{-N}$ levels, and most importantly, reproduces the $\text{NO}_x\text{-N}$ depletion that typically occurs from late spring through summer. In some cases, the model under-predicts the rapidness of the onset of $\text{NO}_x\text{-N}$ depletion, resulting in a net over-prediction of concentrations. The algae of Lake LBJ do not appear to exhibit a great preference for $\text{NH}_4\text{-N}$ over $\text{NO}_x\text{-N}$, as discussed in Section 4.5.4. The overall model AME is 0.13 mg/L, similar to the calibration goal of 0.1 mg/L.

4.5.7.5 Phosphorus

Figures 4-104 to 4-111 compare the observed levels of TP with model predictions. High TP concentrations associated with runoff events tended to decline rapidly, resulting in a baseline TP concentration of approximately 25 $\mu\text{g/L}$ with peaks of 50 to 300 $\mu\text{g/L}$. Total phosphorus concentrations in the upper and middle water column averaged approximately 37 $\mu\text{g/L}$. This average is similar to that measured in Inks Lake and did not vary significantly from upstream to downstream. An increasing trend in TP concentrations over the modeled period appears to be statistically significant, but this may be an artifact of time-varying analytical detection limits.

Table 4-27 summarizes model performance statistics for phosphorus species. The overall model AME of 35 $\mu\text{g/L}$ for TP substantially exceeds the calibration goal of 20 $\mu\text{g/L}$, but does not seem poor in light of the observed concentration range from 0 to 500 $\mu\text{g/L}$. It must also be considered that the typical concentrations are near analytical detection limits, and a substantial number of measurements are below detection. Variance is also inflated by varying analytical detection limits, which ranged from <1 to 100 $\mu\text{g/L}$.

The $\text{PO}_4\text{-P}$ model calibration is shown in Figures 4-112 to 4-119. Surface $\text{PO}_4\text{-P}$ concentrations are typically below detection limits. The model predicts surface $\text{PO}_4\text{-P}$ levels that generally are in agreement with measured data. As with TP, $\text{PO}_4\text{-P}$ levels exhibit high pulses associated with major runoff events. Model predictions of $\text{PO}_4\text{-P}$ are sensitive to boundary concentrations, which in turn are strongly affected by the varying detection limits, as illustrated for model Segment 2 in Figure 4-116. The model simulates very low values of $\text{PO}_4\text{-P}$ in the epilimnion from March to October, and the model predicts that phosphorus is most often the limiting nutrient. As with ammonia, $\text{PO}_4\text{-P}$ levels rise in the deeper areas of the lake in summertime due to the accumulation of $\text{PO}_4\text{-P}$ released from the sediments. The overall model AME for $\text{PO}_4\text{-P}$ is 11.6 $\mu\text{g/L}$, higher than the calibration goal of 10 $\mu\text{g/L}$. However, the AMEs for the upper and middle layers meet the calibration goal.

Table 4-27 Overall Model Performance Metrics for Phosphorus Species in Lake LBJ

Parameter	Depth	Mean Error	Absolute Mean Error	Reliability Index	Number of Samples
TP, µg/L	Upper Third	-5.60	33.4	2.25	808
TP, µg/L	Middle Third	-9.51	28.0	2.15	322
TP, µg/L	Lower Third	14.97	44.5	2.25	427
TP, µg/L	All Depths	-0.77	35.3	2.23	1,557
PO ₄ -P, µg/L	Upper Third	3.70	9.86	3.97	813
PO ₄ -P, µg/L	Middle Third	1.47	8.51	3.62	325
PO ₄ -P, µg/L	Lower Third	6.28	17.26	2.88	433
PO ₄ -P, µg/L	All Depths	3.95	11.62	3.57	1,571

4.5.7.6 Chlorophyll-a

Figures 4-120 to 4-127 show measured and model-predicted temporal variations of chlorophyll-a at eight stations in Lake LBJ. Chlorophyll-a levels exhibit high temporal variability, with a small long-term increasing concentration trend.

The model performs reasonably well in predicting the observed range and variability of chlorophyll-a levels, the normal seasonal fluctuations, and the small increasing trend in concentrations over the modeled period. The model does not accurately predict many of the short-term peaks in chlorophyll-a concentrations, particularly an observed peak in 2008. This results in an average under-prediction of chlorophyll-a levels of 2.54 µg/L. Model performance statistics are summarized in Table 4-28. The overall model AME considering all sites was 4.88 µg/L, and 4.26 µg/L near Wirtz Dam. The calibration goal was 4 µg/L.

The model predicted that, in an average year, cyanobacteria were dominant from May to January, and diatoms were dominant in February, March, and April (Figure 4-128). Although this seasonal pattern is evident in observed algal counts, the model may over-predict the extent of dominance by cyanobacteria. Model performance may also be limited because diatom growth can be limited by availability of silica, and silica was not measured or simulated.

Table 4-28 Overall Model Performance Metrics for Chlorophyll-a in Lake LBJ

Parameter	Depth	Mean Error	Absolute Mean Error	Reliability Index	Number of Samples
Chlorophyll-a, µg/L	Upper Third	2.75	5.09	2.38	764
Chlorophyll-a, µg/L	Middle Third	1.82	4.51	2.33	277
Chlorophyll-a, µg/L	Lower Third	3.21	3.72	3.85	55
Chlorophyll-a, µg/L	All Depths	2.54	4.88	2.43	1,096

In order to understand the factors controlling algal growth throughout Lake LBJ, it is useful to examine the algal growth limitation factors. Figure 4-129 summarizes algal limiting

growth factors by year for Lake LBJ near Wirtz Dam. These illustrate the relative frequency of limitation by light, phosphorus, or nitrogen at a depth of 1 m at noon each day. Figure 4-130 summarizes the same limiting factors by month. At this depth, a surplus of light can limit algal growth by photo-inhibition as much as a deficit of light. Ignoring light limitation because it varies substantially with depth and time of day, the model predicts that phosphorus availability limits algal growth six times more frequently than nitrogen. Nitrogen limitation is predicted to occur most frequently in the summer months, but even in these months phosphorus is predicted to limit algal growth more frequently. The limiting factors did not vary substantially by algal group; nitrogen limitation was slightly less frequent for cyanobacteria.

4.5.7.7 Model Parameters

The parameters of the calibrated Lake LBJ CE-QUAL-W2 model are provided in Table 4-29.

Table 4-29 Default and Calibrated Parameter Values for the Lake LBJ Model

Parameter	Description	Default Value	Calibration Value	Units	Basis
AG	Maximum algal growth rate	2.0	2.0 (all groups)	day ⁻¹	calibration parameter
AR	Maximum algal respiration rate	0.04	0.04 (all groups)	day ⁻¹	model default
AE	Maximum algal excretion	0.04	0.04 (all groups)	day ⁻¹	model default
AM	Maximum algal mortality	0.1	0.16 (all groups)	day ⁻¹	USGS grazing measurements
AS	Algal settling rate	0.1	Group 1: 0.1 Group 2: 0.005 Group 3: 0.1 Group 4: 0.1	m day ⁻¹	calibration parameter
AHSP	Algal half-saturation for phosphorus-limited growth	0.003	0.003 (all groups)	g m ⁻³	model default
AHSN	Algal half-saturation for nitrogen-limited growth	0.014	Group 1: 0.014 Group 2: 0.007 Group 3: 0.014 Group 4: 0.014	g m ⁻³	calibration parameter
ASAT	Light saturation intensity at maximum photosynthetic rate	75	70 (all groups)	W m ⁻²	calibration parameter
AT1	Lower temperature for algal growth	5	Group 1: 7 Group 2: 15 Group 3: 10 Group 4: 10	°C	calibration parameter
AT2	Lower temperature for maximum algal growth	25	Group 1: 17 Group 2: 20 Group 3: 20 Group 4: 20	°C	calibration parameter

Parameter	Description	Default Value	Calibration Value	Units	Basis
AT3	Upper temperature for maximum algal growth	35	Group 1: 20 Group 2: 35 Group 3: 25 Group 4: 25	°C	calibration parameter
AT4	Upper temperature for algal growth	40	Group 1: 25 Group 2: 40 Group 3: 35 Group 4: 35	°C	calibration parameter
AK1	Fraction of algal growth at AT1	0.1	0.1 (all groups)	---	model default
AK2	Fraction of maximum algal growth at AT2	0.99	0.99 (all groups)	---	model default
AK3	Fraction of maximum algal growth at AT3	0.99	0.99 (all groups)	---	model default
AK4	Fraction of algal growth at AT4	0.1	0.1 (all groups)	---	model default
ALGP	Stoichiometric equivalent between algal biomass and phosphorus	0.005	0.007 (all groups)	---	USGS particulate C, total and dissolved P data
ALGN	Stoichiometric equivalent between algal biomass and nitrogen	0.08	0.07 (all groups)	---	USGS particulate C and N data
ALGC	Stoichiometric equivalent between algal biomass and carbon	0.45	0.45 (all groups)	---	model default
ACHLA	Stoichiometric ratio between algal biomass and chlorophyll-a	0.05	0.1 (all groups)	---	USGS particulate C, LCRA chlorophyll-a data
ALPOM	Fraction of algal biomass that is converted to POM when algae die	0.8	0.8 (all groups)	---	model default
ANEQN	Equation number for algal ammonia preference	2	2 (all groups)	---	model default
ANPR	Algal half-saturation constant for ammonia preference	0.001	0.03 (all groups)	g m ⁻³	calibration parameter
LDOMDK	Labile dissolved organic matter (LDOM) decay rate, day ⁻¹	0.1	0.08	day ⁻¹	calibration parameter
RDOMDK	Refractory dissolved organic matter (LDOM) decay rate	0.001	0.001	day ⁻¹	model default
LRDDK	Labile to refractory conversion rate	0.01	0.01	day ⁻¹	model default

Parameter	Description	Default Value	Calibration Value	Units	Basis
LPOMDK	Labile particulate organic matter (LPOM) decay rate	0.08	0.05	day ⁻¹	calibration parameter
RPOMDK	Refractory particulate organic matter (RPOM) decay rate	0.001	0.001	day ⁻¹	model default
LRPDK	Labile to refractory conversion rate	0.01	0.02	day ⁻¹	calibration parameter
POMS	particulate organic matter settling rate	0.1	0.1	m day ⁻¹	model default
OMT1	Lower temperature for organic matter decay	4	4	°C	model default
OMT2	Upper temperature for organic matter decay	25	25	°C	model default
OMK1	Fraction of organic matter decay at OMT1	0.1	0.1	---	model default
OMK2	Fraction of organic matter decay at OMT2	0.99	0.99	---	model default
ORGP	Stoichiometric equivalent between organic matter and phosphorus	0.005	0.004	---	calibration parameter
ORGN	Stoichiometric equivalent between organic matter and nitrogen	0.08	0.06	---	calibration parameter
ORGC	Stoichiometric equivalent between organic matter and carbon	0.45	0.45	---	model default
PO4R	Sediment release rate of phosphorus, fraction of SOD	0.001	0.0001	fraction of SOD as g/m ² /day	calibration parameter
PARTP	Phosphorus partitioning coefficient for suspended solids	0.0	0.0	---	model default
NH4R	Sediment release rate of ammonium, fraction of SOD	0.001	0.018	fraction of SOD as g/m ² /day	calibration parameter
NH4DK	Ammonium decay rate	0.12	0.1	day ⁻¹	calibration parameter
NH4T1	Lower temperature for ammonia decay	5	5	°C	model default
NH4T2	Lower temperature for maximum ammonia decay	25	25	°C	model default
NH4K1	Fraction of nitrification rate at NH4T1	0.1	0.1	---	model default

Parameter	Description	Default Value	Calibration Value	Units	Basis
NH4K2	Fraction of nitrification rate at NH4T2	0.99	0.99	---	model default
NO3DK	Nitrate decay rate	0.03	0.03	day ⁻¹	model default
NO3S	Denitrification rate from sediments	0.001	0.001	m day ⁻¹	model default
FNO3SED	Fraction of NO3N diffused into the sediments that becomes part of organic N in the sediments	0.0	0.0	---	model default
NO3T1	Lower temperature for nitrate decay, °C	5	5	°C	model default
NO3T2	Lower temperature for maximum nitrate decay	25	25	°C	model default
NO3K1	Fraction of denitrification at NO3T1	0.1	0.1	---	model default
NO3K2	Fraction of denitrification at NO3T2	0.99	0.99	---	model default
O2NH4	Oxygen stoichiometry for nitrification	4.57	4.57	---	model default
O2OM	Oxygen stoichiometry for organic matter decay	1.4	1.4	---	model default
O2AR	Oxygen stoichiometry for algal respiration	1.1	1.1	---	model default
O2AG	Oxygen stoichiometry for algal primary production	1.4	1.4	---	model default
KDO	Dissolved oxygen half-saturation constant	0.1	0.2	g m ⁻³	calibration parameter
SOD	Sediment oxygen demand, zero-order	---	0.3 – 1.9	g O ₂ m ⁻² day ⁻¹	calibration parameter
SODT1	Lower temperature for zero-order SOD or first-order sediment decay	4	4	°C	model default
SODT2	Upper temperature for zero-order SOD or first-order sediment decay	25	25	°C	model default
SODK1	Fraction of SOD at SODT1	0.1	0.2	---	calibration parameter
SODK2	Fraction of SOD at SODT2	0.99	0.9	---	calibration parameter
FSOD	Fraction of the zero-order SOD used	1	1	---	model default

4.5.8 Calibration Results for the Lake Marble Falls Model

4.5.8.1 Conservatives (Specific Conductance and Chloride)

Figures 4-131 to 4-134 show the temporal plots of specific conductance in the upper, middle, and lower third of the water column at Lake Marble Falls stations 12319, 12320, 12322, and 12323. These four stations represent the downstream, two middle, and upstream reaches of the reservoir. Figures 4-135 and 4-136 show temporal plots for chloride at stations 12319 and 12323; the other two stations are not shown due to lack of data. Concentrations are similar at the different locations at the same points in time. Overall, the model reproduces the specific conductance and chloride concentrations well throughout the lake. Except for a slight under-prediction during late 1988 and early 1989, the model accurately tracks the lake response to the large salt releases from the Natural Dam Salt Lake in 1987 to 1989 (Raines and Rast 1999), which are observable in the data collected from 1988 through 1990. Model performance metrics at Max Starcke Dam are provided in Table 4-30. Vertical profiles of specific conductivity and chloride are provided in Appendix B.

Table 4-30 Model Performance Metrics for Specific Conductance and Chloride at Station 12319 of Lake Marble Falls

Parameter	Depth	Mean Error	Absolute Mean Error	Reliability Index	Number of Samples
Specific Conductance, $\mu\text{S}/\text{cm}$	Upper Third	19.5	56.4	1.14	206
Specific Conductance, $\mu\text{S}/\text{cm}$	Middle Third	20.8	57.2	1.14	205
Specific Conductance, $\mu\text{S}/\text{cm}$	Lower Third	23.2	58.1	1.14	205
Specific Conductance, $\mu\text{S}/\text{cm}$	All Depths	21.2	57.3	1.14	616
Chloride, mg/L	Upper Third	5.6	10.8	1.25	201
Chloride, mg/L	Middle Third	6.7	14.2	1.34	24
Chloride, mg/L	Lower Third	5.9	11.1	1.26	200
Chloride, mg/L	All Depths	5.8	11.1	1.26	425

4.5.8.2 Dissolved Oxygen

The main drivers of oxygen levels in the lake are surface reaeration, SOD, and to a somewhat lesser degree, algal growth/respiration and organic matter decay. Figure 4-137 compares model-predicted DO concentrations to observed concentrations at Station 12319. Inspection of the temporal plots shows that the model does a good job of capturing the seasonal dynamics of oxygen at surface, middle, and bottom depths. Vertical profiles of DO are provided in Appendix B. Model performance statistics for DO at Max Starcke Dam are provided in Table 4-31. The model tends to under-predict oxygen levels at the surface and middle depths during the winter months, especially during the later years of calibration. This may be due to the fact that the model does not predict the levels of algae observed during the

winter months (see below). Model predictions of the limited DO data collected at the middle stations match well (Figures 4-138 and 4-139). In addition, the model sometimes misses the DO depletion during summer months. These two deficiencies are more pronounced at the upstream station (Figure 4-140).

Table 4-31 Model Performance Metrics for DO at Station 12319 of Lake Marble Falls

Parameter	Depth	Mean Error	Absolute Mean Error	Reliability Index	Number of Samples
DO, mg/L	Upper Third	0.34	0.81	1.15	207
DO, mg/L	Middle Third	-0.09	0.79	1.18	206
DO, mg/L	Lower Third	-0.72	1.14	1.47	206
DO, mg/L	All Depths	-0.15	0.91	1.26	619

4.5.8.3 Organic Matter (Total Organic Carbon)

Figure 4-141 and 4-142 compares model-predicted TOC concentrations to observed concentrations at Stations 12319 and 12323. TOC was not measured at the two middle stations. TOC is observed to be relatively constant at the upstream and downstream ends of the lake at 3-6 mg/L. The model generally under-predicts the measured concentrations of TOC at both stations; this under-prediction is also seen in the TOC calibrations of the lake models for Inks Lake and Lake LBJ. Spikes in predicted TOC concentration mainly correspond to high flow events, which would not be captured in routine data collected during ambient conditions. Model performance statistics for TOC at Max Starcke Dam are provided in Table 4-32. The AME for all depths at Station 12319 was 1.38 mg/L, missing the calibration goal of 0.6 mg/L. However, the reliability indices of 1.6 - 1.7 imply that the model performs relatively well at explaining variations in TOC.

Table 4-32 Model Performance Metrics for TOC at Station 12319 of Lake Marble Falls

Parameter	Depth	Mean Error	Absolute Mean Error	Reliability Index	Number of Samples
TOC, mg/L	Upper Third	0.63	1.39	1.62	200
TOC, mg/L	Middle Third	0.72	1.62	1.68	24
TOC, mg/L	Lower Third	0.58	1.35	1.61	202
TOC, mg/L	All Depths	0.61	1.38	1.62	426

4.5.8.4 Nitrogen

Figures 4-143 to 4-144 compare model-predicted and measured temporal profiles of TKN at Stations 12319 and 12323 of Lake Marble Falls. Plots for the two middle stations are not shown because they either had no TKN data or only one date with data during the calibration period. Observations show that TKN remains at relatively low concentrations (< 1.0 mg/L) at the upstream and downstream ends of the lake. The model reproduces these levels well, particularly in the last decade. The data also show more variability in TKN at the upstream

location with occasional spikes and a more constant signal toward Max Starcke Dam. This feature is also reproduced by the model although TKN spikes are not captured individually.

Figures 4-145 to 4-146 compare model-predicted and measured temporal profiles of NH₄-N at Stations 12319 and 12323 of Lake Marble Falls. Plots for the two middle stations are not shown because they either had no ammonium nitrogen data or only one date with data during the calibration period. NH₄-N levels throughout Lake Marble Falls are generally very low (below 0.1 mg/L). The model also generates comparably low NH₄-N values. There are, however, periods when higher values of NH₄-N were measured but the model under-predicts the concentrations, notably during late 1987 to 1990, mid-1997 to 1999, and 2007-2008. This under-prediction is more evident at the upstream station as the levels measured upstream are higher than those near Max Starcke Dam. Control over model predictions at the upstream station, however, is limited by the output from the Lake LBJ model.

Figures 4-147 to 4-148 compare model-predicted and measured temporal profiles of NO_x-N at Stations 12319 and 12323 of Lake Marble Falls. Plots for the two middle stations are not shown because they either had no NO_x-N data or only one date with data during the calibration period. Observed NO_x-N levels are generally low (< 0.5 mg/L). The model does well to reproduce the surface NO_x-N levels, capturing the timing and magnitude of occasional higher measured concentrations. More importantly, the model reproduces the NO_x-N depletion that typically occurs from late spring through summer.

Model performance statistics for nitrogen at Max Starcke Dam are provided in Table 4-33. The AME goal of 0.4 mg/L for TKN was met with an overall AME of 0.26 mg/L. For NH₄-N, the AME for all depths was 40.5 µg/L, not meeting the AME goal of 30 µg/L; this metric was slightly better at 33.9 µg/L in the top third depth where the majority of data were collected. For NO_x-N, the AME goal was also not met with a value of 130 µg/L compared to the goal of 100 µg/L.

Table 4-33 Model Performance Metrics for Nitrogen Species at Station 12319 of Lake Marble Falls

Parameter	Depth	Mean Error	Absolute Mean Error	Reliability Index	Number of Samples
TKN, mg/L	Upper Third	0.11	0.24	1.82	199
TKN, mg/L	Middle Third	0.35	0.46	2.16	24
TKN, mg/L	Lower Third	0.13	0.26	1.91	201
TKN, mg/L	All Depths	0.13	0.26	1.88	424
NH ₄ -N, µg/L	Upper Third	7.4	33.9	3.00	198
NH ₄ -N, µg/L	Middle Third	19.4	45.8	2.65	24
NH ₄ -N, µg/L	Lower Third	20.5	46.5	2.78	198
NH ₄ -N, µg/L	All Depths	14.3	40.5	2.88	420
NO _x -N, µg/L	Upper Third	-90	130	3.77	181
NO _x -N, µg/L	Middle Third	-130	140	4.87	24
NO _x -N, µg/L	Lower Third	-80	130	3.61	188

Parameter	Depth	Mean Error	Absolute Mean Error	Reliability Index	Number of Samples
NO _x -N, µg/L	All Depths	-90	130	3.76	393

4.5.8.5 Phosphorus

Figures 4-149 through 4-152 compare the observed levels of TP and PO₄-P with model predictions over time at the downstream and upstream stations. Table 4-34 summarizes model performance statistics for the phosphorus species. TP is generally low throughout the lake, with a large number of samples being below the detection limit. Occasional isolated high values (above detection limit) are observed at various locations; these are not typically reproduced by the lake model. The model also does not reproduce the higher levels of TP measured in late 2007 and 2008 at the upstream station, which is reflective of the model's inability to capture the chlorophyll-a concentrations measured during the same period (see below). The model AME of 31 µg/L for TP substantially does not meet the calibration goal of 20 µg/L.

The PO₄-P model calibrations at the downstream and upstream stations are shown in Figures 4-151 and 4-152. Surface PO₄-P concentrations are typically below detection limits. Consequently, no patterns are evident. The model also produces surface PO₄-P levels that generally remain below detection limits. The model simulates very low limiting values of PO₄-P during the summer, but it cannot be verified against observations as the detection limit for the majority of calibration is above typical half-saturation values for PO₄-P limitation. The AME for PO₄-P meets the calibration goal of 10 µg/L.

Table 4-34 Model Performance Metrics for Phosphorus Species at Station 12319 of Lake Marble Falls

Parameter	Depth	Mean Error	Absolute Mean Error	Reliability Index	Number of Samples
TP, µg/L	Upper Third	-7.2	29.9	2.53	198
TP, µg/L	Middle Third	-16.9	23.6	2.48	24
TP, µg/L	Lower Third	0.3	32.7	2.40	200
TP, µg/L	All Depths	-4.2	30.9	2.47	422
PO ₄ -P, µg/L	Upper Third	2.4	7.8	3.29	198
PO ₄ -P, µg/L	Middle Third	3.2	7.1	3.02	24
PO ₄ -P, µg/L	Lower Third	1.9	8.2	2.75	200
PO ₄ -P, µg/L	All Depths	2.2	8.0	3.02	422

4.5.8.6 Chlorophyll-a

Figures 4-153 and 4-154 show measured and model-predicted temporal variations of chlorophyll-a at Max Starcke Dam and at the upstream station of Lake Marble Falls. The model performs reasonably well in predicting average chlorophyll-a levels, as well as the general range and timing with the notable exception of the higher chlorophyll-a values

measured in late 2007 and 2008. The under-predictions during the last two years of simulation reflect the model's under-prediction of phosphorus levels during the same time period (discussed above). Model performance statistics are summarized in Table 4-35. The model AME of 4.67 µg/L did not meet the calibration goal of 4 µg/L.

Table 4-35 Model Performance Metrics for Chlorophyll-a at Station 12319 of Lake Marble Falls

Parameter	Depth	Mean Error	Absolute Mean Error	Reliability Index	Number of Samples
Chlorophyll-a, µg/L	Upper Third	1.56	5.18	2.45	197
Chlorophyll-a, µg/L	Middle Third	1.20	3.40	2.53	21
Chlorophyll-a, µg/L	Lower Third	1.57	3.22	2.16	52
Chlorophyll-a, µg/L	All Depths	1.53	4.67	2.40	270

The model predicted that, in an average year, cyanobacteria were dominant from May to January, and diatoms were dominant in February, March, and April (Figure 4-155) for Lake Marble Falls. This observation is similar to that observed for Lake LBJ. Model performance may be limited because diatom growth can be limited by availability of silica, and silica was not measured or simulated.

The model predicted that, overall, light was the primary algal limiting growth factor. However, considering only the limiting factor at noon in the topmost one m model layer, phosphorus was the primary model-predicted algal limiting growth factor (Figure 4-156) for most of the modeled period. However, the model predicts that due to an increasing phosphorus concentration, nitrogen has increasingly limited algal growth in recent years. It is not clear to what extent these model predictions may be influenced by an increase in reported detection limits for phosphorus in recent years, and use of half of the detection limits in lieu of non-detected values for input data sets. Nitrogen limitation is predicted to occur most frequently in the summer months, but even in these months phosphorus limitation is predicted to occur more frequently (Figure 4-157).

4.5.8.7 Model Parameters

The parameters of the calibrated Lake Marble Falls CE-QUAL-W2 model are provided in Table 4-36.

Table 4-36 Calibrated Parameter Values for the Lake Marble Falls Model

Parameter	Description	Default Value	Calibration Value	Units	Basis
AG	Maximum algal growth rate	2.0	2.0 (all groups)	day ⁻¹	model default
AR	Maximum algal respiration rate	0.04	0.04 (all groups)	day ⁻¹	model default

Parameter	Description	Default Value	Calibration Value	Units	Basis
AE	Maximum algal excretion	0.04	0.04 (all groups)	day ⁻¹	model default
AM	Maximum algal mortality	0.1	0.16 (all groups)	day ⁻¹	USGS grazing measurements
AS	Algal settling rate	0.1	Group 1: 0.1 Group 2: 0.005 Group 3: 0.1 Group 4: 0.1	m day ⁻¹	calibration parameter
AHSP	Algal half-saturation for phosphorus-limited growth	0.003	0.003 (all groups)	g m ⁻³	model default
AHSN	Algal half-saturation for nitrogen-limited growth	0.014	Group 1: 0.014 Group 2: 0.007 Group 3: 0.014 Group 4: 0.014	g m ⁻³	calibration parameter
ASAT	Light saturation intensity at maximum photosynthetic rate	75	70 (all groups)	W m ⁻²	calibration parameter
AT1	Lower temperature for algal growth	5	Group 1: 7 Group 2: 15 Group 3: 10 Group 4: 10	°C	calibration parameter
AT2	Lower temperature for maximum algal growth	25	Group 1: 17 Group 2: 20 Group 3: 20 Group 4: 20	°C	calibration parameter
AT3	Upper temperature for maximum algal growth	35	Group 1: 20 Group 2: 35 Group 3: 25 Group 4: 25	°C	calibration parameter
AT4	Upper temperature for algal growth	40	Group 1: 25 Group 2: 40 Group 3: 35 Group 4: 35	°C	calibration parameter
AK1	Fraction of algal growth at AT1	0.1	0.1 (all groups)	---	model default
AK2	Fraction of maximum algal growth at AT2	0.99	0.99 (all groups)	---	model default
AK3	Fraction of maximum algal growth at AT3	0.99	0.99 (all groups)	---	model default
AK4	Fraction of algal growth at AT4	0.1	0.1 (all groups)	---	model default
ALGP	Stoichiometric equivalent between algal biomass and phosphorus	0.005	0.007 (all groups)	---	USGS particulate C, total and dissolved P data

Parameter	Description	Default Value	Calibration Value	Units	Basis
ALGN	Stoichiometric equivalent between algal biomass and nitrogen	0.08	0.07 (all groups)	---	USGS particulate C and N data
ALGC	Stoichiometric equivalent between algal biomass and carbon	0.45	0.45 (all groups)	---	model default
ACHLA	Stoichiometric ratio between algal biomass and chlorophyll-a	0.05	0.1 (all groups)	---	USGS particulate C, LCRA chlorophyll-a data
ALPOM	Fraction of algal biomass that is converted to POM when algae die	0.8	0.8 (all groups)	---	model default
ANEQN	Equation number for algal ammonia preference	2	2 (all groups)	---	model default
ANPR	Algal half-saturation constant for ammonia preference	0.001	0.03 (all groups)	g m ⁻³	calibration parameter
LDOMDK	Labile dissolved organic matter (LDOM) decay rate, day ⁻¹	0.1	0.014	day ⁻¹	calibration parameter
RDOMDK	Refractory dissolved organic matter (LDOM) decay rate	0.001	0.01	day ⁻¹	calibration parameter
LRDDK	Labile to refractory conversion rate	0.01	0.01	day ⁻¹	model default
LPOMDK	Labile particulate organic matter (LPOM) decay rate	0.08	0.11	day ⁻¹	calibration parameter
RPOMDK	Refractory particulate organic matter (RPOM) decay rate	0.001	0.01	day ⁻¹	calibration parameter
LRPDK	Labile to refractory conversion rate	0.01	0.02	day ⁻¹	calibration parameter
POMS	particulate organic matter settling rate	0.1	0.1	m day ⁻¹	model default
OMT1	Lower temperature for organic matter decay	4	4	°C	model default
OMT2	Upper temperature for organic matter decay	25	25	°C	model default
OMK1	Fraction of organic matter decay at OMT1	0.1	0.1	---	model default
OMK2	Fraction of organic matter decay at OMT2	0.99	0.99	---	model default
ORGP	Stoichiometric equivalent between organic matter and phosphorus	0.005	0.004	---	calibration parameter

Parameter	Description	Default Value	Calibration Value	Units	Basis
ORGN	Stoichiometric equivalent between organic matter and nitrogen	0.08	0.06	---	calibration parameter
ORGC	Stoichiometric equivalent between organic matter and carbon	0.45	0.45	---	model default
PO4R	Sediment release rate of phosphorus, fraction of SOD	0.001	0.0001	---	calibration parameter
PARTP	Phosphorus partitioning coefficient for suspended solids	0.0	0.0	---	model default
NH4R	Sediment release rate of ammonium, fraction of SOD	0.001	0.018	---	calibration parameter
NH4DK	Ammonium decay rate	0.12	0.10	day ⁻¹	calibration parameter
NH4T1	Lower temperature for ammonia decay	5	5	°C	model default
NH4T2	Lower temperature for maximum ammonia decay	25	25	°C	model default
NH4K1	Fraction of nitrification rate at NH4T1	0.1	0.1	---	model default
NH4K2	Fraction of nitrification rate at NH4T2	0.99	0.99	---	model default
NO3DK	Nitrate decay rate	0.03	0.03	day ⁻¹	model default
NO3S	Denitrification rate from sediments	0.001	0.001	m day ⁻¹	model default
FNO3SED	Fraction of NO3N diffused into the sediments that becomes part of organic N in the sediments	0.0	0.0	---	model default
NO3T1	Lower temperature for nitrate decay, °C	5	5	°C	model default
NO3T2	Lower temperature for maximum nitrate decay	25	25	°C	model default
NO3K1	Fraction of denitrification at NO3T1	0.1	0.1	---	model default
NO3K2	Fraction of denitrification at NO3T2	0.99	0.99	---	model default
O2NH4	Oxygen stoichiometry for nitrification	4.57	4.57	---	model default
O2OM	Oxygen stoichiometry for organic matter decay	1.4	1.4	---	model default
O2AR	Oxygen stoichiometry for algal respiration	1.1	1.1	---	model default

Parameter	Description	Default Value	Calibration Value	Units	Basis
O2AG	Oxygen stoichiometry for algal primary production	1.4	1.4	---	model default
KDO	Dissolved oxygen half-saturation constant	0.1	0.2	g m ⁻³	calibration parameter
SOD	Sediment oxygen demand, zero-order	---	1.3	g O ₂ m ⁻² day ⁻¹	calibration parameter
SODT1	Lower temperature for zero-order SOD or first-order sediment decay	4	4	°C	model default
SODT2	Upper temperature for zero-order SOD or first-order sediment decay	25	25	°C	model default
SODK1	Fraction of SOD at SODT1	0.1	0.2	---	calibration parameter
SODK2	Fraction of SOD at SODT2	0.99	0.9	---	calibration parameter
FSOD	Fraction of the zero-order SOD used	1	1	---	model default

4.6 Sensitivity Analysis

To identify the key factors responsible for predictions of chlorophyll-a concentration by the CE-QUAL-W2 model, a model sensitivity analysis was performed. The sensitivity analysis was performed by varying the values of 55 individual parameters and loads, and examining their effects on the resulting predicted chlorophyll-a concentration at a depth of one meter. The sensitivity analysis was performed for only a four year period (1997 to 2000) due to lengthy model run times. This period included years with low, intermediate, and high inflows, as well as one year with frequent algal growth limitation by nitrogen. The sensitivity analysis was performed using the Lake LBJ model because the other lakes were deemed likely to be less sensitive due to shorter retention times.

Three model runs were performed for each parameter; one used the base parameter value from the calibrated model, another the base value minus 50%, and the third used the base value plus 50%. For parameters that varied by algal group, the median value was used as the base value. The ranges of parameter values were confirmed to be within ranges reported in the literature (Bowie et al. 1985; Cole and Wells 2008).

An SI was computed

$$SI_{Chla} = \text{Max} \left(\left| \frac{\overline{Chla}_{\text{low}} - \overline{Chla}_{\text{base}}}{P_{\text{low}}} \right|, \left| \frac{\overline{Chla}_{\text{high}} - \overline{Chla}_{\text{base}}}{P_{\text{high}}} \right| \right)$$

Where:

Chla= chlorophyll-a concentration in µg/L

P_{low} = percent reduction from base parameter value in low run

P_{high} = percent increase from base parameter value in high run

The results of sensitivity analyses are displayed in Table 4-37 and Figure 4-158. The model exhibited greatest sensitivity to the chlorophyll-a content of algae (ACHLA) and the mortality rate of algae (AM), as shown in a scree plot in Figure 4-159. However, neither of these parameters was calibrated; instead, they were calculated from ambient measurements and not varied during calibration. Among calibrated parameters, the greatest changes in chlorophyll-a concentration were caused by changes in maximum algal growth rate (AG), algal phosphorus content (ALGP), and the decay rate of labile particulate organic matter (LPOMDK).

Table 4-37 Sensitivity Indices for Model Parameters and Inputs

Parameter	Description	Base Value	Low	High	Sensitivity Index
BETA	Fraction of incident solar radiation absorbed at the water surface	0.45	0.23	0.68	0.60
EXH2O	Light extinction coefficient for pure water	0.35	0.175	0.525	0.49
EXSS	Light extinction coefficient for inorganic solids	0.01	0.005	0.015	0.06
EXOM	Light extinction coefficient for organic solids	0.2	0.1	0.3	0.68
EXA	Light extinction coefficient for algae	0.2	0.1	0.3	0.14
AG	Maximum algal growth rate	2.0	1.0	3.0	4.23
AR	Maximum algal respiration rate	0.04	0.02	0.06	0.38
AM	Maximum algal mortality rate	0.16	0.08	0.24	5.67
AS	Algal settling rate	0.10	0.05	0.15	0.75
AE	Algal excretion rate	0.04	0.02	0.06	0.13
AHSP	Algal half-saturation concentration for phosphorus-limited growth	0.003	0.0015	0.0045	0.53
AHSN	Algal half-saturation concentration for nitrogen-limited growth	0.014	0.007	0.021	0.03
ASAT	Light saturation intensity at maximum photosynthetic rate	70	35	105	0.49
AT1	Lower temperature for algal growth	10	5	15	0.23
AT2	Lower temperature for maximum algal growth	20	10	30	0.71
AT3	Upper temperature for maximum algal growth	30	15	45	0.79
AT4	Upper temperature for algal growth	40	20	60	0.37

Parameter	Description	Base Value	Low	High	Sensitivity Index
ALGP	Stoichiometric equivalent between algal biomass and phosphorus	0.007	0.0035	0.0105	4.01
ALGN	Stoichiometric equivalent between algal biomass and nitrogen	0.07	0.035	0.105	0.28
ACHLA	Stoichiometric ratio between algal biomass and chlorophyll-a	0.10	0.05	0.15	8.16
ANPR	Algal half-saturation constant for ammonia preference	0.03	0.015	0.045	0.002
LDOMDK	Labile dissolved organic matter decay rate	0.08	0.04	0.12	0.64
LPOMDK	Labile particulate organic matter decay rate	0.05	0.025	0.075	1.64
LRPDK	Labile to refractory conversion rate	0.02	0.01	0.03	0.56
POMS	particulate organic matter settling rate	0.10	0.05	0.15	0.39
ALPOM	fraction of algal mass converted to POM upon death	0.8	0.4	1.0	1.04
ORGP	Stoichiometric equivalent between organic matter and phosphorus	0.004	0.002	0.006	0.002
ORGN	Stoichiometric equivalent between organic matter and nitrogen	0.06	0.04	0.08	0.004
PO4R	Sediment release rate of phosphorus, fraction of SOD	0.0001	0.00005	0.00015	0.010
NH4R	Sediment release rate of ammonium, fraction of SOD	0.018	0.009	0.027	0.002
NH4DK	Ammonium nitrogen decay rate	0.10	0.05	0.15	0.002
NO3DK	Nitrate nitrogen decay rate	0.03	0.015	0.045	0.002
NO3S	Denitrification rate from sediments	0.001	0.0005	0.0015	0.000
KDO	Dissolved oxygen half-saturation constant	0.2	0.1	0.3	0.004
SOD	Sediment oxygen demand	1.0	0.5	1.5	0.02
SODK1	Fraction of SOD at temperature SODT1	0.2	0.1	0.3	0.002
SODK2	Fraction of SOD at temperature SODT2	0.9	0.8	1.0	0.004
SSS	Suspended solids settling rate	0.8	0.4	1.2	0.15
Fraction dissolved of organic carbon in inflows		67%	33%	100%	0.54
Fraction dissolved of organic phosphorus in inflows		60%	30%	90%	0.15
Fraction dissolved of organic nitrogen in inflows		28%	14%	42%	0.04
Labile fraction of organic matter in inflows		25%	12.5%	37.5%	0.51
Orthophosphorus in inflows from SWAT		base	base-50%	base+50%	0.72
Nitrate + nitrite nitrogen in inflows from SWAT		base	base-50%	base+50%	0.11

Parameter	Description	Base Value	Low	High	Sensitivity Index
	Organic phosphorus in inflows from SWAT	base	base-50%	base+50%	0.57
	Organic nitrogen in inflows from SWAT	base	base-50%	base+50%	0.05
	Organic carbon in inflows from SWAT	base	base-50%	base+50%	0.30
	Chlorophyll-a in inflows from SWAT	base	base-50%	base+50%	0.31
	Orthophosphorus in inflows from upstream lake	base	base-50%	base+50%	0.47
	Nitrate nitrogen in inflows from upstream lake	base	base-50%	base+50%	0.002
	Ammonia nitrogen in inflows from upstream lake	base	base-50%	base+50%	0.004
	Organic phosphorus in inflows from upstream lake	base	base-50%	base+50%	0.44
	Organic nitrogen in inflows from upstream lake	base	base-50%	base+50%	0.004
	Organic carbon in inflows from upstream lake	base	base-50%	base+50%	0.01
	Chlorophyll-a in inflows from upstream lake	base	base-50%	base+50%	0.29

4.7 Bounding Calibration

Model uncertainty was addressed with a bounding calibration. In this approach, another acceptable model calibration was established to give an upper-bound prediction of chlorophyll-a, and thereby yield insight into the uncertainty associated with the model predictions (QEA 1999). This approach was necessary because long model run times precluded iterative model runs such as those performed in a Monte Carlo simulation.

Based on the sensitivity analysis, the three most sensitive calibration parameters were adjusted to achieve an upper-bound calibration for surface chlorophyll-a levels over the full calibration period in each lake model. These parameters were the maximum algal growth rate, algal phosphorus content, and the decay rate of labile particulate organic matter. The maximum algal growth rate and decay rate of labile particulate organic matter were increased at fixed percentages (i.e., 10%, 20%, 30%) to increase chlorophyll-a, while algal phosphorus content was reduced at the same fixed percentages.

In each lake, a 30% change in the values of these three most influential calibration parameters was observed to maintain an acceptable calibration, with only moderate reduction in the calibration metric AME. With these changes, the parameter values were still considered reasonable in light of values reported by other investigators using CE-QUAL-W2. Figures 4-160 to 4-183 show temporal plots comparing measured data, the original model calibration, and the bounding calibration for water quality parameters in Inks Lake, Lake LBJ, and Lake Marble Falls. Calibration statistics for the original and bounding calibration are compared in Tables 4-38 (Inks Lake), 4-39 (Lake LBJ), and 4-40 (Lake Marble Falls).

Table 4-38 Inks Lake Model Performance Metrics for Original and Bounding Calibration

Parameter	Model Layer	AME of Original Calibration	AME of Bounding Calibration
Dissolved Oxygen (mg/L)	Top	1.32	1.34
	Middle	1.32	1.34
	Bottom	1.24	1.26
	Overall	1.29	1.31
Total Organic Carbon (mg/L)	Top	0.69	0.70
	Middle	0.74	0.73
	Bottom	0.63	0.64
	Overall	0.67	0.68
Orthophosphorus (µg/L)	Top	9.19	9.48
	Middle	6.49	6.48
	Bottom	15.2	15.3
	Overall	11.4	11.6
Total Phosphorus (µg/L)	Top	21.7	21.3
	Middle	11.0	10.3
	Bottom	32.4	32.1
	Overall	25.4	25.1
Ammonium Nitrogen (µg/L)	Top	30.4	31.0
	Middle	46.2	48.8
	Bottom	130	130
	Overall	71.7	72.5
Nitrate + Nitrite Nitrogen (µg/L)	Top	74.6	72.8
	Middle	107	106
	Bottom	57.5	56.9
	Overall	69.8	68.6
Total Kjeldahl Nitrogen (mg/L)	Top	0.21	0.20
	Middle	0.37	0.36
	Bottom	0.24	0.24
	Overall	0.23	0.23
Chlorophyll-a (µg/L)	Top	4.77	5.14
	Middle	4.20	3.42
	Bottom	4.32	3.94
	Overall	4.68	4.88

Table 4-39 Lake LBJ Model Performance Metrics for Original and Bounding Calibration

Parameter	Model Layer	AME of Original Calibration	AME of Bounding Calibration
Dissolved Oxygen (mg/L)	Top	1.03	1.07
	Middle	1.28	1.27
	Bottom	1.07	1.06
	Overall	1.13	1.13
Total Organic Carbon (mg/L)	Top	1.21	1.15
	Middle	1.59	1.57
	Bottom	1.30	1.21
	Overall	1.28	1.21
Orthophosphorus (µg/L)	Top	9.45	9.66
	Middle	8.45	8.40
	Bottom	24.9	24.8
	Overall	16.3	16.3
Total Phosphorus (µg/L)	Top	32.3	32.2
	Middle	30.9	30.2
	Bottom	49.9	50.0
	Overall	40.0	39.9
Ammonium Nitrogen (µg/L)	Top	34.0	34.8
	Middle	30.8	38.8
	Bottom	364	362
	Overall	182	182
Nitrate + Nitrite Nitrogen (µg/L)	Top	138	120
	Middle	198	170
	Bottom	107	100
	Overall	129	115
Total Kjeldahl Nitrogen (mg/L)	Top	0.21	0.21
	Middle	0.33	0.32
	Bottom	0.46	0.45
	Overall	0.33	0.32
Chlorophyll-a (µg/L)	Top	4.37	4.85
	Middle	4.81	4.71
	Bottom	3.23	3.42
	Overall	4.26	4.65

Table 4-40 Lake Marble Falls Model Performance Metrics for Original and Bounding Calibration

Parameter	Model Layer	AME of Original Calibration	AME of Bounding Calibration
Dissolved Oxygen (mg/L)	Top	0.81	0.78
	Middle	0.79	0.82
	Bottom	1.14	1.17
	Overall	0.91	0.92
Total Organic Carbon (mg/L)	Top	1.39	1.35
	Middle	1.62	1.56
	Bottom	1.35	1.32
	Overall	1.38	1.35
Orthophosphorus (µg/L)	Top	7.8	7.8
	Middle	7.1	7.2
	Bottom	8.2	8.3
	Overall	8.0	8.0
Total Phosphorus (µg/L)	Top	29.9	29.4
	Middle	23.6	23.1
	Bottom	32.7	32.3
	Overall	30.9	30.5
Ammonium Nitrogen (µg/L)	Top	33.9	33.5
	Middle	45.8	45.6
	Bottom	46.5	46.8
	Overall	40.5	40.5
Nitrate + Nitrite Nitrogen (µg/L)	Top	131	127
	Middle	138	127
	Bottom	129	127
	Overall	130	127
Total Kjeldahl Nitrogen (mg/L)	Top	0.24	0.23
	Middle	0.46	0.45
	Bottom	0.26	0.26
	Overall	0.26	0.26
Chlorophyll-a (µg/L)	Top	5.18	5.59
	Middle	3.40	3.26
	Bottom	3.22	3.23
	Overall	4.67	4.95

THIS PAGE INTENTIONALLY LEFT BLANK

SECTION 5 SUMMARY

Phase 3 of the CREMs Project addresses Inks Lake, Lake LBJ, and Lake Marble Falls. These are the second, third, and fourth in a series of six reservoirs on the lower Colorado River known as the Highland Lakes. The Phase 3 effort includes:

1. conducting increased water quality monitoring to aid in the development and calibration of the modeling tools and in the understanding of the Inks Lake, Lake LBJ, and Lake Marble Falls systems;
2. developing comprehensive, linked watershed and water quality modeling tools of the Inks Lake, Lake LBJ, and Lake Marble Falls systems; and
3. evaluating the sensitivity of Inks Lake, Lake LBJ, and Lake Marble Falls to different changes on the watershed, including the impact of land use changes and possible introductions of point source dischargers on the lake.

The Phase 3 monitoring supplemented the existing data record (and existing monitoring program) with 1) expanded routine monitoring conducted for an increased suite of parameters at increased frequencies and at additional monitoring sites, 2) storm event sampling to capture concentrations at high flow events, 3) special continuous monitoring remote sensors, and 4) other special studies aimed at understanding nutrient and algal growth and speciation and zooplankton predation on algae.

The reservoir management tool developed during Phase 3 of the CREMs project consists of hydrodynamic and water quality models of Inks Lake, Lake LBJ, and Lake Marble Falls based on the USACE CE-QUAL-W2 model. To effectively apply the lake models for the current and future management of the basin, tributary loadings and direct runoff under potential watershed scenarios need to be predicted. This was accomplished through the development and calibration of mathematical models of the Inks Lake, Lake LBJ, and Lake Marble Falls watersheds. The watershed modeling software selected for the CREMs project is SWAT2005 (Neitsch et al. 2005), which is the same version of SWAT used to model the Lake Travis watershed in Phase 2 of the CREMs project (Anchor QEA and Parsons 2009). SWAT simulates watershed hydrology, sediment erosion and transport, and nutrient transport and accounts for various land-cover types, land uses, and management practices. SWAT is a semi-lumped watershed model that has been widely applied in Texas to predict changes in constituent loads arising from changes in land use and practices within the watershed, and thereby provided a mechanism to tie activities in the watershed to resultant water quality in the lake.

The watershed models encompass approximately 13,300 km² of land spanning the Edwards Plateau in the Texas Hill Country. The Llano River drains almost 90% of this area and flows into Lake LBJ. Sandy Creek is the second largest tributary and also drains into Lake LBJ. Calibration of the Lake LBJ watershed model focused on matching observed flows and loads at three primary flow gages and monitoring stations on the Llano River and one gage on Sandy Creek from January 1, 1984 through December 31, 2008, following a four year “spin-up” period from 1980 through 1983. No gages or water quality monitoring stations were present in the small Inks Lake watershed; therefore calibration parameters from the Lake LBJ

watershed were applied to the Inks Lake watershed model. Similarly, no water quality monitoring stations were present in the Lake Marble Falls watershed, but limited flow measurements were available for 1998 to 2008 from a gage on Backbone Creek in the Lake Marble Falls watershed. Therefore, flow-related parameters from the calibrated Lake LBJ watershed model were further adjusted to better match these observations in the Lake Marble Falls watershed model.

The watershed model performed well based on the graphical and statistical calibration metrics, particularly at the Llano River near Llano gage, whose drainage area accounts for 84% of the Lake LBJ watershed area. Nash-Sutcliffe model efficiency values for monthly flow ranged from 0.62 to 0.83 for the primary calibration stations. Percent differences between measured and simulated flow volumes ranged from 14% at the Sandy Creek gage to 13% at the Llano River near Mason gage. Calibration of model sediment loads was also considered good, with NS values for TSS from 0.71 to 0.85, and percent differences for TSS ranging from 9% to 29%. Model fits to observed monthly loads were deemed “fair” for nutrients, with NS values of 0.77 for PO₄-P, 0.17 for OrgP, 0.58 for TP, 0.50 for OrgN, and 0.64 for TN and in the Llano River at Llano. However, the model fits for NH₄-N and NO_x-N were poor.

The lake model selected for Phase 3 of CREMs is CE-QUAL-W2 (version 3.6), a two-dimensional laterally averaged hydrodynamic and water quality model. CE-QUAL-W2 simulates important hydrodynamic and water quality processes including: advection, dispersion, sedimentation, algal dynamics (growth, respiration, mortality, excretion, and settling), atmospheric reaeration, nutrient cycling (uptake, organic decomposition, and nitrification/ denitrification), and water-sediment interactions (SOD, anaerobic nutrient releases, and denitrification). Three separate reservoir models were developed: one for each of Lakes Inks, LBJ, and Marble Falls. Although the models were developed independently, and designed to run in stand-alone mode, there were flow and water quality linkages among outputs from the upstream lake and inputs to the next reservoir downstream.

Model segmentation and bathymetry was developed based on recent (2007) bathymetric surveys, and the elevation-volume curves in each lake model matched the measured bathymetry well for all water surface elevations. The lake models were developed and calibrated using data from January 1, 1984 through December 31, 2008, matching the time period of the output from the watershed model calibration.

The numerical stability of CE-QUAL-W2 is highly sensitive to the water balance, and an imbalance between inflows and outflows will result in changes in lake volume and surface elevation in the model. A water balance was developed for the Colorado River system from Buchanan Dam to Max Starcke Dam. The objective of this effort was to achieve daily water balances for the four lake system (Inks, LBJ, Marble Falls, and Travis) while minimizing any required adjustments (in terms of frequency and magnitude) from the reported water release time series. A linked water balance time series facilitates linking of the lake models. The water balance was calculated on a daily time step, and compared to measured water surface elevations for each lake at the dam.

The state and derived constituents simulated in the lake models include temperature, DO, chloride, TDS, specific conductance, ISS, NH₄-N, NO_x-N, OrgN (labile and resistant, dissolved

and particulate), TN, PO₄-P, OrgP (labile and resistant, dissolved and particulate), TP, OM (labile and resistant, dissolved and particulate), and four groups of algae.

Several data limitations were noted that may negatively impact some aspects of model performance. These include the distance from the lakes to the source of meteorological data, the low frequency (monthly) of water quality measurements at the upstream (Lake Buchanan) boundaries, the unavailability of silica data, and the lack of algal speciation data at the upstream boundary.

Calibration of each model occurred in two steps, hydrodynamics and water quality. Hydrodynamic/thermal calibration focused on matching observed lake water levels as well as vertical and temporal profiles of temperature and chloride. Hydrodynamic/thermal calibration was excellent at reproducing observed spatial and temporal trends in temperature, with AMEs of less than 1 °C in Inks Lake and Lake Marble Falls, and 1.14 °C overall for many sites in Lake LBJ. The RI values for temperature ranged from 1.06 for Lake Marble Falls to 1.09 for Inks Lake and Lake LBJ. Of primary importance, the model reproduced the location, depth, and timing of thermal stratification that occurs during the summer months. Concentrations of the conservative constituent chloride were also simulated very well, with RI values from 1.11 to 1.31 in the three reservoirs.

Water quality calibration focused on matching observed temporal profiles of DO, TP, TOC, TKN, NO_x-N, NH₄-N, PO₄-P and chlorophyll-a in upper, middle, and bottom layers of the water column. The AME was the primary metric used to judge quality of calibration. The model accurately simulated DO levels throughout the epilimnion and hypolimnion in each lake, with AMEs of 0.85 to 1.29. The reproduction of hypoxic conditions observed frequently during the summer in the hypolimnion of the deeper parts of the lake was a good indicator of the strength of the model. The levels of TOC simulated by the models were similar in magnitude to those measured in the lakes, but slightly under-predicted. Nutrient levels in the lakes were simulated fairly well, with AME values in most cases similar to those observed in other systems. The models accurately simulated most seasonal nutrient depletion events. The models did predict the observed accumulation of nutrients in the hypolimnion when the lake is stratified, due to fluxes from sediments, but the year-to-year variability in this hypolimnetic accumulation was not simulated well.

Simulation of chlorophyll-a levels in the epilimnion was the primary focus of water quality calibration. To enhance the model's ability to simulate seasonally-variable chlorophyll-a levels, the models simulated four taxonomic groups of algae: diatoms, cyanobacteria, green algae, and flagellates. These groups correspond to the groups enumerated by the USGS in Phase 3 water quality special studies. Most of the values of the algal parameters in the models were kept identical. Exceptions were temperature parameters for algal growth rates, and the settling rates and nitrogen half-saturation concentration for cyanobacteria. In general, the models simulated the seasonal patterns of abundance for the four algal groups. The models perform reasonably well in predicting the observed the range and variability of chlorophyll-a levels, the normal seasonal fluctuations, and the small increasing trend in concentrations over the modeled period. The models do not accurately predict many of the short-term peaks in chlorophyll-a concentration, particularly an observed peak in 2008. This resulted in average under-predictions of chlorophyll-a levels ranging from 1.2 to 2.7 µg/L. Overall AMEs for the upper third of the water column ranged from 4.8 to 5.3 µg/L. The models predict that

phosphorus was most often the nutrient limiting algal growth. However, the models also predict that due to increasing phosphorus concentrations, nitrogen has increasingly limited algal growth in recent years, primarily in the summer months. However, this may be an artifact of an increase in reported detection limits for phosphorus in recent years.

Sensitivity analyses were performed for both the watershed and water quality models to identify the key factors responsible for model predictions. For the watershed models, sensitivity analysis was performed by varying eight key model parameters, and examining their effect on predicted flows and loads of solids and nutrients. For the lake model, sensitivity analysis was performed by varying the values of 55 individual parameters and loads, and examining their effects on the resulting predicted chlorophyll-a concentrations. The sensitivity analysis for the lake water quality model included the assessment of the sensitivity of model results to changes in loadings from upstream and the watershed. With a few exceptions, the sensitivity analyses involved one-at-a-time model parameter changes to a “low” value and a “high” value. Among calibrated parameters, the greatest changes in chlorophyll-a concentration were caused by changes in maximum algal growth rate, algal phosphorus content, and the decay rate of labile particulate organic matter.

Because long model run times prohibited iterative model runs such as those performed in a Monte Carlo simulation, uncertainty was assessed through the establishment of a bounding calibration. The three most sensitive parameters were adjusted to increase the model prediction of surface chlorophyll-a, but keeping the model within the range of the data (i.e., keeping the model calibration line reasonable, given the data). This represents an upper-prediction to help assess model uncertainty in surface chlorophyll-a predictions under different future scenarios.

The Inks Lake, Lake LBJ, and Lake Marble Falls watershed and water quality models developed under Phase 3 of the CREMs project provide predictive tools to facilitate proactive watershed and reservoir management decisions. The models can be used to evaluate the water quality and quantity effects of a wide range of management policies such as the Highland Lakes Watershed Ordinance, the TCEQ point source discharge ban, and land use changes. In addition, the Phase 3 effort has strengthened LCRA’s understanding of the Highland Lakes system through enhanced sampling and data analysis, and expanded the expertise of LCRA staff with respect to watershed and water quality management and modeling issues. In conclusion, CREMs not only provides valuable insights into the relationships between water quality of the Highland Lakes and their surrounding watersheds, but the means to quantify the positive or negative impacts of proposed management activities.

SECTION 6 REFERENCES

- American Public Health Association (APHA), American Water Works Association (AWWA), Water Environment Federation (WEF). 1998. *Standard Methods for the Examination of Water and Wastewater*, 20th Edition.
- Anchor QEA and Parsons. 2009. *Colorado River Environmental Models Phase 2: Lake Travis Final Report*. Final draft submitted to LCRA on March 18, 2009; revised on May 11, 2009.
- Arnold, J.G., R. Srinivasan, R.S. Muttiah, and J.R. Williams. 1998. Large area hydrologic modeling and assessment part I: model development. *J. Am. Water Resources Assn.* 34(1):73-89.
- Asquith, W.H., M.C. Roussel, T.G. Cleveland, X. Fang, and D.B. Thompson. 2006. *Statistical Characteristics of Storm Interevent Time, Depth, and Duration for Eastern New Mexico, Oklahoma, and Texas*: U.S. Geological Survey Professional Paper 1725, 299 p.
- Benaman, J., C.A. Shoemaker, and D.A. Haith. 2005. Calibration and validation of soil and water assessment tools on an agricultural watershed in Upstate New York. *Hydrologic Enginr.* 10(5):363-374.
- Bowie, G.L., W.B. Mills, D.B. Porcella, C.L. Campbell, J.R. Pagenkopt, G.L. Rupp, K.M. Johnson, P.W.H. Chan, S.A. Gherini, and C.E. Chamberlin. 1985. *Rates, Constants, and Kinetics Formulations in Surface Water Quality Modeling (Second Edition)*. EPA/600/3-85/040. United States Environmental Protection Agency (USEPA), Environmental Research Laboratory, Athens, GA.
- Brown, L.C., and T.O. Barnwell. 1987. *The Enhanced Stream Water Quality Models QUAL2E and QUAL2E-UNCAS: Documentation and User Manual*. USEPA, Office of Research and Development, Athens, GA; EPA/600/3-87/007; May 1987.
- CH2M Hill. 2002. *Master Plan for the Colorado River Environmental Models Program*. LCRA, Austin, TX.
- Cerco, C. 2000. *Phytoplankton Kinetics in the Chesapeake Bay Estuary Model*. Technical Report. January 2000. Chesapeake Bay Program Office, Annapolis, MD. <http://www.chesapeakebay.net/modsc.htm>. [Accessed 28 January 2011].
- Cho, S., G.D. Jennings, C. Stallings, and H.A. Devine. 1995. *GIS-based water quality model calibration in the Delaware River Basin*. American Society of Agricultural Engineers Meeting Presentation: Microfiche No. 95-2404.
- Cole, T.M. and S.A. Wells. 2008. *CE-QUAL-W2: A Two-Dimensional, Laterally Averaged, Hydrodynamic and Water Quality Model, Version 3.6*. Department of Civil and Environmental Engineering, Portland State University, Portland, OR.
- Davenport, J.B., B. Maguire, Jr., and E.G. Fruh. 1976. *Phytoplankton succession and the productivity of individual algal species*. Technical Report CRWR-136. Center for Research in Water Resources, University of Texas, Austin, TX.
- Debele, B., R. Srinivasan, and J.-Y. Parlange. 2006. Coupling upland watershed and downstream waterbody hydrodynamic and water quality models (SWAT and CE-

- QUAL-W2) for better water resources management in complex river basins. *Environ Model Assess*, DOI 10.1007/s10666-006-9075-1.
- Di Luzio, M., R. Srinivasan, J.G. Arnold, and S.L. Neitsch. 2002. *Soil and Water Assessment Tool. ArcView GIS Interface Manual: Version 2000*. GSWRL Report 02-03, BRC Report 02-07, Published by Texas Water Resources Institute TR-193, College Station, TX. 346p.
- Egge, J.K., and D.L. Aksnes. 1992. Silicate as regulating nutrient in phytoplankton competition. *Mar. Ecol. Prog. Ser.* 83:281-289.
- Flowers, J.D., L.M. Hauck, and R.L. Kiesling, 2001. *Water quality modeling of Lake Waco using CE-QUAL-W2 for assessment of phosphorus control strategies*. Texas Institute for Applied Environmental Research, Stephenville, TX.
- Fogg, G.E., and A.E. Walsby. 1971. Buoyancy regulation and the growth of planktonic blue-green algae. *Mitt. Int. Ver. Limnol.* 19:182-188.
- Fogg, G.E., W.D.P. Stewart, P. Fay, and A.E. Walsby. 1973. *The Blue-Green Algae*. Academic Press, New York, NY.
- Fruh, E.G., B. Maguire, Jr., and P.S. Schmidt. 1977. *Before and After Studies on the Effects of a Power Plant Installation on Lake Lyndon B. Johnson: After Studies, Final Report*. Technical Report CRWR-151. Center for Research in Water Resources, University of Texas, Austin, TX.
- Gassman, P.W., M.R. Reyes, C.H. Green, and J.G. Arnold. 2007. The soil and water assessment tool: historical development, applications, and future research directions. *Transactions of the ASABE* 50(4):1211-1250.
- LCRA. 2004. Phase 1 Lake Travis Model. LCRA, Austin, TX.
- LCRA. 2006. *Highland Lakes Watershed Ordinance Regulations Handbook*. LCRA, Austin, Texas. Available URL: <http://www.lcra.org/library/media/public/docs/HighlandLakesOrdinanceHandbook.pdf> [Accessed 28 January 2010].
- LCRA. 2009. LCRA Dams and Lakes. Lower Colorado River Authority, Austin, Texas. Available online at <http://www.lcra.org/water/dams> [Accessed 20 January 2010].
- Mace, R. E., E. S. Angle, and W. F. Mullican. 2004. Aquifers of the Edwards Plateau. Texas Water Development Board Report #360. TWDB, Austin, TX.
- McFarland, A., R. Kiesling, and C. Pearson, 2001. *Characterization of a Central Texas Reservoir with Emphasis on Factors Influencing Algal Growth*. TR0104. Texas Institute of Applied Environmental Research, Stephenville, TX.
- Meckel, S. 2008. Personal communication with Jennifer Benaman.
- Meckel, S. 2010. Personal communication with Jennifer Benaman.
- Nash, J. E. and J. V. Sutcliffe. 1970. River flow forecasting through conceptual models part I - A discussion of principles. *J. of Hydrology* 10(3):282-290.
- Natural Resources Conservation Service, United States Department of Agriculture. Official Soil Series Descriptions. Available URL: <http://soils.usda.gov/technical/classification/osd/index.html> [Accessed 22 December 2009]. United States Department of Agriculture NRCS, Lincoln, NE.

- Neitsch, S.L., J.G. Arnold, J.R. Kiniry, and J.R. Williams. 2005. *Soil and Water Assessment Tool Theoretical Documentation: Version 2005*. United States Department of Agriculture Agricultural Research Center and Texas A&M University Agricultural Experiment Station.
- Pascual, P., N. Stiber, and E. Sunderland. 2003. *Draft Guidance on the Development, Evaluation, and Application of Regulatory Environmental Models*. USEPA Office of Science Policy, Council for Regulatory Environmental Modeling, Washington, D.C.; November 2003.
- QEA. 1999. *PCBs in the Upper Hudson River: Volume 2, A Model of PCB Fate, Transport, and Bioaccumulation*. Montvale, NJ: General Electric; June 1999.
- QEA. 2004. Summary of low flow survey, November 9-12, 2004. Memo; Austin, TX: Lower Colorado River Authority; December 2004.
- QEA. 2005. Calibration of QUAL-TX. Austin, TX: Lower Colorado River Authority; August 2005.
- Raines, T.H., and W. Rast, 1999. *Characterization and Simulation of the Quantity and Quality of Water in the Highland Lakes, Texas, 1983–92*. USGS Report 99–4087.
- Runkel, R.L., C.G. Crawford, and T.A. Cohn, 2004. *Load Estimator (LOADEST): A FORTRAN Program for Estimating Constituent Loads in Streams and Rivers*. USGS Techniques and Methods Book 4, Chapter A5. Reston, VA.
- Santhi, C., J.G. Arnold, J.R. Williams, W.A. Dugas, R. Srinivasan and L.M. Hauck. 2001. Validation of the SWAT model on a large river basin with point and nonpoint sources. *J. of American Water Resources Assn.* 37(5):1169-1188.
- Santhi, C., R. Srinivasan, J.G. Arnold, and J.R. Williams. 2006. A modeling approach to evaluate the impacts of water quality management plans implemented in a watershed in Texas. *Environmental Modeling and Software* 21:1141-1157.
- Sommer, U. 1988. Growth and reproductive strategies of planktonic diatoms. In *Growth and Reproductive Strategies of Freshwater Phytoplankton*, C.D. Sandgre, ed. Cambridge University Press. New York, NY.
- Srinivasan, R., T.S. Ramanarayanan, J.G. Arnold, and S.T. Bednarz. 1998. Large area hydrologic modeling and assessment, Part II: Model application. *J. Am. Water Resources Assn.* 34(1):91-101.
- Srinivasan, R. 2009. Personal Communication. Meeting with Jonathan Bumgarner, June 16, 2009.
- Thomann, R.V., and Fitzpatrick, J.F. 1982. *Calibration and verification of a mathematical model of the eutrophication of the Potomac estuary*. Report by Hydroqual, Inc., Mahwah, NJ to DES, District of Columbia.
- Thomann, R.V., R.P. Winfield, and D.M. Di Toro. 1974. Modeling of phytoplankton in Lake Ontario. *Proc. 17th Conf. Great Lakes Res. Internat. Assoc. Great Lakes Res.*, pp. 135-149.
- Tolson, B.A. and C.A. Shoemaker. 2007. Cannonsville reservoir watershed SWAT2000 model development, calibration and validation. *J. Hydrology* 337:68-86.

- TWDB. 1998. Annual Texas Precipitation (Average monthly and annual precipitation for the climatological period 1961-90). Geographical Information Systems (GIS) dataset available online at <http://www.twdb.state.tx.us/mapping/gisdata.asp> [Accessed 22 December 2009].
- TWDB. 2007a. Volumetric and Sedimentation Survey of Inks Lake – April 2007 Survey. Prepared for the Lower Colorado River Authority. Texas Water Development Board, Austin, TX.
- TWDB. 2007b. Volumetric and Sedimentation Survey of Lake Marble Falls – April 2007 Survey. Prepared for the Lower Colorado River Authority. Texas Water Development Board, Austin, TX.
- TWDB. 2009. Volumetric and Sedimentation Survey of Lake Lyndon B. Johnson – May 2007 Survey. Prepared for the Lower Colorado River Authority. Texas Water Development Board, Austin, TX.
- USEPA. 2001. *PLOAD version 3.0, User's Manual, An Arc View GIS Tool to Calculate Nonpoint Sources of Pollution in Watershed and Stormwater Projects*. January 2001.
- Wallace, M.A. 2009. Personal Communication. Email to John Wedig and Dave Bass. July 30, 2009.
- Wetzel. 1983. *Limnology*. 2nd Edition. Saunders College Publishing, Philadelphia, PA.

FIGURES

THIS PAGE INTENTIONALLY LEFT BLANK

APPENDIX A.1
WATER BALANCE METHODOLOGY MEMO

THIS PAGE INTENTIONALLY LEFT BLANK

MEMORANDUM

To: Lisa Hatzenbuehler, LCRA
John Wedig, LCRA
Bryan Cook, LCRA

cc: Elaine Darby, Anchor QEA
Randy Palachek, Parsons
Emily Chen, Anchor QEA
Jim Patek, Parsons
Monica Suarez, Parsons

From: Kirk Dean, Parsons

Subject: Water Balance Methodology for CREMS models of Inks Lake, Lake LBJ,
and Lake Marble Falls

Date: December 11, 2009

This memorandum discusses development of a methodology to develop and optimize water balances for CE-QUAL-W2 models of Inks Lake, Lake LBJ, and Lake Marble Falls as part of Phase 3 of the Colorado River Environmental Modeling System (CREMS). Only a relatively small fraction of the inflows to Inks Lake and Lake Marble Falls is from runoff, with the major part from releases from upstream reservoirs. Thus, adjustments to runoff inflows were insufficient to achieve the water balance. The goal of the effort was to optimize agreement of water balances between the three lakes, while utilizing the runoff inflows from the watershed models.

Water Balance

The governing equations of the CE-QUAL-W2 model are based on the conservation of fluid mass and momentum, and assume that water is an incompressible fluid. Thus, water inflows must be balanced by outflows and changes in system volume (reservoir storage).

For the highland lakes of the Colorado River (Figure 1), inflows include turbine (hydroelectric), floodgate, and spillway releases, runoff from the local watershed and ungaged tributaries, direct precipitation to the lake surface, and TPDES-permitted point source wastewater discharges. Losses from the lakes include evaporation and releases via turbines, floodgates, and spillway. For Lake LBJ, the direct evaporative losses associated with the Ferguson Power Plant represent another water loss. Water withdrawals for local irrigation or

other purposes, groundwater losses and gains, and seepage through the dams were assumed small and ignored. The data sets used in developing the water balances are described below.

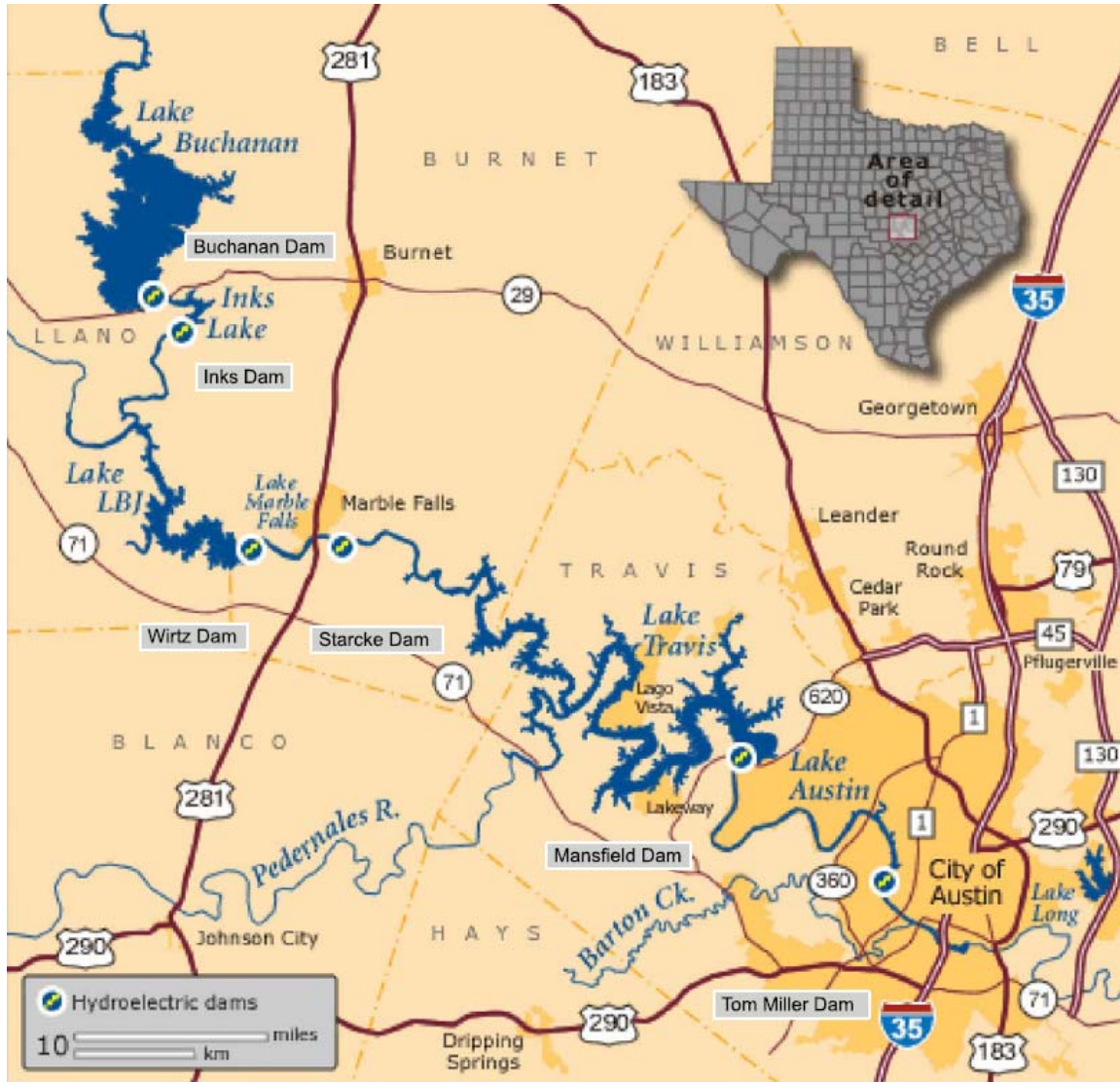


Figure 1. LCRA Highland Lakes and Dams

DATA SOURCES

Reservoir Water Surface Elevation and Storage

Daily water surface elevations for Inks Lake at Inks Dam, Lake LBJ at Wirtz Dam, and Lake Marble Falls at Starcke Dam were provided by the LCRA River Operations Center (ROC). These elevations were recorded each day at approximately midnight. A few extreme short-term

“spikes” in elevation were “scrubbed” from the data set if they were not supported by inflows and/or outflows.

Lake storage and surface area were calculated from the water surface elevation using the elevation-area and elevation-volume tables from several 2007 Texas Water Development Board (TWDB) reports. The Inks Lake report (TWDB 2007a) was based on an April 2007 bathymetry survey. The Lake LBJ report (TWDB 2007b) was based on a May 2007 bathymetric survey. The Lake Marble Falls report (TWDB 2007c) was based on an April 2007 bathymetric survey. Because these tables were developed with 1/10th foot vertical resolution, while lake surface elevation was reported to 1/100th foot of vertical resolution, the volume and area tables were linearly interpolated to 1/100 foot. The elevation datum used was the North American Vertical Datum 1988.

Water Releases at Dams

Releases from Lake Buchanan, Lake LBJ, and Lake Marble Falls are the sum of turbine releases (for hydropower generation) and floodgate releases. Uncontrolled releases over the spillway have not occurred. Releases from Inks Lake are the sum of turbine releases and uncontrolled releases over the spillway. There are no floodgates on Inks Dam. Daily releases records were provided by the ROC. A few anomalous spikes in these release records were identified by comparison with upstream and downstream dam releases and changes in reservoir storage. These anomalous values were replaced by values calculated from changes in reservoir storage, inflows and outflows.

Evaporation and Precipitation

Monthly gross evaporation and precipitation data were obtained from the TWDB web site at <http://midgewater.twdb.state.tx.us/Evaporation/evap.html> for quadrangle 709 for 1984 through 2007. The monthly data were distributed into daily values by simply dividing by the number of days in each month. For 2008, daily pan evaporation measured at Canyon Dam was converted to an estimated lake evaporation using a multiplier of 0.7219, determined from a regression between historical TWDB evaporation estimates for quad 709 and monthly measured pan evaporation at Canyon Dam ($r^2 = 0.963$, $n=273$ months). Daily precipitation estimates for 2008 were based on reported measurements at LCRA Hydromet rain gauges, weighted using a Thiessen polygon approach.

Daily evaporation and precipitation were converted to an evaporated or precipitated volume (cubic meters) and flow rate (cubic meters per second) based on the daily lake surface area (calculated from lake surface elevation and the area-volume table).

Runoff and Tributary Inflows

Runoff inflows to each of the lakes were quantified using a Soil and Water Assessment Tool (SWAT) watershed models. The inflows included gaged and ungaged tributaries, taken from the SWAT reach file output, as well as direct watershed runoff to the lake, taken from the SWAT sub-basin file output.

Point Source Wastewater Discharges

Monthly average point source wastewater discharge flow rates were retrieved from the EPA Permit Compliance System. These discharges included Kingsland Municipal Utility District (TPDES Permit WQ0011549-001) and Aqua Utilities (TPDES Permit WQ0011332-001), with average flow rates of 0.32 and 0.014 mgd, respectively. Both of these facilities discharge to Lake LBJ.

Ferguson Power Plant Evaporation

Water for the Thomas C. Ferguson Power Plant is withdrawn from one point in Lake LBJ and discharged at another. It is assumed that, with the exception of evaporative losses, the withdrawals balance the discharged volume. Daily evaporative losses at the plant were calculated from a formula provided by the LCRA:

$$\text{Evaporative loss (mgd)} = (T_{\text{out}} - T_{\text{in}}) * \text{Circulating Water (mgd)} * 0.00181029$$

where $T_{\text{out}} - T_{\text{in}}$ represents the increase in water temperatures (degrees Celsius) from withdrawal to discharge. Daily data for water temperatures and circulating water rate were provided by the LCRA for the period since 1996. Prior to 1996, monthly average values were available.

APPROACH

Several challenges were presented in developing the water balance.

- There is uncertainty associated with estimates of water releases at the dams, particularly with floodgate and spillway releases. Cole and Wells (2004) state that reservoir outflow measurements have typical errors of five to ten percent. In the case of spillage and floodgate measurements, the uncertainty is likely even higher.
- Water surface elevations vary spatially and fluctuate over a daily cycle, but the elevation measurements used were taken from the dam at midnight.
- There is uncertainty associated with the runoff flows predicted by the watershed model, particularly since there were no gages in the Inks Lake watershed, and because

of limited gaged inflows in the LBJ watershed, the LBJ SWAT model was calibrated primarily based on gaged flows from the Llano River.

- Daily precipitation and evaporation values were calculated from monthly estimates.
- There is uncertainty associated with the lake elevation-volume and elevation-area relationships.
- There is a time lag between inflows and outflow from the system. This time lag is more pronounced under low flow conditions. This time often exceeded the daily time step used in the water balance.

For a daily period, the generalized flow balance for the highland lakes can be expressed as:

$$V_t = V_y + Q_{ud} + Q_{tr} + Q_{ws} + Q_{ps} + Pr - Ev - Q_{dd}$$

V_t = lake storage today, acre-feet

V_y = lake storage yesterday, acre-feet

Q_{ud} = inflow from upstream dam⁴, acre-feet/day

Q_{tr} = inflow from tributaries, acre-feet/day

Q_{ws} = runoff inflow from watershed, acre-feet/day

Q_{ps} = inflow from point source wastewater discharges, acre-feet/day

Pr = precipitation, acre-feet/day

Ev = evaporation, acre-feet/day

Q_{dd} = outflow over downstream dam¹, acre-feet/day

For Lake LBJ, the evaporation from the Ferguson Power Plant represents an additional loss term.

Figure 2 compares the annual daily average of measured releases from Inks Lake with those calculated from the water balance. With the exception of 1997, there is good agreement between the water balance and measured outflows on an annual basis. However, on a daily basis, there is more scatter between reported releases and those predicted by the water balance (Figure 3). Figures 4 and 5 present annual water balances for Lakes LBJ and Marble Falls.

⁴ Including turbine, floodgate, and spillways

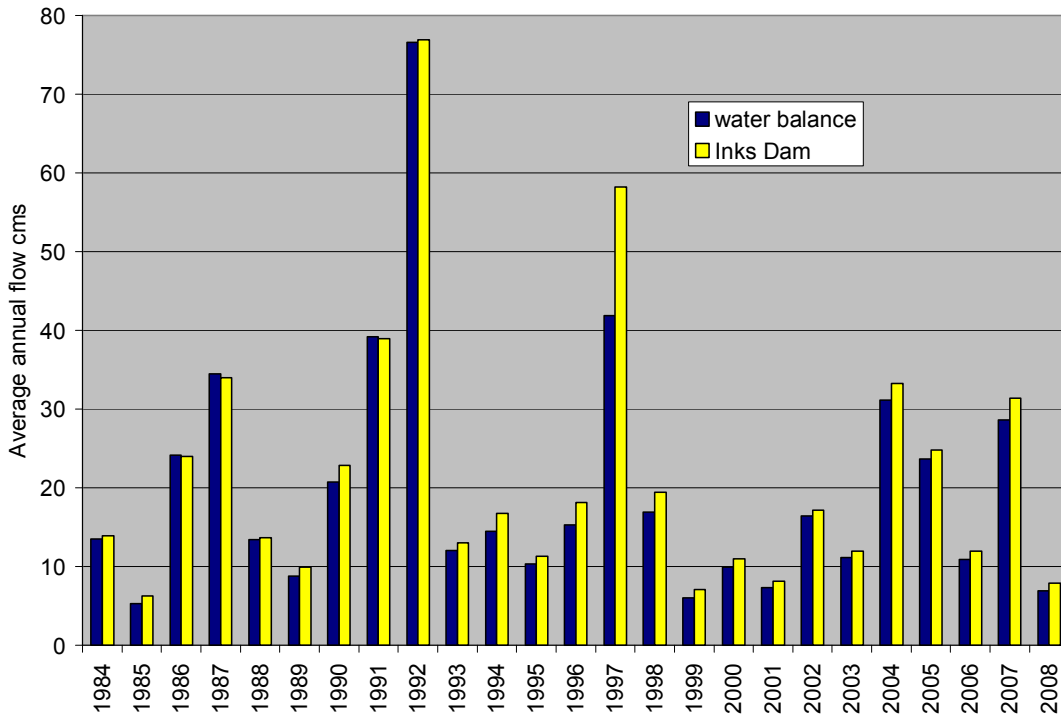


Figure 2. Comparison of measured annual average releases at Inks Dam with those predicted from the water balance.

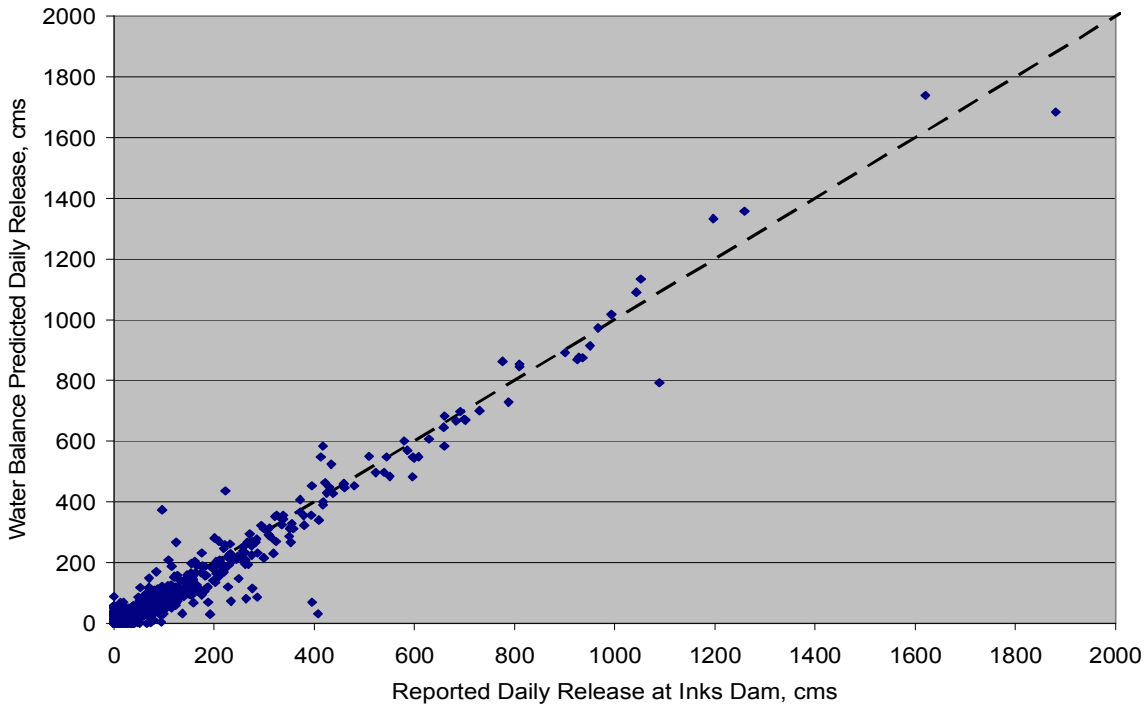


Figure 3. Comparison of daily reported releases from Inks Lake to those predicted by the water balance.

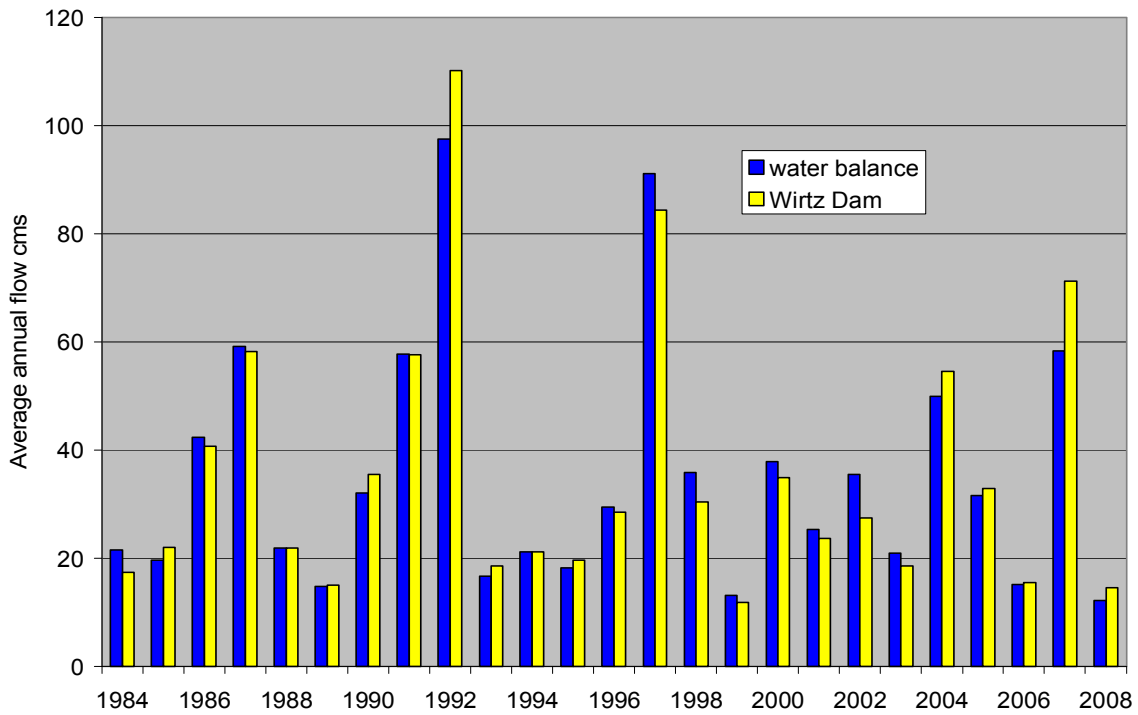


Figure 4. Comparison of measured annual average releases at Wirtz Dam with those predicted from the water balance.

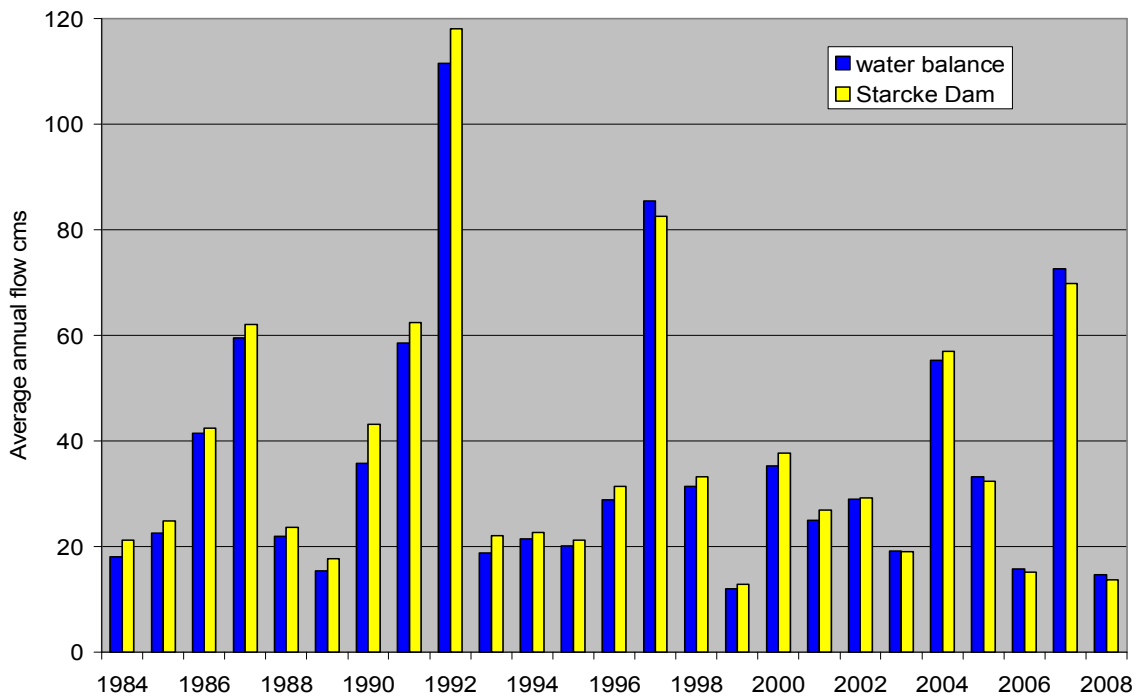


Figure 5. Comparison of measured annual average releases at Starcke Dam with those predicted from the water balance.

Given the model requirement for mass balance, an imbalance between inflows and outflows will result in changes in lake volume and surface elevation in the model. Because lake surface elevation measurements are reported from just one location (at the dam) and at one time (midnight), some deviation from the reported elevation is reasonable and expected. In fact, inspection of hourly surface elevation data from Inks Dam and the Highway 29 bridge frequently reveals intra-day and intra-lake variation of several tenths of a foot. Large daily or systematic discrepancies between inflows and outflows are not physically realistic for small lakes such as Inks Lake and Lake Marble Falls, and will quickly result in unrealistic lake elevations and volumes in the model. When adjustments to inflows and or outflows were required to achieve a daily water balance, it was typically necessary to adjust the inflows and/or outflows at the dams. While there is significant uncertainty in the watershed and tributary inflows predicted by the SWAT watershed model, these inflows were small compared to the total inflow and often insufficient to make up the required volume. This was especially true for Inks Lake and Lake Marble Falls.

The objective of this effort was to achieve daily water balances for the four lake system (Inks, LBJ, Marble Falls, Travis) while minimizing any required adjustments (in terms of frequency and magnitude) from the reported water release time series. A linked water balance time series facilitates linking of the lake models.

METHODOLOGY

To close the water balance, the modeled lake elevation and volume was allowed to deviate from measured elevations to a small extent as a buffer for short-term variations and uncertainties in inflows and outflows. However, the difference from measured elevation was not allowed to exceed 0.5 feet. When the calculated elevation deviation exceeded 0.5 feet, changes in inflow and outflow volumes were necessary to achieve a water balance.

A water balance utility was implemented as a Microsoft Windows application in the RealBasic programming language. Seven different versions were written that differed slightly in their methodology as described below.

Version 1 - This version attempts to make all 4 models (Travis, Marble Falls, LBJ, and Inks) link up with a common water release time series at each dam. Because the Travis model is complete, the balance uses the Starcke Dam water release time series from the Lake Travis model, then works its way sequentially upstream to Lake Marble Falls, Lake LBJ, and then Inks Lake. It then repeats the process ten times, using the dam releases from the previous iteration as a starting point, in an attempt to smooth out any differences between the calculated time series as Wirtz and Inks Dams between lakes.

It was noted that there were substantial differences between the reported water releases over Starcke Dam and the water release time series used in the Lake Travis model. This was believed to be because Lake Travis has a very large storage capacity, and achieving closure in the Lake Travis water balance often required large revisions to inflows as releases from Starcke Dam. Only version 1 uses the Starcke Dam flows from the Lake Travis model.

Version 2 - This version works the same as version 1, but uses the reported releases from Starcke Dam rather than those from the Lake Travis model. It does allow adjustments to the releases at Starcke Dam to aid in the water balance.

Version 3 - This version is based on the observation that Lakes Inks and Marble Falls are the smallest lakes, and therefore the most sensitive to any errors or adjustments to their inflows and outflows. Therefore, it first balances Inks Lake by adjusting releases at Buchanan Dam preferentially, but also at Inks Dam when required (because releases at Buchanan Dam cannot be negative). Next it balances Lake Marble Falls by adjusting releases at Starcke Dam preferentially, but also at Wirtz Dam as required. Finally, it balances Lake LBJ, preferentially adjusting flows at Inks Dam, and at Wirtz only as required. It goes through ten iterations, using the dam releases from the previous iteration as a starting point.

Version 4 - This version first balances Lake LBJ by preferentially adjusting releases from Inks Dam, then those at Wirtz Dam only as required. Next, it balances Marble Falls by adjusting releases at Starcke Dam preferentially, and at Wirtz Dam only as required. Finally, it balances Inks Lake by preferentially adjusting flows at Buchanan Dam, and at Inks Dam only as required. It goes through ten iterations, using the dam releases from the previous iteration as a starting point.

Version 5 - This version balances only Lake LBJ, independently of the other lakes. It preferentially modifies inflows over Inks Dam, and adjusts Wirtz Dam flows only as necessary. It goes through ten iterations, using the dam releases from the previous iteration as a starting point.

Version 6 - This version balances only Lake Marble Falls, independently of other lakes. It preferentially modifies inflows over Starcke Dam, and adjusts Wirtz Dam flows only as necessary. It goes through ten iterations, using the dam releases from the previous iteration as a starting point.

Version 7 - This version balances only Inks Lake, independently of other lakes. It preferentially modifies inflows over Inks Dam, and adjusts Buchanan Dam flows only as necessary. It goes through ten iterations, using the dam releases from the previous iteration as a starting point.

RESULTS

The several versions of the water balance utility were evaluated with respect to the following objectives:

1. minimizing the adjustments to reported water releases at dams,
2. minimizing deviations from reported water surface elevations, and
3. minimizing differences between adjacent lake models in adjusted water release time series at dams, in order to maximize the model linkage.

Minimizing Adjustments to Reported Water Releases at Dams

Tables A.1 shows the percentage of days when the various versions of the water balances for each lake required an alteration to the reported water release at each dam. Table A.2 shows the average absolute magnitude of those alterations. Figures A.1 through A.6 show histograms of these alterations in water release for each version and dam.

Water balance versions 5, 6, and 7, which balance each lake independently, require the least adjustments from reported water releases to achieve a daily flow balance. Version 1 requires the greatest adjustments. Versions 2, 3, and 4 produce similar results, with Version 4 performing slightly better on the Lake Marble Falls water balance.

Table A1. Percentage of days requiring a water release adjustment of 1 cms or more

Model	Inks Lake		Lake LBJ		Lake Marble Falls	
Dam	Buchanan Dam	Inks Dam	Inks Dam	Wirtz Dam	Wirtz Dam	Starcke Dam
Version 1	39%	30%	30%	54%	50%	0.6%
Version 2	34%	24%	24%	14%	14%	48%
Version 3	40%	25%	24%	14%	14%	48%
Version 4	34%	24%	24%	14%	14%	43%
Version 5	-	-	23%	12%	-	-
Version 6	-	-	-	-	2%	38%
Version 7	30%	0%	-	-	-	-

Table A2. Average absolute water release adjustment from reported values, in cms

Model	Inks Lake		Lake LBJ		Lake Marble Falls	
	Buchanan Dam	Inks Dam	Inks Dam	Wirtz Dam	Wirtz Dam	Starcke Dam
Reported release	20.0	22.6	22.6	35.6	35.6	37.8
Version 1	10.8	11.2	11.2	11.7	10.7	0.02
Version 2	7.1	7.7	7.6	3.4	3.4	5.3
Version 3	7.5	7.7	7.6	3.4	3.4	5.3
Version 4	7.1	7.7	7.7	3.4	3.4	5.0
Version 5	-	-	6.9	2.6	-	-
Version 6	-	-	-	-	1.0	3.1
Version 7	3.9	0.1	-	-	-	-

Minimizing Deviations from Reported Water Surface Elevations

All water balance versions perform similarly on matching reported water surface elevations, as illustrated in Table A.3..

Table A3. Average water surface elevation difference from reported values, in feet. Averages are of absolute differences (relative differences in parentheses).

Model	Inks Lake	Lake LBJ	Lake Marble Falls
Version 1	0.37 (-0.19)	0.34 (0.01)	0.41 (-0.03)
Version 2	0.38 (-0.17)	0.34 (0.08)	0.39 (0.05)
Version 3	0.39 (-0.02)	0.34 (0.08)	0.38 (0.07)
Version 4	0.38 (-0.18)	0.33 (0.06)	0.40 (-0.06)
Version 5	-	0.34 (0.08)	-
Version 6	-	-	0.41 (-0.20)
Version 7	0.39 (-0.29)	-	-

Minimizing Differences between Adjacent Lake Models in Water Release Time Series

As expected, the independently developed water balances of versions 5, 6, and 7 permitted the greatest discrepancies in water releases at dams between adjacent lakes (Table A.4). Also, with only version 1 attempting to match the water release time series at Starcke Dam from the Lake Travis model, versions 2 through 5 exhibited a large flow difference with the Travis model at Starcke Dam. Versions 2 through 4 produced similar results, with version 4 probably performing the best.

Table A4. Discrepancies in water releases at dams between lake models

Dam	% of Days with Difference in Water Release of 1 cms or more			Average Absolute Difference in Water Release (cms)		
	Inks	Wirtz	Starcke	Inks	Wirtz	Starcke
Version 1	0.53%	9.0%	0.64%	0.04	2.21	0.02
Version 2	0.55%	0.00%	57.4%	0.05	0.00	11.8
Version 3	1.20%	0.00%	57.8%	0.08	0.00	11.8
Version 4	0.53%	0.00%	53.8%	0.05	0.00	11.6
Version 5	-	-	50.2%	6.99	-	-
Version 6	-	-	-	-	3.27	10.9
Version 7	23.3%	13.7%	-	-	-	-

RECOMMENDATIONS

Version 1, which is based on Starcke Dam water releases from the Lake Travis model, is not recommended because it exhibits large differences from reported water releases, and these differences are propagated upstream and significantly affect the water balances of upstream lakes.

Version 5 is not recommended because it permits large differences between models in the flow time series at dams. If the models are intended to be run in series, this can result in significant water and mass losses from the models.

Versions 2 through 4 produce similar results, with version 4 recommended because it requires slightly less difference from reported water releases and slightly less difference between models in the flow time series at dams.

REFERENCES

Cole, TM, and SA Wells. 2008. CE-QUAL-W2: A Two-Dimensional, Laterally Averaged, Hydrodynamic and Water Quality Model, Version 3.6. User Manual. Instruction Report EL-08-1. U. S. Army Corps of Engineers. Washington, DC.

TWDB (Texas Water Development Board). 2007a. Volumetric and Sedimentation Survey of Inks Lake. Texas Water Development Board. Austin, Texas.

TWDB (Texas Water Development Board). 2007b. Volumetric and Sedimentation Survey of Lake Lyndon B. Johnson. Texas Water Development Board. Austin, Texas.

TWDB (Texas Water Development Board). 2007c. Volumetric and Sedimentation Survey of Lake Marble Falls. Texas Water Development Board. Austin, Texas.

THIS PAGE INTENTIONALLY LEFT BLANK

APPENDIX A.2
SUMMARY OF WATER BALANCE DISCUSSIONS WITH ROC

THIS PAGE INTENTIONALLY LEFT BLANK

SUMMARY OF WATER BALANCE DISCUSSIONS WITH ROC

Lake water quality modeling calibration generally starts by first calibrating the water balance, then temperature and finally water quality. For Lakes and Reservoirs, the water balance is checked by comparing predicted surface water elevations with observed elevations.

The water balance for a lake or reservoir is the change in volume per time calculated by the differences in inflows and outflows. The change in volume or storage, can be determined from the day to day variations in surface water elevation provided a surface elevation to volume rating curve is available or can be estimated from the bathymetry of the model. The team's approach was to estimate inflows from measured data and SWAT-generated watershed inflows and outflows from reported flows over the dams, use precipitation and evaporation estimates from historical data, and assume groundwater flows were negligible. The water balance calculates a daily water surface elevation that is compared to the measured water surface elevations for each lake. For Phase 3, the modeling team planned to balance each lake independently, assuming any necessary adjustments would be minor and within the error of measurement of the reported flows over the dams and observed surface elevations, particularly during storm flows. The initial water balance approach worked well for Inks Lake, but not Lake LBJ or Lake Marble Falls. The team determined that flows (and particularly storm water flows) at Wirtz Dam were possibly causing discrepancies in the calculations of both flow balances for Lake LBJ and Lake Marble Falls. The team investigated scrubbing flow data for time periods in which the lake elevations changed more than +/- 2 feet and reviewed the data in question with LCRA's River Operations Center (ROC) personnel. Because the adjustments at Wirtz would impact both flow balances of Lake LBJ and Lake Marble Falls, the team developed a flow balance methodology to minimize adjustments in flows at all three dams. A memo describing the methodology and the review comments from Limno Tech, Inc. are included in this appendix.

This approach was reviewed with LCRA's ROC personnel on April 6, 2010. During this meeting, modeling team members also discussed measurement techniques for measuring flow and surface water elevations with ROC personnel to gain an understanding in the uncertainty associated with the measures and initiated a joint review of specific data. ROC personnel reviewed spreadsheets provided by the modeling team and confirmed missing data and data associated with managed lowering of lake levels in certain years.

The modeling team used the water balance utility as a starting point for each lake's water balance; however, final calibration for each lake required minor adjustments to the flow balance generated from the utility and some estimation of flows on days when data was missing or considered inaccurate. Overall, the adjustments were minor as noted in the attached water balance methodology memo.

THIS PAGE INTENTIONALLY LEFT BLANK

APPENDIX B
VERTICAL PROFILES OF TEMPERATURE, SPECIFIC
CONDUCTANCE, CHLORIDE, AND DISSOLVED OXYGEN

THIS PAGE INTENTIONALLY LEFT BLANK

LIST OF FIGURES

- Figure B-1 Water temperature vertical profiles for the Inks Lake model
- Figure B-2 Specific conductance vertical profiles for the Inks Lake model
- Figure B-3 Chloride vertical profiles for the Inks Lake model
- Figure B-4 Dissolved oxygen vertical profiles for the Inks Lake model
- Figure B-5 Water temperature vertical profiles for Lake LBJ near Wirtz Dam
- Figure B-6 Water temperature vertical profiles for Lake LBJ at confluence with Sandy Creek Arm
- Figure B-7 Water temperature vertical profiles for Lake LBJ at confluence with Llano River Arm
- Figure B-8 Water temperature vertical profiles for Lake LBJ at Kingsland Cove
- Figure B-9 Water temperature vertical profiles for Lake LBJ at Lake Shore Drive
- Figure B-10 Water temperature vertical profiles for Lake LBJ at Horseshoe Bay Cove
- Figure B-11 Specific conductance vertical profiles for Lake LBJ near Wirtz Dam
- Figure B-12 Specific conductance vertical profiles for Lake LBJ at confluence with Sandy Creek Arm
- Figure B-13 Specific conductance vertical profiles for Lake LBJ near confluence with Llano River Arm
- Figure B-14 Specific conductance vertical profiles for Lake LBJ at Kingsland Cove
- Figure B-15 Specific conductance vertical profiles for Lake LBJ near Lake Shore Drive
- Figure B-16 Specific conductance vertical profiles for Lake LBJ at Horseshoe Bay Cove
- Figure B-17 Chloride vertical profiles for Lake LBJ near Wirtz Dam
- Figure B-18 Chloride vertical profiles for Lake LBJ near Sandy Creek confluence
- Figure B-19 Chloride vertical profiles for Lake LBJ near confluence with Llano River Arm
- Figure B-20 Chloride vertical profiles for Lake LBJ at Kingsland Cove
- Figure B-21 Chloride vertical profiles for Lake LBJ near Lake Shore Drive
- Figure B-22 Chloride vertical profiles for Lake LBJ at Horseshoe Bay Cove
- Figure B-23 Dissolved Oxygen vertical profiles for Lake LBJ near Wirtz Dam
- Figure B-24 Dissolved Oxygen vertical profiles for Lake LBJ near Sandy Creek confluence
- Figure B-25 Dissolved Oxygen vertical profiles for Lake LBJ near confluence with Llano River Arm
- Figure B-26 Dissolved Oxygen vertical profiles for Lake LBJ at Kingsland Cove
- Figure B-27 Dissolved Oxygen vertical profiles for Lake LBJ near Lake Shore Drive
- Figure B-28 Dissolved Oxygen vertical profiles for Lake LBJ at Horseshoe Bay Cove
- Figure B-29 Water temperature vertical profiles for Lake Marble Falls near Max Starcke Dam
- Figure B-30 Water temperature vertical profiles for Lake Marble Falls near US 281 Bridge
- Figure B-31 Water temperature vertical profiles for Lake Marble Falls at Hefner Ranch

- Figure B-32 Water temperature vertical profiles for Lake Marble Falls at Headwaters
- Figure B-33 Specific conductance vertical profiles for Lake Marble Falls near Max Starcke Dam
- Figure B-34 Specific conductance vertical profiles for Lake Marble Falls near US 281 Bridge
- Figure B-35 Specific conductance vertical profiles for Lake Marble Falls at Hefner Ranch
- Figure B-36 Specific conductance vertical profiles for Lake Marble Falls at Headwaters
- Figure B-37 Chloride vertical profiles for Lake Marble Falls near Max Starcke Dam
- Figure B-38 Chloride vertical profiles for Lake Marble Falls at Headwaters
- Figure B-39 Dissolved Oxygen vertical profiles for Lake Marble Falls near Max Starcke Dam
- Figure B-40 Dissolved Oxygen vertical profiles for Lake Marble Falls near US 281 Bridge
- Figure B-41 Dissolved Oxygen vertical profiles for Lake Marble Falls at Hefner Ranch
- Figure B-42 Dissolved Oxygen vertical profiles for Lake Marble Falls at Headwaters

APPENDIX C

CE-QUAL-W2 MODEL CALIBRATION METRICS AND OBJECTIVES

THIS PAGE INTENTIONALLY LEFT BLANK

MEMORANDUM

TO: CREMS Lake Travis Team **DATE:** 4/9/2007
FROM: Kirk Dean **RE:** Water quality calibration of Lake
Travis CE-QUAL-W2 model
CC: **JOB#:**

This memorandum discusses several issues pertinent to the calibration of the Lake Travis water quality model. Recommendations are made regarding the most suitable approaches for the Lake Travis model for CREMS.

1. Manual Calibration or Numerical Optimization?

One key decision is whether to utilize 1) a formal numerical optimization procedure, or 2) statistical and graphical comparisons between model predictions and observations in a manual trial and error approach, with the modeler providing interpretation and judgment as to the optimum calibration. The latter is the more common approach. However, as the number of interacting parameters simulated increases, the model calibration becomes more complex because varying one parameter affects many others. Because a eutrophication model includes multiple biological responses to multiple chemical and physical driving parameters, it can be difficult and time-consuming for a modeler to find the optimum values of model calibration parameters. Thus, a numerical optimization procedure may be recommended. However, numerical optimization procedures should not be considered 'black boxes' that feed out the ultimate answer, but should be used as a tool with statistical and graphical analysis by an experienced modeler.

Formal numerical optimization procedures can be of several types. For a small number of parameters, an optimum numerical solution may be obtained by minimizing an objective function using calculus-based solver algorithms. UCODE uses nonlinear regression, with a modified Gauss-Newton method to adjust parameter values to minimize the weighted least-squares objective function. PEST is a similar program using the Marquardt-Levenburg method of nonlinear parameter estimation. Either of these tools will work with most models. These programs may, however, have problems with numerical instability when fitting functions do not vary smoothly.

Another option would be to run a Monte Carlo Analysis. In Monte Carlo Analysis, key parameters are varied within a range of potential values, the model is run with each combination of parameter values, and model goodness of fit is judged with one or more statistics until a best fit is identified.

More recently, genetic algorithms (GAs) have been used commonly in model calibration. They are based on the biological principles of natural selection, with optimal combinations of parameters selected from a “population” of potential values through many “generations” of variations. In each generation, combinations of parameters that improve model fit tend to be more favored for selection in the next generation. GA’s tend to be more stable and robust than calculus-based numerical algorithms, and tend to converge to a solution more efficiently than Monte Carlo analysis. Mulligan and Brown (1998) report use of a genetic algorithm to calibrate Streeter-Phelps and QUAL2E stream models. Pelletier et al. (2006) applied a publicly-available GA (PIKAIA) to calibrate a QUAL2Kw eutrophication model. Ostfeld and Salomons (2005) report application of a hybrid genetic algorithm to calibrate a CE-QUAL-W2 model. In this report, the efficiency of the genetic algorithm was enhanced using hurdle-race and k-nearest neighbor algorithms to eliminate most of the excess computational effort.

Although the numerical optimization methods offer certain advantages, many modelers feel more comfortable with a manual trial-and error approach based on statistical and graphical analysis. Given the time required to develop a numerical optimization program, the manual approach is recommended for the Lake Travis model.

2. Calibration then Verification or Combined Calibration/Verification?

Typically, it is recommended that models should be calibrated to one dataset, then verified using an independent dataset. Often, this is performed by splitting the available dataset in half, using the first half for calibration and the second half for verification. If the model fits the verification dataset well (without adjusting the calibrated model parameters), it lends confidence in model predictions of future conditions. Cole and Wells (2002) point out, however, that the separation between calibration and verification is a false one, because if the verification run does not fit well, then the model calibration coefficients will inevitably be adjusted until the model fits both calibration and verification periods. Thus, they recommend that the model should be calibrated to all available data continuously, i.e. not broken into separate runs by years or seasons. However, the model should exhibit good fit to all periods, including individual years, droughts, and flood periods. Ideally, the calibration data set should encompass the full range of variations and extreme conditions that might be anticipated in the future.

3. Measures of Model Goodness of Fit

While some modelers do not use statistical measures of goodness of fit (GOF), choosing to rely instead on graphical illustration of GOF, it is generally recommended (Reckhow et al. 1990) that one or more quantitative measures of GOF be used in calibration and verification/confirmation of models. Numerous statistical measures of model goodness of fit (GOF) are available, and some are listed below and summarized in Table 1. The similarity of most of these measures is readily noticeable when they are expressed using common notation. The table lists the number of times each GOF statistic was used in a brief review of modeling reports.

Several authors recommend that several GOF measures be used, to quantify 1) model bias, 2) absolute error, and 3) relative error. This may lead to situations where different calibrations show improved performance with respect to some GOF statistics, but poorer performance for others. For this reason, it is recommended that acceptable ranges of GOF statistics are decided in advance, as well as a hierarchy of importance of GOF statistics. To facilitate calibration, an automated or semi-automated method should be implemented to calculate and summarize the various GOF statistics, compare them to acceptable ranges, and calculate an overall calibration score.

Cole and Wells (2002) recommend using the absolute mean error (AME) as an indicator of CE-QUAL-W2 model accuracy, since it is simply calculated and directly interpretable, i.e., it is in the same units as the measurement. A similar statistic is the root mean square error (RMSE), with the difference that it provides an extra penalty for the outlying predictions that are very different from observations. The RMSE is commonly used in the objective minimization functions of parameter optimization algorithms. Neither the AME nor RMSE provide information on model bias, as deviations in either directions from observed values are penalized equally. For quantification of the bias of model predictions, the mean error (ME) or mean percent error (M%E) are recommended.

The reliability index (RI) of Leggett and Williams (1981) has been used by many CE-QUAL-W2 modelers to evaluate model performance. Wlosinski (1984) considered the RI to be the best statistic for reporting aggregate model performance for CE-QUAL-R1, the predecessor to CE-QUAL-W2. The RI indicates the average factor by which model predictions differ from observations. A RI of 1.0 indicates a perfect fit. If all predicted values are one-half order of magnitude apart, a RI of 5 will result. RI values of less than 3 are generally considered to be acceptable for most parameters. RI values of greater than 10 usually indicate extremely low values near detection limits, as often found with some nutrient species, or highly variable parameters, such as algae biomass. One of the weaknesses of the RI is that the values are difficult to interpret since they are unitless and their range is expected to vary by parameter. The RI should be used with other measures of absolute and relative error.

The modeling efficiency (MEF) measures how much better a model predicts observed values than the average of the observed values. A value of 1 indicates a perfect match, whereas a value of 0 indicates that the model performs no better at predicting observed values than the average of the observed values.

Theil's inequality coefficient is similar to a correlation coefficient, but is a measure of distance instead of similarity. One advantage of Theil's inequality coefficient is that it can be decomposed into bias, variance, and fit quality components (Smith and Rose, 1995). However, the interpretation of these quantities may not be as straightforward as the more direct measures.

While the modeler has substantial leeway in selecting GOF statistics, we recommend using mean error (ME) to evaluate bias, root mean square error (RMSE) to evaluate absolute error, and Leggett and Williams' (1986) reliability index (RI). These are straightforward to calculate and interpret. Since they have been used in other modeling studies, it will facilitate comparison of model performance with other studies.

Table 1. Summary of model goodness of fit statistics and their characteristics

Statistic	Statistic name	Use [‡]	Measure of?	Penalizes outliers?	Units?	Range ^{†,*}
ME	mean error	9	absolute bias	N	Same as observation	$-\infty - +\infty$ 0*
M%E	mean percent error	2	relative bias	N	Unitless % of observation	$-\infty - +\infty$ 0*
MSE	mean square error	2	absolute error	Y	Square of observation	0* – ∞
MAE	mean absolute error	10	absolute error	N	Same as observation	0* – ∞
MA%E	mean absolute percent error	2	relative error	N	Unitless % of observation	0* – ∞
RMSE	root mean square error	11	absolute error	Y	Same as observation	0* – ∞
RMAE	relative mean absolute error	1	relative error	N	Unitless % of observation	0* – ∞
GSD	general standard deviation	1	relative error	Y	Unitless % of observation	0* – ∞
U	Theil's inequality coefficient	1	fit quality index	Y	unitless	0* – 1
E	Nash-Sutcliffe coefficient of efficiency	1	fit quality index	Y	unitless	$-\infty - 1^*$
E'	modified coefficient of efficiency	1	fit quality index	N	unitless	$-\infty - +\infty$ 1*
J	Janus quotient	1	fit quality index	Y	unitless	0* – ∞
R ²	coefficient of determination	8	fit quality index	Y	unitless	0 – 1*
d	index of agreement	1	fit quality index	Y	unitless	0 – 1*
d'	modified index of agreement	1	fit quality index	N	unitless	0 – 1*
L _k	likelihood function	1	fit quality index	Y	Square root of observation	0* – ∞
k _g or RI	reliability index	6	fit quality index	Y	unitless	1* – ∞
d	functional distance	1	fit quality index	N	logarithm of y	0* – ∞
MEF	modeling efficiency	1	fit quality index	Y	unitless	$-\infty - 1^*$

- † assuming observed data are positive numbers
- ‡ number of modeling reports and papers using this statistic
- * asterisk indicates value for a perfect model fit to observed data

4. Model Verification and Confirmation

For model confirmation, several authors recommend that statistical hypothesis tests should be used in lieu of, or as a supplement to, descriptive GOF statistics. If model predictions fall within confidence limits of measured data, the model cannot be said to differ from the real system and confidence in model predictions is increased, even in the case of poor GOF statistics commonly observed for highly variable or near-detection limit parameters. To evaluate model predictive capacity, one can test the hypothesis that average prediction errors are, for example, less than 1 mg/l for dissolved oxygen and less than 10 µg/l for chlorophyll a. Many hypothesis tests, such as the t-test, Wilcoxon-Mann-Witney test, or the Kolmogorov-Smirnov test are capable. All of these tests require independent samples drawn from a population, but water quality model simulations are typically very strongly autocorrelated with respect to time and location. Reckhow et al. (1990) describe methods to adjust for this autocorrelation. The t-test also requires normally distributed values, which is unusual for most environmental parameters but may be achievable through log-transformation.

Cole and Wells (2002) do not provide guidelines regarding *a priori* acceptable levels of error for CE-QUAL-W2. Ultimately, acceptable levels of error should be based on model uncertainty versus water quality prediction requirements of lake managers. However, based on a review of reported model errors in other systems, we can identify calibration goals for some parameters that may be achievable. These are average absolute mean errors for the system as a whole, and may not be met at all places and times.

Table 2. Calibration goals for system-wide average absolute mean error, based on CE-QUAL-W2 modeling results in other systems

water level	0.2 meters	total Kjeldahl nitrogen	0.4 mg/l
water temperature	1°C	ammonia nitrogen	0.03 mg/l
pH	0.3 su	nitrate nitrogen	0.1 mg/l
total organic carbon	0.6 mg/l	total phosphorus	0.02 mg/l
chlorophyll a	4 µg/L	orthophosphate phosphorus	0.01 mg/L

Model Goodness of Fit Statistic Formulas

In these formulas:

y_i represents a measured value at point i in time and space

\hat{y}_i represents a model predicted value at point i in time and space

i represents a point in time and space

n represents the number of observations

\bar{y} represents the average measured value

$\bar{\hat{y}}$ represents the average predicted value

$$\text{Mean error } ME = \left(\sum_{i=1}^n (y_i - \hat{y}_i) \right) / n$$

$$\text{Mean \% error } M\%E = 100 \left[\sum_{i=1}^n (y_i - \hat{y}_i) / y_i \right] / n$$

$$\text{Mean square error } MSE = \left[\sum_{i=1}^n (y_i - \hat{y}_i)^2 \right] / n$$

$$\text{Mean absolute error } MAE = \left(\sum_{i=1}^n |y_i - \hat{y}_i| \right) / n$$

$$\text{Mean absolute \% error } MA\%E = 100 \left[\sum_{i=1}^n (|y_i - \hat{y}_i| / |y_i|) \right] / n$$

$$\text{Root mean square error } RMSE = \left\{ \left[\sum_{i=1}^n (y_i - \hat{y}_i)^2 \right] / n \right\}^{0.5}$$

$$\text{Relative mean absolute error } RMAE = \left(\sum_{i=1}^n |y_i - \hat{y}_i| \right) / (n * \bar{y}) = MAE / \bar{y}$$

$$\text{General standard deviation } GSD = RMSE / \bar{y}$$

$$\text{Theil's inequality coefficient (Theil, 1966) } U = \sqrt{\left[\sum_{i=1}^n (y_i - \hat{y}_i)^2 \right] / \sum_{i=1}^n y_i^2}$$

$$U_{bias} = [\bar{y} - \bar{\hat{y}}]^2 / \left[(1/n) \sum_{i=1}^n (y_i - \hat{y}_i)^2 \right]$$

$$U_{variance} = [s - \hat{s}]^2 / \left[(1/n) \sum_{i=1}^n (y_i - \hat{y}_i)^2 \right]$$

where $\hat{s} = \sqrt{\frac{1}{n} \sum_{i=1}^n (\hat{y}_i - \bar{\hat{y}})^2}$ and $s = \sqrt{\frac{1}{n} \sum_{i=1}^n (y_i - \bar{y})^2}$

$$U_{covariance} = [2(1 - r_{y\hat{y}}) * s * \hat{s}] / \left[(1/n) \sum_{i=1}^n (y_i - \hat{y}_i)^2 \right]$$

Nash-Sutcliffe coefficient of efficiency (Nash and Sutcliffe 1970)

$$E = 1 - \frac{\sum_{i=1}^n (y_i - \hat{y}_i)^2}{\sum_{i=1}^n (y_i - \bar{y})^2}$$

Modified coefficient of efficiency reduces the impact of outliers:

$$E' = 1 - \frac{\sum_{i=1}^n (y_i - \hat{y}_i)}{\sum_{i=1}^n (y_i - \bar{y})}$$

Janus quotient (Gadd and Wold, 1964) $J^2 = \left\{ \frac{\sum_{i=1}^m (y_i - \hat{y}_i)^2 / m}{\sum_{i=1}^n (y_i - \hat{y}_i)^2 / n} \right\}$

Coefficient of determination $r^2 = \left\{ \frac{\sum_{i=1}^n (y_i - \bar{y})(\hat{y}_i - \bar{\hat{y}})}{\left[\sum_{i=1}^n (y_i - \bar{y})^2 \right]^{0.5} * \left[\sum_{i=1}^n (\hat{y}_i - \bar{\hat{y}})^2 \right]^{0.5}} \right\}^2$

Index of Agreement (Willmott et al., 1985) $d = 1 - \frac{\sum_{i=1}^n (y_i - \hat{y}_i)^2}{\sum_{i=1}^n (|\hat{y}_i - \bar{y}| + |y_i - \bar{y}|)^2}$

Modified index of agreement
$$d' = 1 - \frac{\sum_{i=1}^n (y_i - \hat{y}_i)}{\sum_{i=1}^n (|\hat{y}_i - \bar{y}| + |y_i - \bar{y}|)}$$

Likelihood function for parameter k
$$L_k = \sqrt{\frac{1}{n_k} * \sum_{i=1}^{n_k} \frac{(\hat{y}_{i,k} - y_{i,k})^2}{y_{i,k}}}$$

Reliability index (Leggett and Williams 1981)
$$k_g = \frac{1 + \sqrt{\frac{1}{n} \sum_{i=1}^n \left[\frac{1 - (y_i / \hat{y}_i)}{1 + (y_i / \hat{y}_i)} \right]^2}}{1 - \sqrt{\frac{1}{n} \sum_{i=1}^n \left[\frac{1 - (y_i / \hat{y}_i)}{1 + (y_i / \hat{y}_i)} \right]^2}}$$

Functional distance
$$d = \sqrt{\sum_{i=1}^n (\ln y_i - \ln \hat{y}_i)^2 / n}$$

Modeling efficiency
$$MEF = \frac{\sum_{i=1}^n (y_i - \bar{y})^2 - \sum_{i=1}^n (\hat{y}_i - y_i)^2}{\sum_{i=1}^n (y_i - \bar{y})^2}$$

Autocorrelation coefficient for time lag k
$$r_k = \frac{\text{cov ar}[y_i, y_{i+k}]}{s(y_i) * s(y_{i+k})}$$

References

Berger, C.J., R.L. Annear, Jr, and S.A. Wells. 2003. "Upper Spokane River Model: Model Calibration, 2001". Technical Report EWR-1-03, Department of Civil and Environmental Engineering, Portland State University, Portland, OR, 89 pages.

Cole, TM, and SA Wells. 2002. CE-QUAL-W2: A two-dimensional, laterally averaged, hydrodynamic and water quality model, version 3.1: user manual. Instruction report EL-02-1. U.S. Army Corps of Engineers, Washington DC, August 2002.

Mulligan, AE, and LC Brown. 1998. Genetic algorithms for calibrating water quality models. J. Environ. Eng. 124: 202-211.

Ostfeld, A and S Salomons. 2005. A hybrid genetic-instance based learning algorithm for CE-QUAL-W2 calibration. J. Hydrol. 310: 122-142.

Pelletier, GJ, SC Chapra, and H. Tao. 2006. QUAL2Kw – A framework for modeling water quality in streams and rivers using a genetic algorithm for calibration. Environ. Modeling and Software 21: 419-425.

Reckhow, KH, JT Clements, and RC Dodd. 1990. Statistical evaluation of mechanistic water-quality models. J. Environ. Eng. 116: 250-268.

Smith, EP, and KA Rose. 1995. Model goodness-of-fit analysis using regression and related techniques. Ecol. Modelling 77:49-64.

Wlosinski, JH. 1984. Evaluation techniques for CE-QUAL-R1 – a one-dimensional reservoir water quality model. Miscellaneous Paper E-84-1. U.S. Army Corps of Engineers Waterways Experiment Station, Vicksburg, MS.